Lucília Celina Silva Pebre Pereira

Licenciada em Biologia Celular e Molecular

Exploring the chemotherapeutic potential of *Brassicaceae* extracts in colorectal cancer cell spheroids

Dissertação para obtenção do Grau de Mestre em
Genética Molecular e Biomedicina

Orientador: Teresa Serra, PhD, iBET/ITQB

FACULDADE DE CIÊNCIAS E TECNOLOGIA
UNIVERSIDADE NOVA DE LISBOA

Setembro 2016

Lucília Celina Silva Pebre Pereira

Licenciada em Biologia Celular e Molecular

Exploring the chemotherapeutic potential of *Brassicaceae* extracts in colorectal cancer cell spheroids

Dissertação para obtenção do Grau de Mestre em
Genética Molecular e Biomedicina

Orientador: Teresa Serra, PhD, iBET/ITQB

FACULDADE DE CIÊNCIAS E TECNOLOGIA
UNIVERSIDADE NOVA DE LISBOA

Setembro 2016

Exploring the chemotherapeutic potential of *Brassicaceae* extracts in colorectal cancer cell spheroids

Acknowledgments

Gostaria de agradecer a todos os que me apoiaram e/ou contribuíram direta ou indiretamente na concretização deste trabalho.

À Dr.ª. Teresa Serra, por toda a orientação e incansável apoio durante este último ano lectivo. Agradeço especialmente todos os nossos diálogos que contribuíram para o meu desenvolvimento pessoal e académico, e por demonstrar que todas as adversidades podem ser ultrapassadas e que servem para fortalecer o nosso carácter e perseverança. Um grande obrigado por toda a boa-disposição, dedicação e motivação que demonstrou para comigo e com este projeto, e por me ajudar a concretizar esta grande etapa do meu percurso académico.

À Dr.ª. Catarina Duarte, pela compreensão, receção e acolhimento no grupo Nutraceuticals and Delivery. Agradeço o facto de me ter dado a oportunidade de recomeçar (e terminar) uma tese de mestrado num laboratório com boas condições de trabalho e orientação.

À Professora Paula Gonçalves, Coordenadora de Mestrado, pela sua compreensão e apoio quando mais precisei antes de iniciar este ano letivo.

À Dr.ª. Cristina Albuquerque do IPO por me ter acolhido e dado a oportunidade de completar ainda mais a minha tese. Agradeço a sua disponibilidade e orientação, apesar de não ser sua aluna. Ao Bruno, à Marlene, à Ana e à Soraia por me terem orientado no laboratório e me esclarecerem dúvidas pontuais.

Ao grupo do TCA, pela disponibilidade de equipamentos e materiais que contribuíram para o desenvolvimento deste trabalho. À Dr.ª. Margarida Serra pela formação no microscópio de contraste de fase. Ao Hugo pela formação inicial no citómetro de fluxo. Ao Marcos Sousa pela disponibilidade e ajuda na manipulação do software do microscópio quando este não colaborava.

Ao Nuno Pimpão e ao Hugo do IGC pela formação e apoio na manipulação do microscópio confocal de fluorescência.

A todo o núcleo do grupo Nutraceuticals and Delivery pela boa disposição e acolhimento. Gostaria de agradecer especialmente à Liliana Rodrigues pela produção dos extractos naturais, e pela prontidão com que sempre me ajudou. À Joana Poejo pelo apoio na cultura de células.

Às colegas Carolina Pereira, Joana Guerreiro, Ana Roda e Anyse Pereira, pelo convívio, pelos desabafos e pelos bons momentos que passamos neste último ano. Agradeço especialmente à Carolina Pereira por toda a ajuda inicial com a cultura 3D, por me transmitir os ensinamentos dados pela Inês e por todos os nossos debates sobre os esferoides, que tanto nos acompanharam horas a fio. Agradeço também à Joana Guerreiro por todo o apoio e amizade nos momentos em que as coisas nem sempre corriam como esperado.

Às meninas dos “MIGs”, Sara Costa e Andreia Ferreira, por sempre me motivarem e darem força cada vez que nos cruzávamos nos corredores. Ao Pedro Fonseca por todo o apoio desde a licenciatura.

Aos colegas que me acompanharam na Faculdade de Farmácia, Diana Rafael, Sérgio Silva, Raquel Tavares, Rita Leones, Maria Nunes, Sara Moreira e Carolina Abreu Pereira, que me deram força para recomeçar o passado ano lectivo num novo laboratório. Nunca irei esquecer o vosso gesto!

À minha grande amiga Aida Lima, que nem tenho palavras para exprimir o incondicional apoio, amizade e força durante estes últimos 2anos.

À Luna, minha “bigodes” (que também merece), por sempre me ter acompanhado fosse dia ou noite.

Ao Miguel, pelo amor, companheirismo e infindável compreensão. Obrigada por teres sempre acreditado em mim e por todo o carinho nas alturas mais difíceis.

À minha família, em especial ao meu mano piolho e à minha tia-madrinha Zi por toda a força e apoio, mesmo estando longe.

À minha mãe, por todo o amor e apoio incondicionais. Obrigada por toda a paciência e motivação, por me ajudares a ultrapassar todas as adversidades, por me enxugares as lágrimas quando tudo parecia perdido e por teres sempre acreditado em mim. Nunca irei esquecer todo o esforço que fizeste para eu concretizar esta etapa, serás sempre para mim a minha heroína e mãe guerreira!

Aos meus avós que sempre se esforçaram por me ajudar a prosseguir os meus estudos. À minha avó Argentina, por todo o apoio, motivação, carinho e amor que sempre me deu. E em especial ao meu avô, que apesar de ter partido a meio deste meu percurso, sei que sempre esteve comigo. Um dia serei a “Doutora” que sempre desejaste que eu fosse. Obrigada por todo o amor, carinho e preocupação mesmo quando a saúde se esvanecia.

Abstract

Colorectal cancer is the third most common cause of mortality worldwide. Given the growth and increasing life expectancy of the world's population, as well as the acquisition of unhealthy lifestyle habits, the global burden of colorectal cancer is estimated to increase in the next years. Despite the efforts made so far, its treatment is still very challenging due to cancer recurrence usually associated with prevalence of cancer stem cells (CSCs) after treatment. Hence, it is imperative to seek new therapeutic strategies that target colorectal CSCs.

Epidemiological data have reported a positive correlation between cruciferous vegetables intake and decreased risk of colorectal cancer. Their chemo-preventive effect is mainly due to their high content in glucosinolates, the precursors of isothiocyanates (ITCs) that are known to modulate and target several aspects of carcinogenesis.

Hence, by recurring to a green and sustainable high pressure extraction process to recover ITCs from cruciferous vegetables, namely watercress and broccoli, we intended to explore the anticancer mechanisms of *Brassicaceae* vegetables and respective ITCs in a tri-dimensional (3D) cell model of colorectal cancer (i.e. in cell spheroids), since this approach resembles best with the tumor microenvironment in comparison with the conventional two-dimensional (2D) cells models. Our results revealed that *Brassicaceae* extracts and ITCs have the potential to prevent cell proliferation and chemo-resistance, to induce apoptosis, and to target colorectal CSC population and its self-renewal ability. Therefore, our research provides new insights on colorectal cancer therapy using nutraceuticals derived from cruciferous vegetables.

Keywords: Colorectal cancer, cancer stem cells, isothiocyanates, cruciferous vegetables, *Brassicaceae* extracts

Resumo

O cancro colorrectal é a terceira causa mais comum de morte a nível mundial. Dado o aumento do crescimento e esperança média de vida da população mundial, bem como a aquisição e hábitos alimentares pouco saudáveis, estima-se que a taxa de cancro colorrectal aumente nos próximos anos. Apesar dos esforços feitos até agora, o seu tratamento é ainda muito desafiante devido à recidiva da doença que usualmente está associada à prevalência das células estaminais tumorais (CET) após o tratamento. Desta forma, é crucial desvendar novas estratégias terapêuticas com seletividade para as CETs.

Dados epidemiológicos têm reportado uma correlação positiva entre o consumo de vegetais crucíferos e menor risco de cancro colorrectal. O seu efeito quimio-terapêutico deve-se maioritariamente ao seu elevado teor em glucosinolatos, precursores dos isotiocianatos (ITCs) conhecidos por modularem e atingirem diversos aspetos do desenvolvimento tumoral.

Assim, ao recorrer a um processo "verde" e "sustentável" de extração a alta pressão para recuperação de ITCs a partir de vegetais crucíferos, nomeadamente de agrião e brócolos, nós pretendemos explorar os efeitos anti tumorais dos vegetais *Brassicaceae* e respetivos ITCs num modelo tri-dimensional (3D) de cancro colorrectal (i.e. em esferoídes celulares), uma vez que esta abordagem assemelha-se melhor ao microambiente tumoral em comparação com os convencionais modelos celulares bi-dimensionais (2D). Os nossos resultados revelaram que os extratos de *Brassicaceae* e ITCs têm o potencial de prevenir a proliferação e quimio-resistência, de induzir a apoptose e actuar na sob-população das CET e na sua capacidade de autorrenovação. Assim, a nossa pesquisa fornece novas perspetivas na terapia do cancro colorrectal usando nutracêuticos derivados de vegetais crucíferos.

Termos-chave: Cancro colorrectal, células estaminais tumorais, isotiocianatos, vegetais crucíferos, extratos de *Brassicaceae*

Table of Contents

List of Figures

List of Tables

List of Abbreviations

2D	Two-dimensional
3D	Tri-dimensional
5-Fu	5-Fluorouracil
ABC transporters	ATP-binding cassette transporters
ALDH	Aldehyde Dehydrogenase
Allyl ITC	Allyl isothiocyanate
AMPK	AMP-activated protein kinase
APC	Adenomatous polyposis coli
CD133	Prominin-1
CD44	CD44 molecule (Indian blood group)
CDK	Cyclin-dependent kinase
cDNA	complementary DNA
CIN	Chromosomal instability
DCC	Deleted in Colorectal Carcinoma
DMSO	Dimethyl Sulfoxide
DNA	Deoxyribonucleic acid
EGF	Epidermal Growth Factor
EGFR	Epidermal Growth Factor Receptor
ECM	Extracellular matrix
EMT	Epithelial-to-mesenchymal transition
EtOH	Ethanol
FAP	Familial adenomatous polyposis
FBS	Fetal Bovine Serum
GAE	Gallic Acid Equivalents
GAPDH	Glyceraldehyde-3-phosphate dehydrogenase
GC-MS	Gas Chromatography – Mass Spectrometry
GSK-3ß	Glycogen synthase kinase-3 beta
GST	Glutathione-S-transferase
HCAs	Heterocyclicamines
HDAC	Histone deacetylases
HNPCC	Hereditary nonpolyposis colorectal cancer
HPLC-DAD	High-Performance Liquid Chromatography with Diode Array Detection
ITCs	Isothiocyanates
KRAS	Kirsten Ras
LGR5	Leucine-rich repeat-containing G-protein coupled receptor 5
MAPK	Mitogen-activated protein kinase

MMP	Matrix metalloproteinase
MSI	Microsatellite instability
MTS	3-(4,5-dimethylthiazol-2-yl)-5-(3-carboxymethoxyphenyl)-2-(4-sulfophenyl)-2H-tetrazolium, inner salt
NF-kB	Nuclear factor kappa B
NOCs	N-nitroso compounds
PAHs	Polycyclic aromatic hydrocarbons
PBS	Phosphate Buffered Saline
PEITC	Phenethyl isothiocyanate
PenStrep	Penicillin and streptomycin
Ptch	Patched
ROS	Reactive oxygen species
RPMI 1640	Roswell Park Memorial Institute 1640
RNA	Ribonucleic acid
RNS	Reactive nitrogen species
$ScCO_2$	Supercritical carbon dioxide
SFE	Supercritical fluid extraction
SFN	Sulforaphane
Smo	Smoothened
PI	Propidium Iodide
qPCR	Real-time quantitative polymerase chain reaction
TCF	T-cell factor
TP53	Tumor protein p53

1. Introduction

1.1. Large Intestine: anatomy and physiology in brief

The large intestine is part of the gastrointestinal system and comprises the colon, a muscular tube with approximately 5 feet long responsible for the absorption of water and nutrients during digestion, and the rectum, a final extension of the large intestine with about 6 inches through which the fecal matter resultant from digestion is excreted from the anus, see Figure 1.1.A. The colon is sectioned into four main regions named: the ascending, transverse, descending and sigmoid colon, with the latter connecting the colon to the anus, as depicted in Figure 1.1.A. The colon region comprising collectively the ascending and transverse regions is denominated as the proximal colon, whereas the region involving the descending and sigmoid colon is designated as the distal colon (American Cancer Society., 2014).

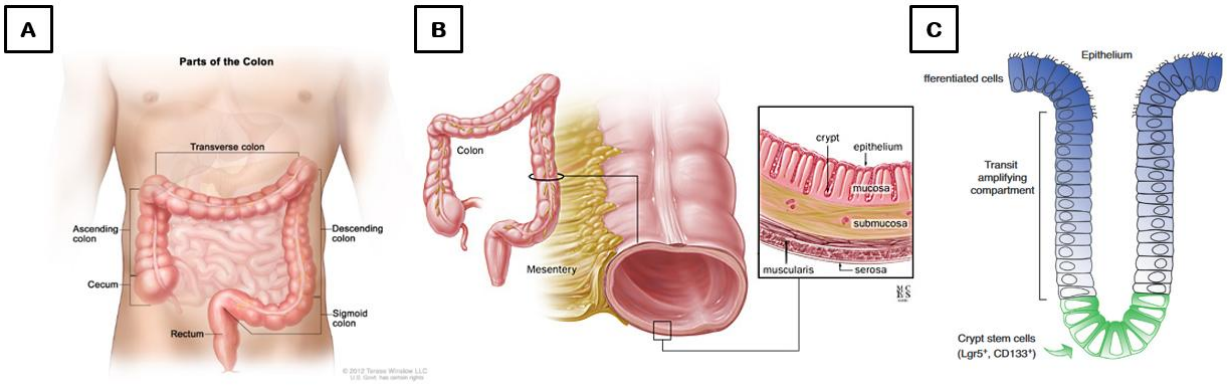

Figure 1.1. ***Illustration of the large intestine sections***. **(A)** Proximal region comprises the ascending and transverse colon, while distal region englobes the descending and sigmoid colon. **(B)** Colon wall architecture, with colonic crypts embedded in the mucosa layer. **(C)** Colonic crypt with stem cell population residing at the base of the crypt and progenitor cells migrating and differentiating in the upward direction, towards the intestinal lumen. Adapted from (Degirolamo et al., 2011; Hepatology., 2016; National Institutes of Health, 2016).

As part of the gastrointestinal tract, its wall's architecture encompasses four layers, namely: the serosa, the muscularis, the submucosa and the mucosa. This latter layer is then subdivided in three sublayers: the muscularis mucosa, the lamina propria and the epithelium, as shown in Figure 1.1.B. In turn, the epithelium, consisting in a single layer of columnar epithelial cells (including enterocytes, goblet cells and endocrine cells), folds into finger-like invaginations so-called the colonic crypts, as depicted in Figure 1.1.B-C. (Fredericks, 2015; Humphries and Wright, 2008; Vaiopoulos et al., 2012). In the bottom of these crypts resides a subpopulation of intestinal stem cells responsible for the renewal of the epithelium (Fredericks, 2015; Humphries and Wright, 2008; Vaiopoulos et al., 2012). The intestinal stem cells perform asymmetric division, undergoing self-renewal alongside with generation of a population of progenitor cells that migrate upwardly in the crypt, proliferate and differentiate into goblet, columnar, among other cell types (Boman and Huang, 2008; Vaiopoulos et al., 2012). However, due to their high proliferation rate, both stem cells and progenitor cells are prone

to acquire mutations and undergo malignant transformation towards colorectal cancer (Huels and Sansom, 2015).

1.2. Epidemiologic scenario: incidence and mortality of colorectal cancer

Colorectal cancer is classified as the third most common cause of mortality worldwide and the fourth leading cause in the ranking of the cancer-related deaths. The incidence of this pathology rises with increasing age, being the age range from 40 to 50years the most critical for colorectal cancer incidence. Notwithstanding, there is a significant difference in incidence between genders, having males the highest incidence rate of colorectal cancer in comparison to females (Ait Ouakrim et al., 2015; Favoriti et al., 2016).

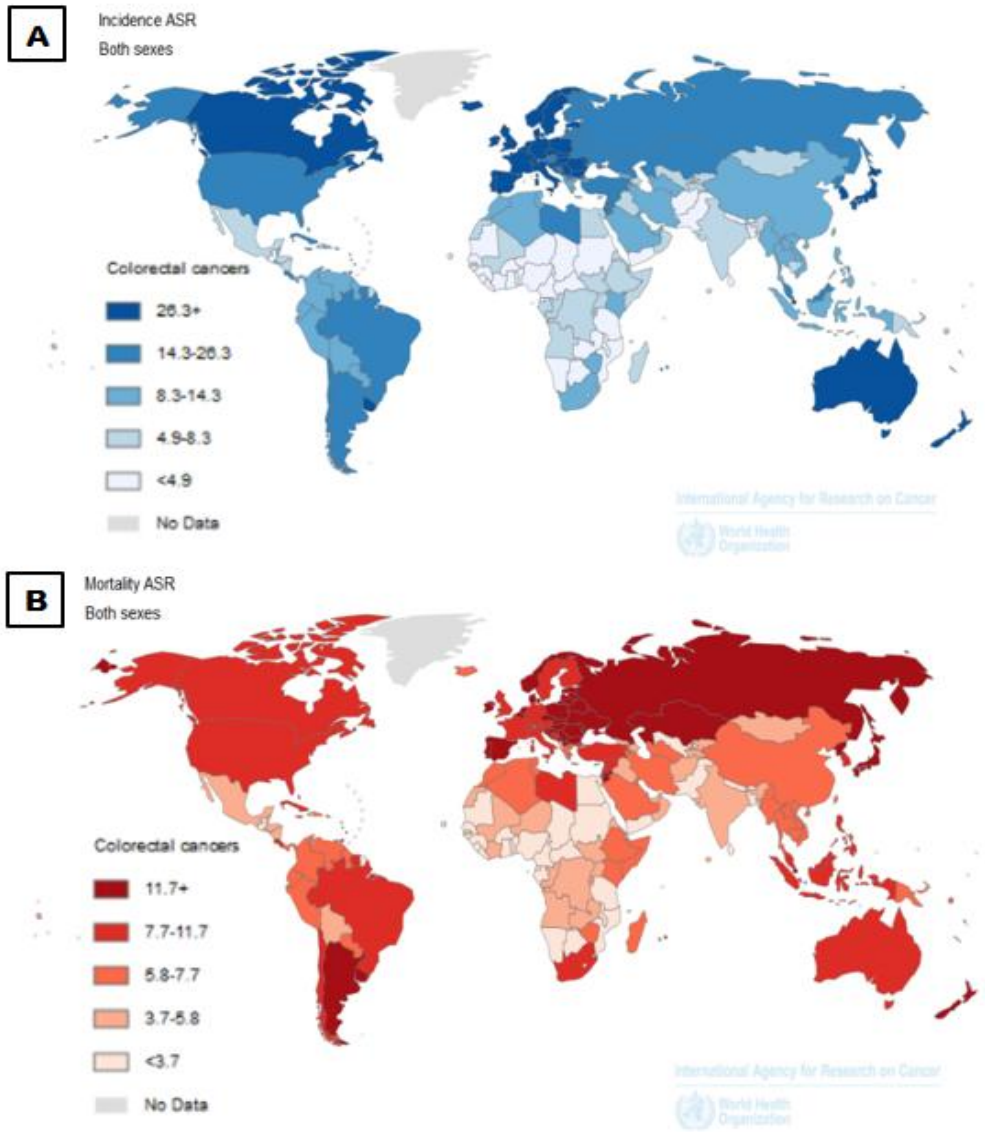

Figure 1.2. ***Worldwide colorectal cancer incidence and mortality rates in age-standardized rate (ASR), per 100.000 individuals of the world standard population, estimated in 2012.*** **(A)** Colorectal cancer incidence. **(B)** Colorectal cancer mortality. Adapted from (GLOBOCAN, 2012).

The disparity in the geographical distribution of colorectal cancer burden can be correlated with the human development index of the countries, with the more developed countries accounting for more than two-thirds of diagnosed cases (Arnold et al., 2016). Moreover, this discrepancy can also be associated not only with the environmental exposure and different dietary habits inherent to the geographic area, but also with the genetic background and/or higher genetic susceptibility (Favoriti et al., 2016). Nonetheless, there has been an increasing trend in the incidence of colorectal cancer in the developing countries that can be correlated with the acquisition of western lifestyle habits (Arnold et al., 2016; Favoriti et al., 2016).

Given the growth and increasing life expectancy of the world's population, as well as the acquisition of unhealthy lifestyle habits, the global burden of colorectal cancer is estimated to increase to almost 2.5 million cases and 1.3 million deaths by 2035 (Favoriti et al., 2016; GLOBOCAN, 2012).

1.3. Colorectal cancer etiology

Colorectal cancer derives from the imbalance between normal cell growth and death in colonic epithelium. It can be described as the progression from a normal to dysplastic epithelium, to adenoma which then evolves towards a carcinoma and, eventually, to metastases. This stepwise progression known as "adenoma-carcinoma sequence", depicted in Figure 1.3, arises from the accumulation of genetic alterations. The adenoma-carcinoma sequence accounts for about 90% of all sporadic colorectal cancers, while the remaining 10% are attributed to the "serrated neoplasia pathway" (Fredericks, 2015).

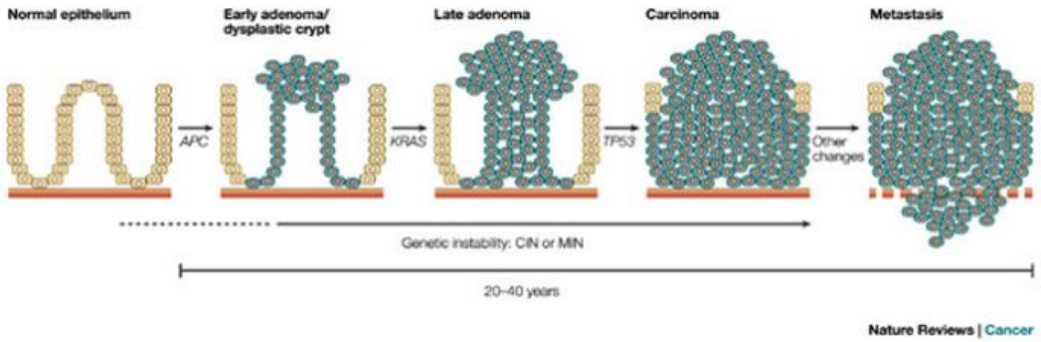

Figure 1.3. ***Adenoma-carcinoma sequence in colorectal cancer onset.*** Evolution from a normal mucosa to hyperplasia, followed by adenoma development (benign polyp) that culminates in the establishment of a carcinoma that, upon accumulation of mutations in critical genes, may metastasize to other organs. Adapted from (Rajagopalan et al., 2003).

Genomic instability driving colorectal cancer can be attributed to two major genetic phenomena: chromosomal instability (CIN) that accounts for up to almost 85% of colorectal cancers, and microsatellite instability (MSI) (Fredericks, 2015). In the most likely scenario of genetic instability, the CIN pathway, the colonic adenomas arise from mutations in the *APC* (Adenomatous polyposis coli)

tumor suppressor gene that lead to formation of dysplastic crypts (Cappell, 2008; Lamprecht and Fich, 2015) – Figure 1.3.

Mutations leading to dysfunctional APC protein consequently drive the deregulation of Wnt/β-catenin signaling pathway (Fredericks, 2015; Huels and Sansom, 2015). In this context, APC loss results in the translocation of β-catenin towards cell nuclei where it accumulates and binds to T-cell factor (TCF), prompting unrestrained transcription of target genes that control cell growth, proliferation and invasion (namely *Axin2, Cyclin D1* and *CD44*) (Fredericks, 2015) – see Figure 1.4.

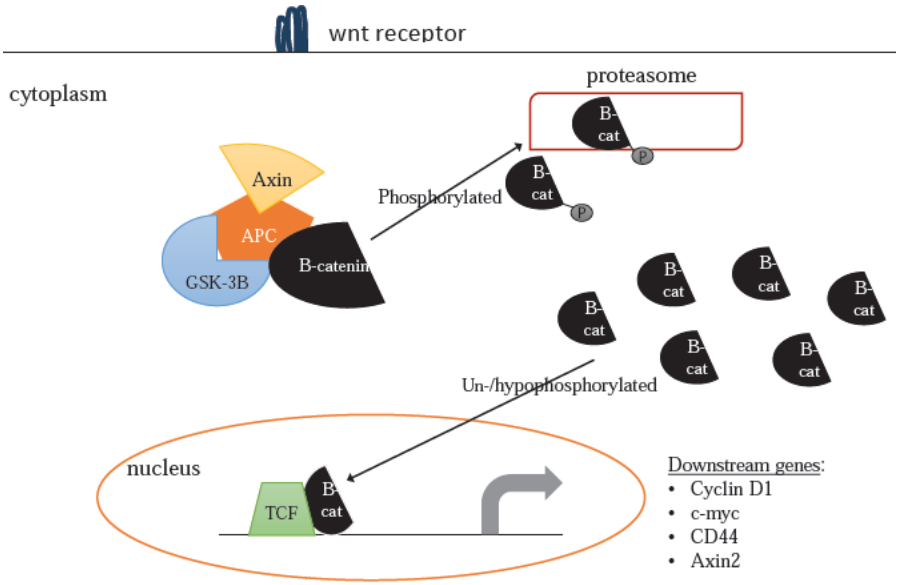

Figure 1.4. ***Wnt signaling pathway.*** In the absence of Wnt receptor ligands, β-catenin is phosphorylated and routed for proteasome degradation upon interaction with a multimeric complex composed by Axin, APC and Glycogen synthase kinase-3β (GSK-3β). Contrary, upon stimulation of Wnt receptors or in the case of mutated APC, β-catenin translocates towards cell nuclei where it interacts with TCF, activating the transcriptional expression of target genes. Adapted from (Fredericks, 2015).

Afterwards, the resultant mutant clone population can further acquire a more aggressive phenotype towards adenoma establishment upon additional mutations affecting oncogenes, like *KRAS* (Kirsten Ras), and tumor suppressor genes, like *TP53* (tumor protein p53) and *DCC* (Deleted in Colorectal Carcinoma) (Fredericks, 2015; Huels and Sansom, 2015; Humphries and Wright, 2008). Notwithstanding, epigenetic alterations, namely those prompted by deoxyribonucleic acid (DNA) methylation, can also contribute to the genetic instability of intestinal cells and to tumorigenesis, as proposed for the serrated neoplasia pathway (Jass et al., 2002).

Although normally adenomas remain benign, the accumulation of genetic alterations can drive them towards malignant transformation, i.e. to establishment of carcinomas (Cappell, 2008). In fact, every normal cell (either stem, progenitor or differentiated cell) has the potential to become the cancer cell of origin, as the result of successive mutations (Vaiopoulos et al., 2012). Thereby, two possible models of colorectal carcinogenesis have been suggested: the “top-down” and the “bottom-up” models (Huels and Sansom, 2015).

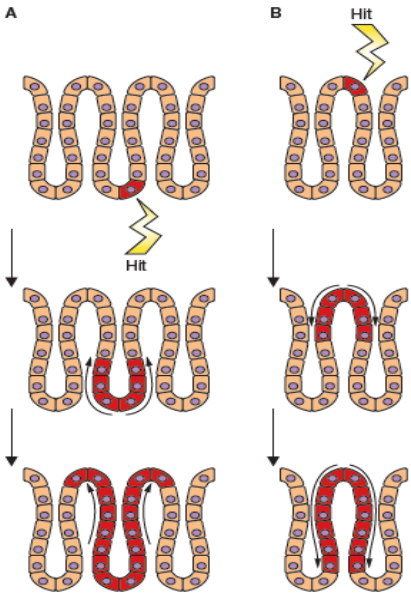

Figure 1.5. ***Proposed mechanisms for colorectal tumorigenesis*****. (A)** "Bottom-up" model assumes that genetic instability affects the intestinal stem cell niche. **(B)** "Top-down" model assumes that more differentiated cells affected by genetic mutations can propagate the mutated clones. Adapted from (McDonald et al., 2006).

The "top-down" model assumes that tumor begins at the top of the colonic crypt, with mutations affecting the differentiated or progenitor intestinal cells, resulting in tumor propagation in the lateral directions and downwards toward the crypt base (Huels and Sansom, 2015) - see Figure 1.5-B.

However, due to the rapid turnover of the colonic epithelial cells (in approximately 4-5 days these cells are shed from the colonic epithelium), the stem cell niche at the base of the crypt appears to be the most likely cancer cell origin in colorectal carcinogenesis. In this context, the "bottom-up" model assumes that intestinal stem cells upon malignant transformation become the trigger for tumor onset, and spreading of mutant clone occurs upwards the crypt (Huels and Sansom, 2015), as represented in Figure 1.5-A. The propagation of the stem cell mutant clone eventually begins by replacing the normal cells inside the intestinal stem cell niche, a phenomena called niche succession. This event can then be followed by monoclonal conversion when the mutant stem cells take control of the crypt and end up filling the entire colonic crypt with their offspring (Humphries and Wright, 2008).

Several markers of the colorectal CSCs have been discovered. For instance, LGR5 (Leucine-rich repeat-containing G-protein coupled receptor 5) has demonstrated to modulate proliferation, migration and colony formation *in vitro* and to provide tumorigenic potential *in* vivo (Hirsch et al., 2014; Lin et al., 2015). Content of $LGR5^{+}$ cells also proved to correlate positively with invasiveness, lymph node and distant metastasis (Wu et al., 2012), as well as with resistance to common therapeutic agents (Liu et al., 2013b). Besides CD44 (CD44 molecule - Indian blood group), CD133 (Prominin-1) has also been proposed as a putative colorectal CSC marker, with application in clinical prognosis (Ren et al., 2013; Schneider et al., 2012; Wang et al., 2012).

Nonetheless, colorectal cancer can be classified based on its level of invasiveness. One of the most well-known classification scales is the Dukes' classification that stages colorectal cancer from A through D, as illustrated in Figure 1.6. In stage A, colorectal cancer penetrates beyond the muscularis layer into the submucosa. At initial stage B (B1) it crosses submucosa layer into the muscularis layer, and further progression beyond muscularis into serosa is classified as late stage B (B2). Upon reaching regional lymph node, colorectal cancer now in its metastatic phase, is rated as stage C. Further progression with establishment of metastases at distant organs (e.g. liver and lungs) is devised as stage D. More recently this classification system was upgraded to the "Tumor, Node, Metastases" (TNM) system, in which stage A and B1 correlate with stage I of TNM scale, and stage B2 and C correspond to stage II and stage III, respectively. The worst case scenario characterized by distant metastases in Dukes' D stage corresponds to TNM stage IV (Cappell, 2008).

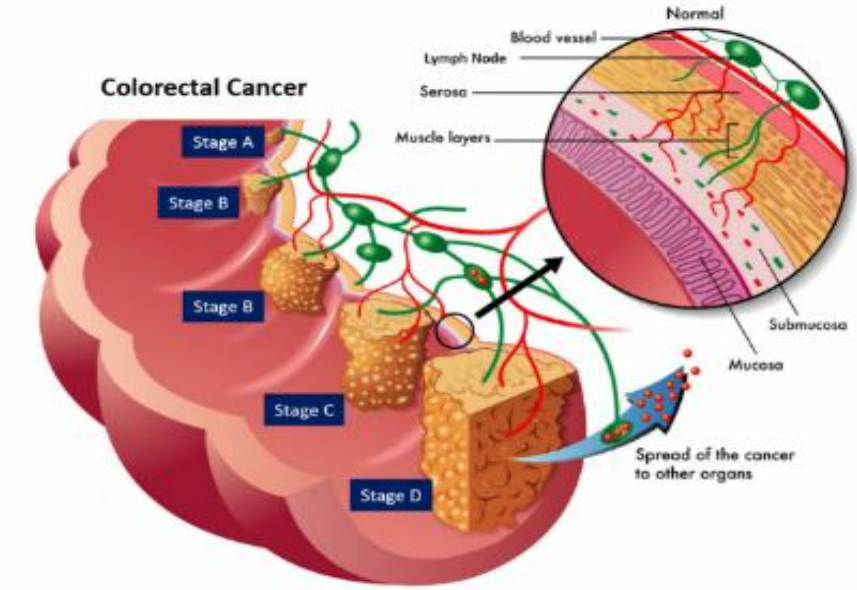

Figure 1.6. ***Colorectal cancer staging by Dukes' stratification.*** Adapted from (University., 2015).

1.3.1. Hallmarks underlying tumor development and progression

Regardless of the genetic instability pathway that drives tumorigenesis, there is a general consensus that all cancers are characterized by a plethora of molecular and cellular processes, so-called hallmarks, that sustain the malignant phenotype, summarized in Figure 1.7. These functional capabilities of cancer cells that endow them with an enhanced fitness encompass: sustained proliferation signaling, replicative immortality and evasion of growth suppressors (overall, eliciting unrestrained proliferation and tumor growth); evasion of immune destruction and apoptosis; activation of invasion and metastasis; angiogenesis induction and deregulation of cellular energetics (Hanahan and Weinberg, 2011).

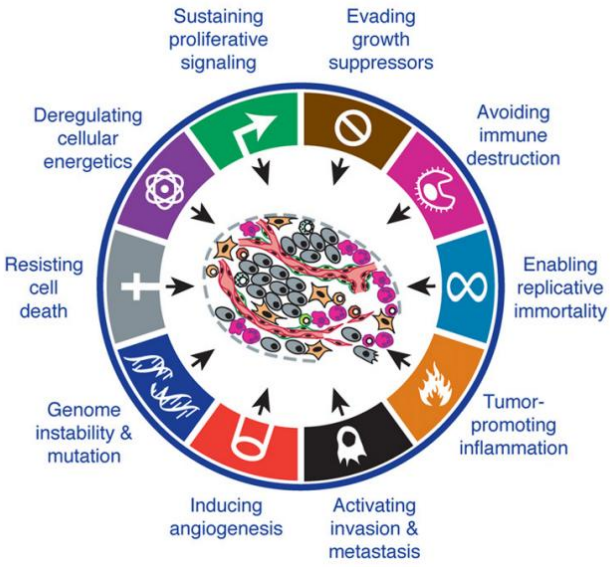

Figure 1.7. *Cancer hallmarks*. Adapted from (Hanahan and Weinberg, 2011).

To note that, due to their intrinsic self-renewal capability and plasticity, colorectal CSCs can contribute to all of cancer hallmarks, and hence to tumor establishment and progression (Mathonnet et al., 2014; Vaiopoulos et al., 2012; Zeuner et al., 2014).

1.3.2. Deregulation of signaling pathways in colorectal CSCs

The intestinal homeostasis, resultant from the balance between cell proliferation, differentiation, migration and self-renewal, is tightly controlled by a complex crosstalk network involving several signaling pathways, namely Wnt/β-catenin, Hedgehog and Notch pathways. However, in colorectal cancer the genetic instability imposed to precursor cancer cells may prompt the deregulation of these intricate signaling networks, with consequent unrestrained cell growth (Beachy et al., 2004).

Wnt/β-catenin signaling pathway

As already mentioned above, the Wnt/β-catenin signaling pathway modulates several crucial events in colorectal cancer onset by enhancing the expression of tumorigenesis “driver” genes, an event elicited by the accumulation of β-catenin in the presence of a dysfunctional APC protein (please review Figure 1.4.). Upon stimulation of Wnt ligand receptors, β-catenin is no longer degraded by proteasomes and accumulates in cytosol. After shuttling towards nucleus, β-catenin interacts with TCF forming a complex that functions as a transcriptional activator of Wnt target genes, such as CD44, Axin2, cyclin D1 and *c-myc* (Brabletz et al., 2005; Krausova and Korinek, 2014).

Additionally, Wnt/β-catenin signaling pathway has been linked to epithelial-to-mesenchymal transition (EMT), in which cells lose their intercellular contact and become more “motile”, events that facilitate cell migration. β-catenin is generally associated to membranous E-cadherin, a known adhesion molecule. Translocation of β-catenin towards cell nuclei leads to the loss of membranous E-cadherin, as well as to downregulation of its expression, which decreases the epithelial cell phenotype and favors a more mesenchymal and motile one (Brabletz et al., 2005; Nelson and Nusse, 2004). Moreover, intra-nuclear β-catenin increases survivin expression, an anti-apoptotic protein that also induces cell proliferation (Salama and Platell, 2009).

Hedgehog signaling pathway

Another major signaling pathway involved in cancer growth, metastasis, CSC self-renewal and recurrence, is the Hedgehog pathway. In the absence of hedgehog ligands (Sonic Hedgehog, Desert Hedgehog and Indian Hedgehog) the respective transmembrane receptor Patched (Ptch) interacts with Smoothened (Smo) blocking its function. On the other hand, in the presence of the Hedgehog ligands the repression of Smo is relieved favoring the activation of Gli transcription factors that modulate the expression of cyclin D, EGF (Epidermal Growth Factor), among other genes (Hanna and Shevde, 2016), as illustrated in Figure 1.8.

Furthermore, Hedgehog-Gli1 signaling axis has been associated with the acquisition of a metastatic phenotype via EMT in colorectal cancer, despite promoting cell growth, survival and CSC self-renewal (Varnat et al., 2009).

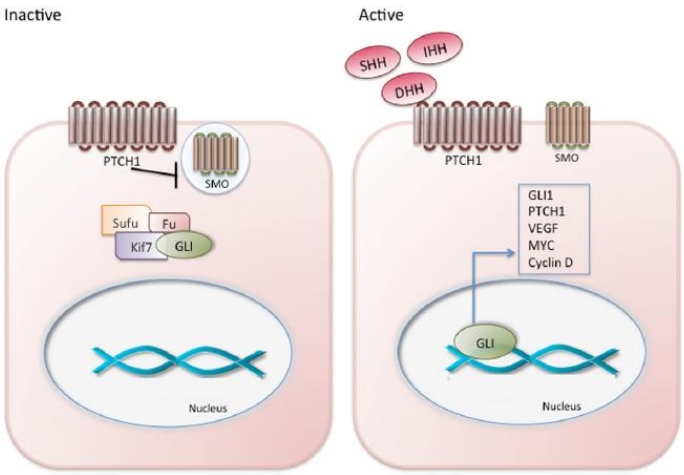

Figure 1.8. ***Hedgehog signaling pathway.*** Upon stimulation by receptor Ptch ligands, Smo inhibition is attenuated with consequent transcription activation of target genes (related to CSC self-renewal and cancer metastasis) by Gli. Adapted from (Hanna and Shevde, 2016).

Notch signaling pathway

Briefly, this signaling pathway is activated by direct cell-to-cell contact between a Notch ligand and a Notch membrane receptors, Notch and Delta. This interaction leads to the proteolytic cleavage of the intracellular domain of Notch (NICD) that shuttles to cell nuclei, where it interacts with transcription

factors and modulates the expression of numerous genes controlling cell proliferation, differentiation, apoptosis - e.g. c-myc, EGFR (Epidermal Growth Factor Receptor), cyclin D1, p21 and Nuclear Factor kappa B (NF-kB) (Qiao and Wong, 2009) - and EMT (e.g. Snail and Slug) (Espinoza et al., 2013).

1.4. Risk factors: lifestyle habits and genetic influence

The striking numbers of the incidence and mortality rates that follow colorectal cancer are in part due to various risk factors of different natures, namely genetic predisposition, history of inflammatory bowel disease, family history of colorectal cancer and/or lifestyle habits, among others.

A small portion of the colorectal cancer cases is derived from genetic syndromes. Individuals who suffer from inflammatory bowel disease, either ulcerative colitis or Crohn's disease, are more prone to develop colorectal cancer, since inflammation is one of the hallmarks of cancer as previously described. In the other hand, individuals that have family history of colorectal cancer affecting at least one first-degree relative have increased risk to develop this pathology. The most common inherited forms of colorectal cancers are familial adenomatous polyposis (FAP, that is inherited in an autosomal dominant way) and hereditary nonpolyposis colorectal cancer (HNPCC) (Haggar and Boushey, 2009).

One of the most critical factors that influence the development of colorectal cancer is diet. In fact, food consumption patterns are responsible for the majority of the colorectal cancer cases and, in this context, the adoption of a western diet (rich in animal derived-products and fats and poor in vegetables and fruits) has led to an increasing trend in the colorectal cancer incidence (Bishehsari et al., 2014). The high consumption of red and processed meats (e.g. beef and pork) has been associated to a higher risk of colorectal cancer, which can be resultant from the presence of potential mutagenic and carcinogenic compounds, namely N-nitroso compounds (NOCs), heterocyclicamines (HCAs), polycyclic aromatic hydrocarbons (PAHs) and heme iron. For instance, NOCs could be synthetized exogenously from nitrites, nitrates, amines or amides during meat processing (like it happens in bacon and sausages) (Aykan, 2015; Song et al., 2015). Moreover, NOCs can be also produced endogenously in the colon after consumption of these animal-derived products due to the presence of amines and amides in the colon originated from the amino acid decarboxylation performed by colon microflora. Additionally, HCAs and PAHs are produced from pyrolysis of meat during high temperature or open flame cooking (e.g. like grilling or barbecuing meat for too long) (Aykan, 2015). Red meats are highly rich in heme iron that is degraded in the small intestine. The resultant free ferrous iron can further promote carcinogenesis by intervening in endogenous production of NOCs, fat peroxidation, and oxidative stress which can subsequently induce genetic mutations and cytokines expression that incites inflammation (Aykan, 2015; Durko and Malecka-Panas, 2014; Song et al., 2015). Nonetheless, colorectal cancer can also be prompted by infectious pathogens acquired via red meat consumption, like *Fusobacterium nucleatum* that promote reactive oxygen and nitrogen species (ROS and RNS, respectively) production leading to colon inflammation (zur Hausen, 2012).

Despite the inconsistency among epidemiologic studies, one could not exclude the possible correlation between high intake of saturated animal fats and increase in colorectal cancer incidence (Pericleous et al., 2013). Diets rich in fats may enhance intestinal excretion of bile acids and modulate colon flora composition towards a pro-oncogenic microenvironment (Song et al., 2015).

Another risk factor is the regular consumption of alcohol whose metabolism leads to acetaldehyde production, a known carcinogenic agent that prompts DNA damage in a dose-dependent manner. Moreover, its regular consumption decreases the absorption of B vitamins, making cells more prone to oxidative stress (Durko and Malecka-Panas, 2014).

Other lifestyle habits, such as tobacco smoking, can be associated with increased colorectal cancer risk. Tobacco contains a plethora of carcinogens, including aromatic amines, NOCs, HCAs and PAHs that, upon metabolism via cytochrome P450, can induce mutations in crucial genes - e.g. *KRAS* and *BRAF* (B-Raf) (Durko and Malecka-Panas, 2014). Additionally, a sedentary lifestyle and obesity, two risk factors that may co-exist, are convincingly associated with increased incidence of colorectal cancer (Haggar and Boushey, 2009).

1.5. Management of colorectal cancer: therapeutic guidelines, drawbacks and cancer recurrence

Nowadays, colorectal cancer treatment is still very challenging due to cancer recurrence. The gold standard therapy for localized colorectal cancers (stage I and II) is surgical resection, but this approach often ends in tumor relapse within a few years after surgery. Moreover, for patients that have stage III or IV and reduced long-term survival, an adjuvant therapy based on radiation or chemotherapy is applied before surgery (Cappell, 2008; Dent et al., 2016; Hellinger and Santiago, 2006).

One of the most currently used chemotherapeutic agents in colorectal cancer therapy is 5-Fluorouracil (5-Fu) (Subramaniam et al., 2010). This drug has the ability to be incorporated into DNA instead of thymidine, thus inhibiting DNA replication and favoring cell death (Hammond et al., 2016). However, drug's biological effect may be counteracted due to drug efflux carried out by ATP-binding cassette transporters (ABC transporters) (Hlavata et al., 2012) and to Aldehyde Dehydrogenase (ALDH) activity, among other mechanisms (Abdullah and Chow, 2013).

Despite the efforts made so far, CSCs can prevail even after chemotherapy, explaining why colorectal cancer eradication is so difficult to attain and often results in a high incidence of tumor relapse (Mertins, 2014; Subramaniam et al., 2010). This chemo-resistant profile of colorectal CSCs has been demonstrated in some reports (Colak et al., 2014; Dylla et al., 2008).

Therefore, it is imperative to design therapeutic strategies targeting essential CSC-related processes, namely: developmental signaling pathways (like Wnt, Hedgehog and Notch); survival pathways (e.g. Phosphoinositide 3-kinase-Mammalian target of rapamycin axis, abbreviated PI3K-mTOR axis); evasion of apoptosis and chemo-resistance. Moreover, it seems also plausible to target components

involved in EMT, as well as surface CSC markers (Mertins, 2014; Vaiopoulos et al., 2012; Zeuner et al., 2014).

In this context, and based on the epidemiological data retrieved from nutrition patterns, natural bioactive compounds present in fruits, vegetables and other natural sources, arise has one appealing strategy to target colorectal cancer, including CSC niche, self-renewal and metabolism (Pistollato et al., 2015).

1.6. Natural compounds as potential therapeutic agents for colorectal cancer: lessons learned from the preventive role of nutrition

As highlighted above, diet is one of the crucial determinants accounting for colorectal carcinogenesis. Inversely, various dietary factors have demonstrated to have protective qualities against this pathology (Durko and Malecka-Panas, 2014). Evidences from epidemiological studies have established a positive correlation between plant-based dietary patterns and a lower risk of colorectal cancer, as reviewed by (Lanou and Svenson, 2010). More recently, after a follow-up study of about 7years with nearly 80.000 participants with different dietary patterns (encompassing non-vegetarianism, vegan diet, lacto-ovo-vegetarianism, pesco-vegetarianism and semi-vegetarianism), it was determined that in overall vegetarian diets are associated with a lower risk to develop colorectal cancer comparing with non-vegetarianism, and that pesco-vegetarianism correlates with a decreased risk comparing with non-vegetarianism (Orlich et al., 2015), observations consistent with the association between red meat consumption and risk of developing this pathology.

In fact, diets rich in vegetables, fruits, whole grains, spices and seeds have shown to counteract the incidence of colorectal cancer, and therefore naturally-occurring dietary compounds have been drawn attention due to their efficacy in colorectal cancer prevention and therapy (Lanou and Svenson, 2010; Pericleous et al., 2013; Song et al., 2015).

Hence, several phytochemicals, so called nutraceuticals, have been identified in these natural sources with the purpose of decrease the colorectal cancer incidence and slow its progression by targeting critical aspects of carcinogenesis, namely cell proliferation, differentiation, apoptosis, inflammation, angiogenesis and metastasis (Kuppusamy et al., 2014; Pan et al., 2011). Furthermore, nutraceuticals stand out by their capacity to modulate gene expression in colorectal cancer by acting at the epigenetic level, either by influencing DNA methylation, histone modification (by acetylation, methylation or phosphorylation) or micro-ribonucleic acid (micro-RNA) expression. Their potential to reverse epigenetic deregulation, or in other words, to reprogram the epigenome, may unveil new targets for colorectal cancer therapy and therefore the possibility of new therapeutic outcomes (Chang and Yu, 2016; Chen and Xu, 2010). Lastly, but more importantly, phytochemicals also have gain widespread attention by showing their potential in targeting the CSC sob-population (Pistollato et al., 2015).

In an oversimplified way, phytochemicals can be classified into: i) phenolics (including phenolic acids, flavonoids, stilbenes, coumarins and tannins); ii) carotenoids; iii) alkaloids; iv) nitrogen-containing compounds and v) organosulfur compounds (Liu, 2004), as depicted in Figure 1.9.

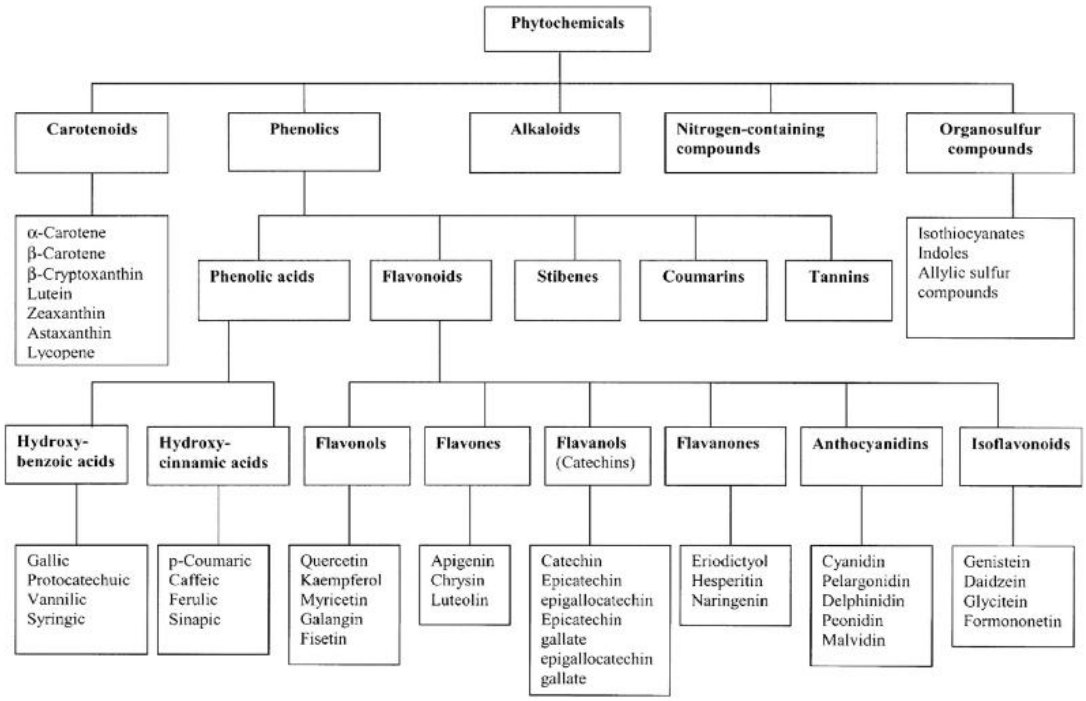

Figure 1.9. ***Classification of phytochemicals.*** Phytochemicals comprise carotenoids, phenolic compounds, alkaloids, nitrogen-containing compounds and organosulfur compounds. Some examples are listed for some categories. Adapted from (Liu, 2004).

Within the phytochemicals panel, phenolic compounds and carotenoids are the most well studied. Several phenolic compounds have been identified in numerous plant species and are resultant from plant metabolism. These plant secondary metabolites can be further subdivided in monophenolic or polyphenolic if they possess one or more aromatic rings in their structure, respectively, with one or more hydroxyl groups attached (Wahle et al., 2010). Among the natural sources of these compounds, apples, grapes, plums, cherries, strawberries and citrus fruits stand out due to their high content in phenolic compounds (Scalbert and Williamson, 2000).

On the other hand, carotenoids are fat-soluble pigments naturally present in yellow/orange vegetables and fruits (such as carrots, pumpkins, tomatoes, papayas and oranges) (Liu, 2004; Pan et al., 2011). These phytochemicals possess a 40-carbon structure of isoprene units, being characterized by their long series of conjugated double bonds that constitute the central portion of the molecule, which in turn can me cyclized at one or both ends, in addition to other degrees of complexity at structural level (Liu, 2004).

Last, but not least, organosulfur compounds are another main class of phytochemicals that is characterized by the presence of at least one atom of sulfur in their structure. These phytochemicals encompass allyl sulfur compounds (mostly present in garlic) and glucosinolates (typical of cruciferous

vegetables) (Gonzalez-Vallinas et al., 2013). The latter subclass will further be addressed in more detail in the following section.

In overall, phytochemicals have been demonstrated to have the ability to block carcinogenesis and impair tumor progression by inducing several responses, namely: modulation of gene expression (inhibiting and prompting the expression of oncogenes and tumor suppressor genes, respectively), signal transduction pathways; metabolic and detoxification systems; induction of apoptosis and of cell cycle arrest; inhibition of cell proliferation, angiogenesis and metastasis, besides exerting anti-inflammatory effects and counteracting oxidative stress (Araujo et al., 2011; Gonzalez-Vallinas et al., 2013; Kuppusamy et al., 2014; Liu, 2004; Pan et al., 2011; Priyadarsini and Nagini, 2012). Table 1.1. summarizes some of the most representative nutraceuticals and their anticancer effects reported in colorectal cancer.

Table 1.1. Representative nutraceuticals and respective anticancer mechanisms exposed in colorectal cancer.

	Natural compound	Proposed anticancer mechanism	Cancer model	Ref.
Phenolic compounds	Epigallocatechin Gallate (EGCG)	G1 cell cycle arrest; ↓cell proliferation; ↑apoptosis	HCT116, SW480	(Du et al., 2012)
	Resveratrol	G0/G1-S cell cycle arrest; ↓cell proliferation; ↑apoptosis	HT29	(Vanamala et al., 2010)
	Fisetin	↑apoptosis; ↓ cell growth	HT29	(Suh et al., 2009)
	Luteolin	↓chemo-resistance to oxaliplatin	SW480	(Qu et al., 2014)
Carotenoids	Lycopene	↓ cell growth; ↓cell proliferation	HT29	(Tang et al., 2008a)

1.6.1. Cruciferous vegetables as natural sources of nutraceuticals

Cruciferous vegetables can also be termed by *Brassica* vegetables, an ambiguity that derives from the fact that they descend from a family than can either be named *Cruciferae* or, alternatively, *Brassicaceae* (Higdon et al., 2007). This family englobes not only vegetables from the *Brassica* genus (e.g. broccoli, cauliflower, Brussels sprouts, cabbage, mustard, among others), but also watercress and wasabi, among other cruciferous vegetables belonging to others genus (Higdon et al., 2007; Kapusta-Duch et al., 2012).

According to the parallelism between high consumption of plant-derived foods and a lower risk in colorectal cancer, as already mentioned, also the intake of cruciferous vegetables has been associated with a decreased risk of colorectal cancer (Higdon et al., 2007; Marshall, 2008; Verhoeven

et al., 1996) (Wu et al., 2013a). In fact, the same trend has also been reported in gastric (Wu et al., 2013b), pancreatic (Li et al., 2015), bladder (Tang et al., 2008b), lung (Tang et al., 2010) and breast (Liu and Lv, 2013) cancers.

The chemo-preventive and therapeutic potential of these vegetables can be attributed to their phytochemical composition in phenolic compounds (namely phenolic acids, flavonoids and other polyphenols) and in organosulfur compounds (glucosinolates and their derivatives) (Mann and Khanna, 2013).

1.6.1.1. Phenolic compounds from cruciferous vegetables

Numerous phenolic compounds have been identified in cruciferous vegetables, including anthocyanins (a pigment that assigns a reddish or purplish color to some cruciferous vegetables, like red cabbage and purple cauliflower), flavonols (such as quercetin and kaempferol, and their derivatives) and Hydroxyacinnamic acids (e.g. p-coumaric acid, ferulic acid, caffeic acid and 3-O-Caffeoylquinic acid) and their conjugates, revised by (Cartea et al., 2011). Some studies have asserted the anticancer mechanisms prompted by phenolic compounds in colorectal cancer. For instance, Cho and Park reported the potential antiproliferative effect of kaempferol in HT29 cells, in which treatment with this bioactive compound has demonstrated to arrest cell cycle at G1 and G2/M phases by decreasing the levels of CDK2 and CDK4, as well as those of cyclin A, D1 and E (Cho and Park, 2013). Moreover, kaempferol has also demonstrated to induce apoptosis in HCT116 cells by the ATM-p53-Bax pathway, involving activation of caspase-3 and decrease in Bcl-2 protein levels (Wu et al., 2009). Likewise, the pro-apoptotic activity of quercetin was also reported in colorectal cancer cells, which was verified by the inhibition of NF-kB pathway, upregulation of Bax levels and downregulation of Bcl-2 levels (Zhang et al., 2015). Additionally, quercetin has demonstrated to inhibit migration and invasion in Caco-2 cells by inhibiting Toll like receptor 4 (TLR4)/NF-kB pathway, confirmed by the downregulation of matrix metalloproteinase-2 and -9 (MMP-2 and MMP-9, respectively) and upregulation of E-cadherin (Han et al., 2016).

1.6.1.2. Glucosinolates, the precursors of isothiocyanates (ITCs)

Nonetheless, the chemo-protective effects of cruciferous vegetables are mainly resultant of their relatively high content of glucosinolates (Verhoeven et al., 1996). These compounds occur naturally in these plants being responsible for their natural defense against insects, as well as by their peculiar bitter taste to the consumer, which leads to some consumer's resistance to include cruciferous vegetables in diet (Drewnowski and Gomez-Carneros, 2000).

The general structure of glucosilonates comprises a β-D-thioglucose group, a sulfonated oxime group and a variable side chain. Although these compounds are biologically inert, they can be converted into

more bioactive products – namely ITCs or indoles – by a hydrolysis reaction catalyzed by myrosinase (Cheung and Kong, 2010; Lynn et al., 2006), as depicted in Figure 1.10. In fact, ITCs are the main bioactive compounds in cruciferous vegetables that are responsible for their chemo-preventive activity in colorectal cancer (Lynn et al., 2006). Regardless of, since myrosinase and glucosinolates exist in different compartments of plant cells (i.e. in external surface of plant cell wall and in cytoplasm, respectively), the hydrolysis reaction only occurs when the plant tissue is disrupted (either by chewing or chopping cruciferous vegetables during culinary processing) (Cheung and Kong, 2010; Lynn et al., 2006). However, ITCs absorption derived from the consumption of cruciferous vegetables can also be attained through the activity of the gut microflora, a reaction catalyzed by β-thioglucosidase (Navarro et al., 2011). In Figure 1.10. are represented the general conversion of glucosinolates into ITCs, as well as examples of the more representative ITCs, namely Phenethyl isothiocyanate (PEITC), Sulforaphane (SFN) and Allyl isothiocyanate (Allyl ITC).

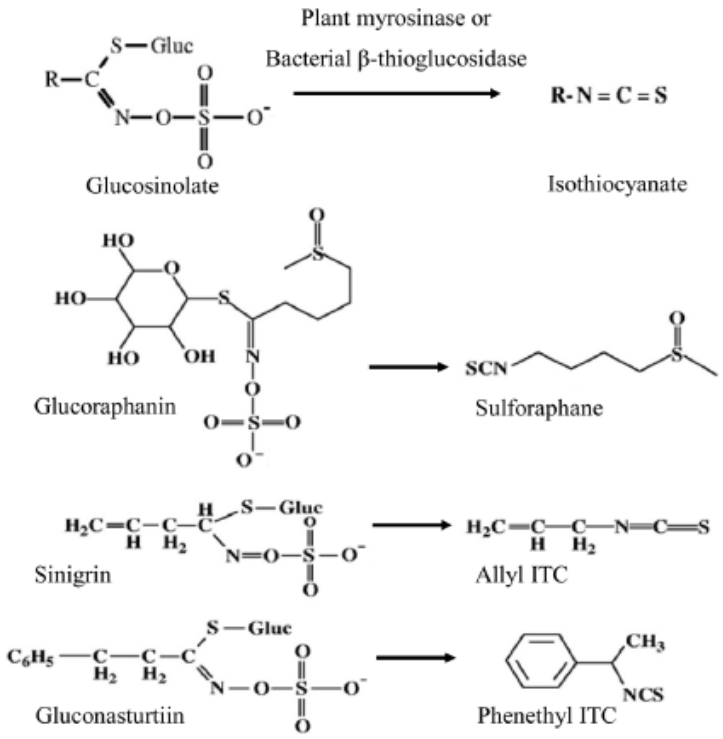

Figure 1.10. ***Conversion of glucosinolates into corresponding ITCs*****.** Adapted from (Navarro et al., 2011).

Once ingested or generated in the gut lumen, ITCs can cross the intestinal epithelial barrier and capillary endothelium by passive diffusion (Wu et al., 2009). Upon uptake by passive diffusion, ITCs are metabolized *in vivo* by the mercapturic acid pathway, in which they are initially conjugated with glutathione in a reaction that is catalyzed by glutathione-S-transferase (GST). Then, the resultant glutathione conjugates undergo consecutive enzymatic modifications that culminate in the generation of mercapturic acids, eventually excreted in urine (Lampe and Peterson, 2002; Wu et al., 2009; Zhang, 2012). Due to their metabolism pathway, ITCs have been implicated in the modulation of the expression of biotransformation enzymes involved in xenobiotic metabolism - namely in the

upregulation of phase II enzymes, such as GST - by increasing the expression of genes that contain an antioxidant response element (ARE) (Higdon et al., 2007; Lampe and Peterson, 2002).
Nonetheless, although ITCs have been implicated in the modulation of cellular processes in colorectal cancer, exemplified in Table 1.2., until today there is no evidence of ITCs biological effect in colorectal CSCs. However, some studies report SFN anticancer effect in CSCs of other solid tumors, namely in breast (Li et al., 2010b) and pancreatic cancer (Li et al., 2013).

Table 1.2. ***Representative ITCs and respective anticancer mechanisms exposed in colorectal cancer.***

ITC	Proposed anticancer mechanism	Cancer model	Ref.
PEITC	G1 cell cycle arrest [↓cyclin A, D, E – by p38/Mitogen-activated protein kinase (MAPK) activation]	HT29	(Cheung et al., 2008)
	↓migration and invasion	HT29	(Lai et al., 2010)
	↑apoptosis; ↑tumor regression	HCT116	(Roy et al., 2013)
SFN	↑DNA damage; ↑Apoptosis	HCT116 p53KO	(Rudolf and Cervinka, 2011)
	Metaphase and subG1 cell cycle arrest; ↓cell growth; ↑apoptosis	Primary cell lines of colon cancer; SCID mice	(Chen et al., 2012)
	↓cell proliferation	HT29, HCT116, LoVo, DLD-1	(Baenas et al., 2015) (Chung et al., 2015)
	↓cell growth and proliferation; ↑apoptosis	SW620	(Andelova et al., 2007)
	↓Histone deacetylase (HDAC) activity; ↓cell growth	HCT116	(Myzak et al., 2004)
	G2-M Cell cycle arrest (↑cyclin A and B1); ↑ apoptosis	HT29	(Gamet-Payrastre et al., 2000)
	↓migration; ↓angiogenesis	HCT116	(Kim et al., 2015a)
Allyl ITC	↓invasion/migration ⇨ ↓metastasis	HT29	(Lai et al., 2014)

1.7. Taking advantage from nature for colorectal cancer therapy: Therapeutic insights

1.7.1. Natural extracts and bioactive compounds in colorectal CSCs: *quo vadis*?

Although dietary modification might be a promising preventive measure to reduce the global burden of this pathology, the intake of nutraceuticals in daily diet may not be sufficient to counteract the carcinogenesis process. Indeed, several factors can explain the limitations inherent to uptake and/or absorption of ITCs through diet, some of which are referred below. For instance, ITC content in cruciferous vegetables may decrease significantly during cooking due to the volatility of some ITCs that may experience hydrolysis at high temperatures (Wu et al., 2009). Moreover, myrosinase enzyme

involved in glucosinolates hydrolysis can also be inactivated at high temperatures during some cooking procedures (Higdon et al., 2007). Another factor contributing to the bioavailability of ITCs is dependent on the individuals *per se*, since the conversion of glucosinolates into ITCs by the gut microflora might be dependent on interactions of the diurnal cycles of individual's microbiota metabolism with daily cycling of human enzymes, which can explain the low efficiency of glucosinolates conversion into ITCs (Fahey et al., 2012). Besides the hydrolysis by colon microflora, as well as the amount of cruciferous vegetables intake, the inter-individual differences may also be influenced by the intensity/time of mastication and by individual's genetic variations in enzymes involved in ITCs metabolism (e.g. in GST) (Lampe and Peterson, 2002). Therefore, individuals possessing GST polymorphisms rendering a reduced GST activity will have ITCs with longer half-lives in circulation and, hence, an enhanced chemo-protective effect (Lampe and Peterson, 2002).

Overall, the possible conjunction of some or all the above-mentioned factors might not provide the attainment of a therapeutic concentration through the daily diet, capable of exercising anticancer effects.

Therefore, to circumvent the limitations of ITCs natural uptake, there is an urgent need to develop new processes enabling the efficient and selective recovery of these valuable phytochemicals. Over time, several extraction techniques have been developed towards the generation of extracts from natural sources, like fruits and vegetables, namely solvent extraction, pressurized liquid extraction (PLE), supercritical fluid extraction (SFE), among other procedures, well revised in (Gil-Chávez, 2013).

1.7.1.1. Extracting bioactive compounds from natural sources: High-pressure extraction allied to "green" technology

Conventional solvent extractions often offer several drawbacks, namely higher environmental pollution, long extraction periods and utilization of hazardous organic solvents, which is a limiting factor when considering food and pharmaceutical industries. This rises the need for developing alternative "green" technologies, in order to substitute the conventional extraction methods (Chemat et al., 2012; Herrero et al., 2013).

In this context, high-pressure based technologies have been emerged towards the concept of a "green"-based technology, i.e. ensuring the generation and recovery of more "clean" bioactive compounds from natural matrices by reducing energy consumption (e.g. using moderate temperatures) and introducing the use of non-toxic solvents, while providing higher extraction yields, higher selectivity and shorter extraction periods (Chemat et al., 2012; Gil-Chávez, 2013; Herrero et al., 2013; Pereira and Meireles, 2009).

As a high-pressured based process, SFE has been applied in food, pharmaceutical and chemical industries for the extraction of natural compounds from plants and other natural matrices, since it can be an environmentally friendly technology (Chemat et al., 2012; da Silva et al., 2016; Gil-Chávez, 2013; Pereira and Meireles, 2009). Briefly, this extraction process consists in the extraction of soluble compounds from a solid matrix using a supercritical solvent, followed by the separation of these compounds from the supercritical solvent after system decompression (da Silva et al., 2016; Pereira

and Meireles, 2009). This extraction methodology utilizes supercritical fluids, which above their critical point display both liquid and gas properties. One of the more widely used supercritical solvents is carbon dioxide (CO_2) that offers less expensive and safer extractions, since it is recognized by EFSA (European Food Safety Authority) and by FDA (U.S. Food and Drug Administration) as a "generally recognized as safe" solvent (GRAS solvent). Besides, since it utilizes a moderate critical temperature (attained at 31.1ºC at a pressure of 7.39MPa) it ensures minimal alteration of the bioactive compounds, as well as of their functional properties. Moreover, since CO_2 is a gas at room temperature and pressure, the recovery of the compounds is easier and solvent-free, upon system depressurization (da Silva et al., 2016; Gil-Chávez, 2013; Herrero et al., 2013).

Although CO_2 supercritical fluid is compatible with the extraction of lipophilic compounds (e.g. lipids and essential oils), due to CO_2 low polarity the extraction of more polar compounds requires the utilization of a co-solvent, like ethanol, to increment and enrich the extracts with polar compounds (such as phenolic compounds) by modifying the solubility of the target compounds in the supercritical fluid (Gil-Chávez, 2013; Pereira and Meireles, 2009).

Although still in its infancy, the application of high-pressure extraction to extract target compounds from cruciferous vegetables has gained attention in the last years. By applying SFE for the generation of broccoli leaves extracts from different cultivars, Arnaiz and co-workers were able to characterize and identify the fatty acid content of different varieties of broccoli (Arnáiz et al., 2011). Wu and colleagues also succeeded in extracting Allyl ITC from horseradish, using CO_2 supercritical fluid extraction (Wu et al., 2009). It was also reported Allyl ITC CO_2-supercritical fluid extraction from wasabi (Li et al., 2010a). Moreover, it was also reported the extraction of glucosinolates and phenols from rocket salad, using water as a co-solvent (Solana et al., 2016).

Moreover, our group has recently developed a green and sustainable high-pressure extraction process to recover PEITC and/or phenolic compounds from watercress, while assuring high selectivity for ITCs and a high recovery yield. *In vitro* assays revealed promising antiproliferative effects of PEITC-rich watercress extracts in colorectal cancer cells, an effect that was further enhanced in the presence of phenolic compounds (Rodrigues et al., 2016).

Until now, very few studies have explored the anticancer potential and mechanisms of ITCs in colorectal cancer, especially regarding their action in colorectal CSCs.

1.8. Cell models for cancer research

Drug development is a highly complex and stepwise process, englobing the identification of a potential therapeutic compound, its preclinical testing (recurring to *in vitro* and *in vivo* studies) and ultimately its clinical testing in humans (encompassing several stages of clinical trials). Besides the current efforts to attain effective chemotherapeutic agents, the rate of success is still very disappointing, due to lack of clinical efficacy in parallel with unacceptable toxicity. Clinical testing is one of the most time-consuming and expensive phases of the drug development process, raising the need to discard the less

promising compounds even prior to animal experimentation (Breslin and O'Driscoll, 2013; LaBarbera et al., 2012).

Thus, preclinical testing arises as one of the most critical stages during drug development process. In fact, the development of *in vitro* cell models that best contribute to the understanding of the therapeutic response (in terms of pharmacokinetic, pharmacological and cytotoxic profile) is one of the goals of the pharmaceutical industry in the field of cancer research. *In vitro* studies play a crucial role in preclinical testing and the development of cell models that best mimic the target tissue, i.e. tumor microenvironment, has becoming an imperative need (Breslin and O'Driscoll, 2013).

1.8.1. Conventional *in vitro* cell models and their limitations

Several human cell lines derived from colorectal cancers, at different cancer stages and with different genetic profiles, are commercially available for cancer research. Indeed, conventional experiments using colorectal cancer cell lines provide a powerful tool to elucidate the complex signaling network that its inherent to tumorigenesis (Golovko et al., 2015).

Usually these cell lines are cultured in two-dimensional (2D) systems, i.e. by recurring to artificial plastic surfaces where cells attach and proliferate towards the formation of a cell monolayer (Amann et al., 2015; Breslin and O'Driscoll, 2013). Although 2D cell culture offers a convenient and less expensive approach for *in vitro* screening of the drug's biological effect, this cell model presents several limitations that derive from the culture system itself. Indeed, the surrounding cell microenvironment strongly influences its cellular behavior in terms of proliferation, differentiation and metabolism (Amann et al., 2015; Golovko et al., 2015; Rimann and Graf-Hausner, 2012).

Cells growing in monolayers fail one of the most characteristic features of solid tumors, since they do not generate a three-dimensional (3D) cellular structure (Hickman et al., 2014). Consequently, since monolayers do not translate the 3D architecture of the tumor, they do not recapitulate the functional, cellular and genetic heterogeneity of human solid cancers, a main feature when considering therapeutic resistance. Moreover, 2D systems do not allow to mimic the *in vivo* cellular morphology, polarity, receptor and oncogene expression, and also interaction with extracellular matrix (ECM) components and tumor stroma (Breslin and O'Driscoll, 2013; Golovko et al., 2015; Hickman et al., 2014).

On the other hand, it is also possible to culture human colon tissue samples (obtained by colonoscopy biopsy or surgical resection) in the form of 3D organoids (Golovko et al., 2015).

1.8.2. 3D cell models

More recently, efforts have been made towards the development and optimization of 3D cell models in an attempt to better recapitulate the *in vivo* tumor cellular and functional behavior, circumventing the limitations of 2D cell models, already described. In this context, multicellular tumor spheroids, hereinafter only called spheroids, have shown to be a promising *in vitro* 3D approach for cancer

research by allowing to study protein interactions, cellular signaling, gene expression and cellular processes (LaBarbera et al., 2012).

By fulfilling several cellular and functional parameters, 3D cell models fill the gaps between *in vitro* and *in vivo* studies. For instance, cancer cells cultured under a 3D system may present differences in cell morphology, alignment and polarization, as well as in cell differentiation. Inversely to what happens in 2D cell models in which monolayer-derived cells are more prone to apoptosis, cells grown in a 3D culture system present enhanced cell viability prompted by intercellular interaction (an important feature when considering cellular response to potential drugs). Moreover, cell's response to stimuli (either drug treatment, radiation exposure or growth factor stimulation), cellular metabolism upon drug treatment, as well as gene expression and protein synthesis, can also be influenced depending on the cell culture approach (Gupta et al., 2016).

Regarding tumor spheroids, all the prior characteristics can be derived from their specific architecture, encompassing complex cell-cell and cell-matrix interactions. When spheroids reach a mean diameter of 500µm a hierarchy of pathophysiological gradients (regarding oxygen and nutrients bioavailability and catabolites accumulation) is established, as depicted in Figure 1.11.A-B (Hirschhaeuser et al., 2010; LaBarbera et al., 2012).

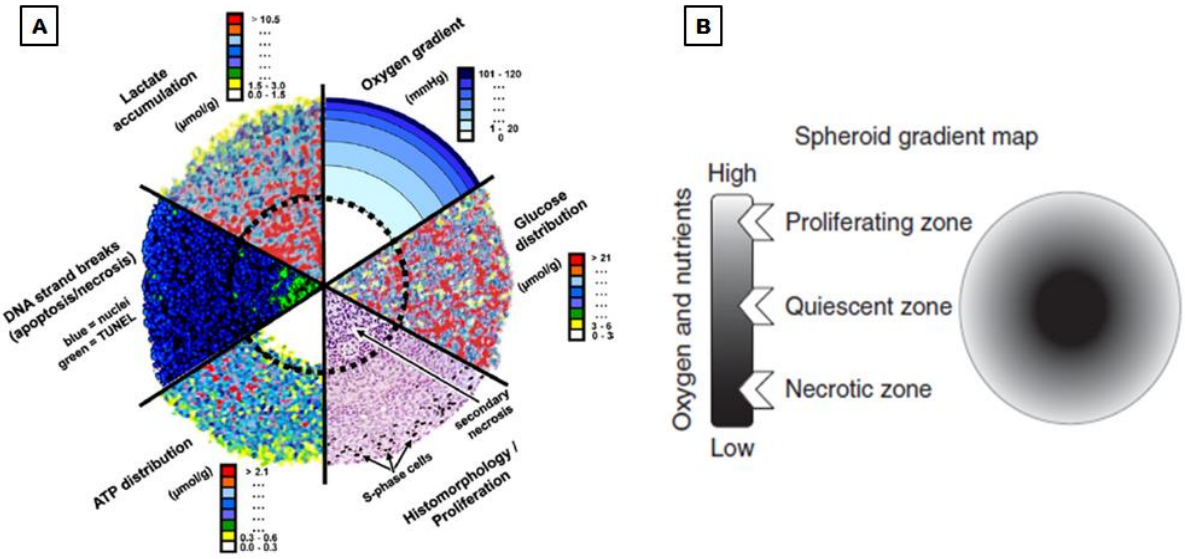

Figure 1.11. *Spheroid characterization*. (A) Combinatory layout of a cell spheroid gathering analytical images of spheroid median sections obtained by different technologies (tunnel assay, bio-luminescence imaging and probing with oxygen microelectrodes). A concentric organization of cell proliferation, cell cycle staging and viability is possible to observe. **(B)** Spheroid hierarchy in terms of cell viability and proliferation, according to oxygen and nutrient bio-availability. Adapted from (Hirschhaeuser et al., 2010; LaBarbera et al., 2012).

At this stage, tumor spheroids are composed by a central necrotic core, by an intermediate inner layer named quiescent zone and by an outer layer termed proliferating zone - Figure 1.11.B. These gradients reflect the *in vivo* tumor hierarchy, in which actively proliferating cells of the spheroid outer layer mimic the tumor cells adjacent to capillaries, whereas those of the spheroid quiescent zone

mimic the most inner tumor cells that eventually die via apoptosis, depending on the oxygen and nutrient bioavailability (Hirschhaeuser et al., 2010; LaBarbera et al., 2012).

In an oversimplified way, the methods of 3D cell culture can be classified into four major categories: non-adherent surface method, stirred culture method, scaffolds or matrices, and microfluidic method (Breslin and O'Driscoll, 2013; Gupta et al., 2016).

The non-adherent surface method, also known as liquid overlay technique, encompasses the forced-floating and the hanging drop methods, in which the culture vessel is subject to a non-adherent coating (like the one promoted by agarose), in order to prevent cells attachment to the substrate (Breslin and O'Driscoll, 2013; Katt et al., 2016). In the hanging drop method (Figure 1.12-A), the plate is inverted after cell seeding and the small cell suspension volume turns into a hanging drop. Gravity leads cells to concentrate and to aggregate at the tip of the drop, where upon continuous proliferation a spheroid is formed. In the forced-floating method (Figure 1.12-B), cells are seeded and centrifuged to promote cell co-localization and cell-cell contacts, with subsequent cell aggregation and spheroid formation (Breslin and O'Driscoll, 2013; Gupta et al., 2016; Katt et al., 2016).

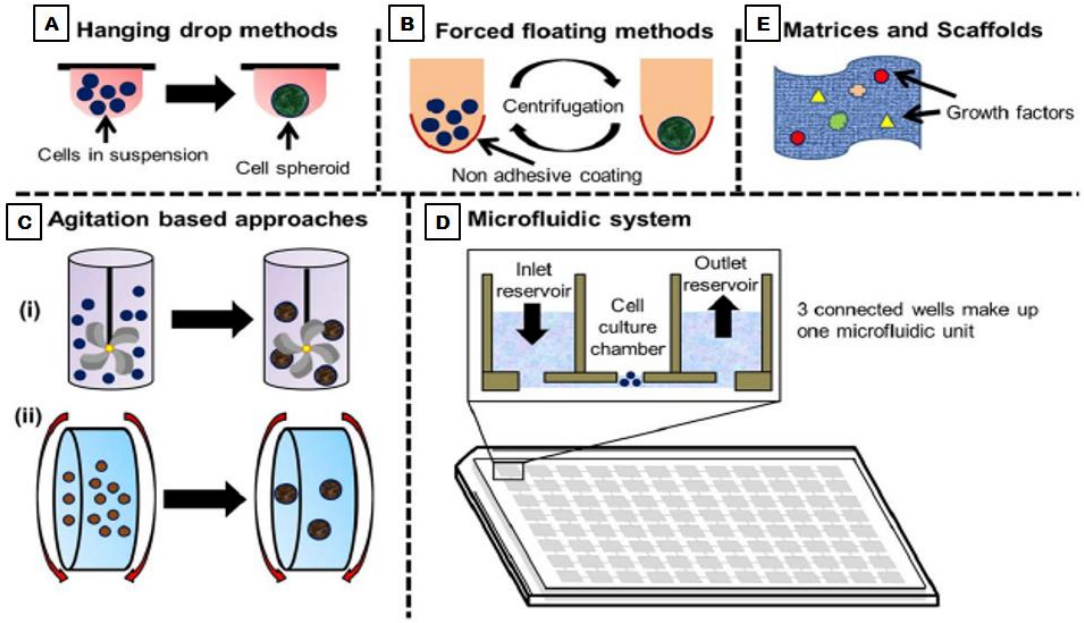

Figure 1.12. ***Spheroid-forming methods in 3D cell culture*** *(Gupta et al., 2016)*.

In stirred culture (Figure 1.12-C), such as that promoted by spinner flask bioreactors and rotating bioreactors, cells are maintained in suspension through constant agitation that also provides nutrients and removal of waste products (Gupta et al., 2016). The main difference between the two is that, in the spinner vessels agitation is promoted by a spinner bar, whereas in the rotating bioreactors the whole container is subject to rotation leading to a lower sheer force. Stirred bioreactors have also been coupled to perfusion systems, allowing constant cell feeding with culture medium (Gupta et al., 2016).

In microfluidics-based culture (Figure 1.12-D) the microenvironment is controlled by a continuous perfusion system, i.e. by adjustment of fluid flow, and cell-cell interactions are prompted by micro-

chamber arrays where cells remain trapped (Breslin and O'Driscoll, 2013; Hickman et al., 2014; Mehta et al., 2012).

Finally, one of the most exciting features of stirred bioreactors it's their capacity to couple another strategy of 3D cell culture that gives 3D support to cells, called scaffolds (Figure 1.12-E). In this case, scaffolds formed by hydrogels in the form of micro-carriers (whose pore size can be optimized) can be coated with substrates that promote cell adhesion (such as gelatin or collagen) (Breslin and O'Driscoll, 2013; Hickman et al., 2014).

An overview of the main advantages and disadvantages for each 3D cell culture method is summarized in Table 1.3. (Amann et al., 2015; Breslin and O'Driscoll, 2013; Gupta et al., 2016; Katt et al., 2016; LaBarbera et al., 2012; Mehta et al., 2012).

Table 1.3. ***Advantages and limitations of different 3D cell models spheroid-forming methods.***

Culture method	Advantages	Limitations
Hanging drop	✓ Simple ✓ Low-cost if using micro-well plates ✓ Control of spheroid diameter ✓ Uniformity in spheroid size ✓ Enables co-culture with defined cellular composition	× Limited long-term culture × Time-consuming × Low stability × Low efficiency × Low throughput
Forced-floating	✓ Simple ✓ Low-cost ✓ Ease sample recovery for analysis ✓ High throughput	× Heterogeneity in spheroid size and shape × Plate-coating
Matrices and scaffolds	✓ 3D support that mimics *in vivo* ✓ Possible inclusion of growth factors ✓ Long-term culture ✓ Uniformity in spheroid size ✓ Spheroids immobilization → easy handling ✓ High throughput	× Difficult sample recovery for analysis × Expensive for scale-up production × Biocompatibility and biodegradability of scaffold materials
Stirring-based	✓ Simple ✓ High throughput / easy large-scale production ✓ Long-term culture ✓ Ease sample recovery for analysis	× Special equipment is required × High shear force for cells × Heterogeneity in spheroid size × No individual compartment for spheroids
Microfluidic systems	✓ Control of spheroid diameter and cellular composition ✓ Quick spheroid formation ✓ High throughput ✓ Control of spheroid growth parameters ✓ Continuous perfusion → long-term culture	× Difficult sample recovery for analysis × Required technical training for customized devices × Limited long-term culture

Besides providing the establishment of intercellular and cell-ECM interactions in monoculture, 3D cell models also allow to perform co-cultures between different cell types. This enables to increment the complexity of the tumor spheroid and a better recapitulation of what occurs in the *in vivo* tumor microenvironment (Edmondson et al., 2014). In this field, in the last years several studies and approaches have been addressed in order to mimic the tumor stroma, by co-culturing colorectal cancer cells with fibroblasts in 3D cell spheroids (Dolznig et al., 2011; Jeong et al., 2016; Kim et al., 2015b; Park et al., 2016).

2. Aim

The present work was the conclusion of a project developed in the host lab (NutraBrass - Nutraceuticals from *Brassicaceae*: High Pressure Processing of Cruciferous food plants to recover biologically active ingredients with health promoting effects - PTDC/AGR-TEC/3790/2012, funded by FCT, Portugal) which aimed the production of extracts from cruciferous vegetables by high-pressure extraction processes with possible application in cancer therapy.

Considering the pre-clinical and therapeutic gaps in the development of effective treatments towards colorectal cancer eradication, this work intended to explore the effect of natural extracts from cruciferous vegetables (namely watercress and broccoli), and respective ITCs, in a 3D colorectal cancer cell model that mimics the tumor *in vivo* and whose cells possess a CSC-like phenotype. The potential of these compounds to target CSCs will open the door for new therapeutic strategies, since until to date these cells are responsible for tumor relapse. For this purpose, after phytochemical characterization and screening of the biological effect of extracts and ITCs using a 2D cell model, colorectal cancer cell spheroids generated by a stirred-based 3D cell culture system (previously developed in the lab) were used to explore the anticancer effects of these phytochemicals in terms of cell proliferation, viability, chemo-resistance and CSC targeting. The main tasks of this work are summarized below in Figure 2.1.

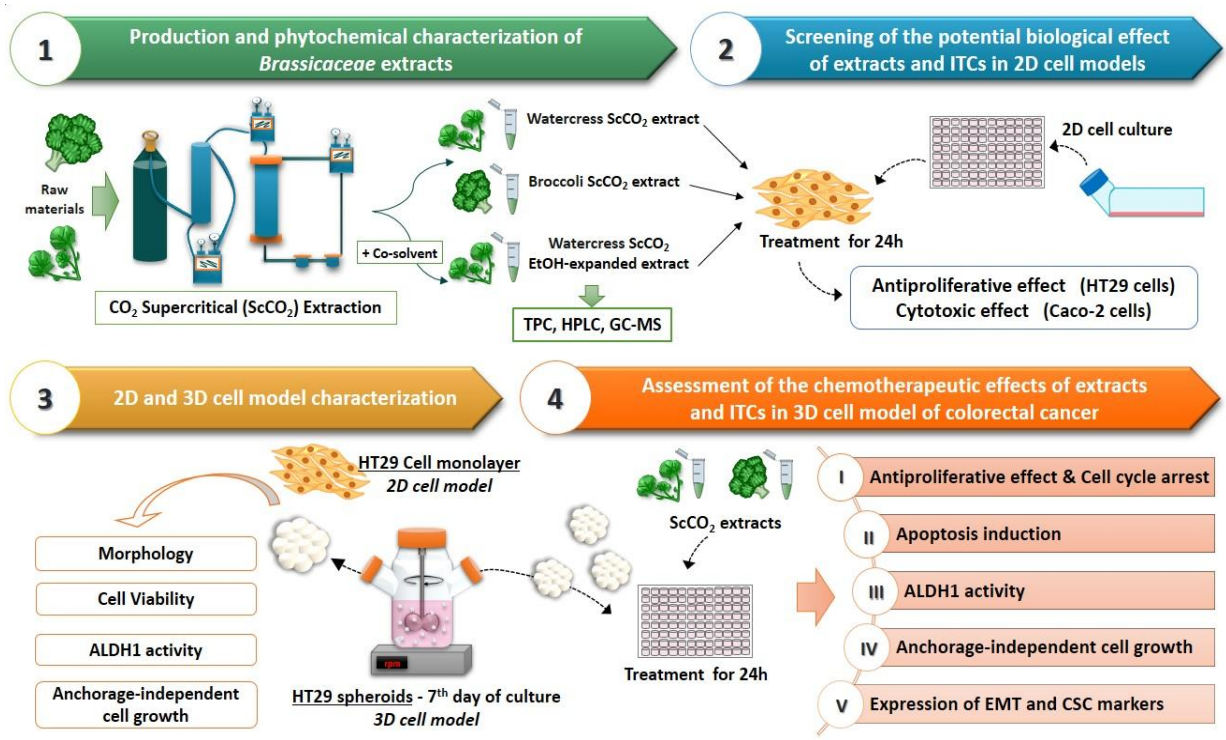

Figure 2.1. ***Illustration of the main tasks.*** This work was divided in 4 main tasks encompassing extracts production and phytochemical characterization, screening of their cytotoxic and antiproliferative effect in 2D cell models, cell models characterization (2D vs. 3D) and evaluation of the chemotherapeutic potential of extracts and ITCs in terms of preventing cell proliferation, inducing apoptosis, and targeting cell self-renewal and CSC sob-population. *Student authorship image (MSO-PPT Drawing Tools).*

3. Materials and Methods

3.1. Chemotherapeutic agents

3.1.1. *Brassicaceae* natural extracts

As raw materials for natural extracts production two different cruciferous vegetables were selected: watercress and broccoli. Watercress was kindly provided by the Vitacress® company of the RAR Group in the Fresh Produce Market, whereas broccoli was purchased by the host lab in an ordinary fresh market.

Broccoli and watercress natural extracts were produced by Nutraceuticals and Delivery Group of IBET (Oeiras, Portugal), using high pressure technology-based extraction processes. Supercritical carbon dioxide ($ScCO_2$) extraction was used to obtain a natural extract for each cruciferous vegetable. Additionally, a CO_2 -expanded ethanol (CO_2-expanded EtOH) high pressure extraction was performed to obtain another watercress natural extract. The conditioning and treatment of the raw material and both the extraction methodologies were performed as described previously by the host lab (Rodrigues et al., 2016). All the extracts were recovered in ethanol and quantified in terms of ITC equivalents by High-Performance Liquid Chromatography with Diode Array Detection (HPLC-DAD), as described elsewhere (Rodrigues et al., 2016). To note that broccoli $ScCO_2$ extract required an additional step of concentration using rotatory vapor. In Table 3.1. are summarized the settings applied in each extraction procedure for the production of cruciferous natural extracts, as well as concentration of each extract in respective ITC equivalents, i.e. in µM of the respective ITC (watercress extracts were quantified in terms of PEITC equivalents, whereas broccoli extract was quantified in terms of SFN equivalents).

Table 3.1. ***Settings applied to high pressure extraction of natural bioactive compounds present in watercress and broccoli extracts.*** The main conditions established included the pretreatment of the raw material, pressure, temperature, time, flow rate and solvent.

Extract	Pretreatment	Pressure (MPa)	Temperature (ºC)	Time (min.)	Flow rate (g/min.)	Solvent mixture	Concentration (µM)
Broccoli $ScCO_2$ extract	60 minutes at 35ºC	25	35	120	10	CO_2	3410
Watercress $ScCO_2$ extract	60 minutes at 35ºC	25	35	120	10	CO_2	7314
Watercress *CO_2-expanded EtOH* extract	60 minutes at 35ºC	25	35	120	10	60% CO_2 40%EtOH	1229

Due to light sensibility, all the experiments and handling of extracts were performed under protection from light. Storage was made at 4ºC.

3.1.2. Bioactive compounds and drugs

As bioactive compounds representative of the class of ITCs naturally derived from cruciferous vegetables, two ITCs were selected: SFN (LKT Laboratories) and PEITC standard (99%) (Sigma). For biological testing purposes, a 10-30mM stock dilution was prepared for each ITC. SFN was diluted in Dimethyl Sulfoxide (DMSO) Hybri-Max™ grade, sterile-filtered bioreagent (Sigma) followed by storage at -20ºC, whereas PEITC was diluted in absolute ethanol for analysis (Sigma) followed by storage at 4ºC. 5-Fu was used as chemotherapeutic agent and a stock dilution in sterile water was made at a final concentration of 50mM, followed by filtration with a 0.2µM cellulose filter and storage at -20ºC. Due to light sensibility, all the experiments with 5-Fu were also performed under light protection.

3.2. Phytochemical characterization

3.2.1. Total Phenolic Content quantification by Folin-Ciocalteau method

The concentration of total phenolic compounds present in *Brassicaceae* extracts was determined according to the colorimetric method of Folin-Ciocalteau described by (Singleton and Rossi, 1965) and adapted by the host lab for readings in a microplate spectrophotometer. Briefly, in a non-sterile, clear 96-well polystyrene microplate with flat bottom (Greiner), 3µL of the appropriate dilutions of samples in distilled water were added to 237µL of distilled water. Additionally, 3µL of water were added as blank and 3µL of gallic acid (Sigma) dilutions (with 50, 100, 200, 400, 600 and 800 mg/L of gallic acid in distilled water) were added as standard to perform a calibration curve. Then, 15µL of Folin-Ciocalteu's Reagent for clinical diagnosis (PanReac AppliChem) were added to each well and after a brief incubation of a few seconds the reaction was neutralized by the addition of 45µL of a Sodium Carbonate solution (Na_2CO_3 from Sigma) at 200g/L in distilled water, followed by brief shaking in an Orbit™ 300 Multipurpose Digital Vortexer (Citomed). After incubating the plate at 40ºC for 30 minutes, sample absorbances were measured at 765nm using a Spark® 10M Multimode Microplate Reader (Tecan Trading AG). The results were expressed as means of independent triplicates in milligrams of Gallic Acid Equivalents (mg GAE) per liter of extract (mg GAE/L extract).

3.2.2. Analysis of phenolic compounds by HLPC-DAD

Identification of phenolic compounds present in watercress CO_2-expanded EtOH extract was performed by HPLC-DAD by Nutraceuticals and Delivery Group of IBET (Oeiras, Portugal), using a Surveyor apparatus (Thermo Finnigan - Surveyor) with a photodiode-array detector coupled to an

Dionex ED40 electrochemical detector, as well detailed in (Rodrigues et al., 2016). This result was recently published by the group, serving only to contextualize the composition of the CO_2-expanded EtOH extract used in this thesis.

3.2.3. Gas Chromatography – Mass Spectrometry (GC-MS) analysis of $ScCO_2$ extracts

Identification of some compounds present in watercress and broccoli $ScCO_2$ natural extracts was made by GC-MS by Nutraceuticals and Delivery Group of IBET (Oeiras, Portugal), using a Shimadzu-QP2010 gas chromatograph (Shimadzu Corporation) with a quadrupole mass spectrometer coupled with an electronic impact source. A VF-5MS capillary column, 30m x 0.25mm I.D. and 0.25µm phase thickness was used in the separation of sample components under the conditions previously described by the host lab (Rodrigues et al., 2016). Data acquisition was performed by GCMS Solutions software and some of the extracts compounds were identified by comparison with mass spectra from a set of libraries (NIST21, NIST27, NIST107, NIST147 and WILEY229). Based on the highest degree of similarity of the potentially present compounds, it was carried out a survey in the literature to define some the most likely extract components.

3.3. Cell culture

3.3.1. Human cell lines

The human colon cancer cell lines, Caco-2 and HT29, were obtained from Deutsche Sammlung von Microorganismen und Zellkulturen (Barunshweig, Germany) and from American Type Culture Collection (ATCC, USA), respectively. Both cells lines, derived from a colorectal adenocarcinoma, have an epithelial morphology and an adherent growth profile.

3.3.2. Cell culture and maintenance

Both cell lines were routinely cultured in 75 or 175cm^2 ventilated t-flasks (Nunc, Thermo Scientific) in RPMI 1640 medium (Roswell Park Memorial Institute 1640; Gibco) supplemented with 10% (v/v) of heat-inactivated sterile filtered Fetal Bovine Serum (FBS; Biowest). Additionally, Caco-2 cells culture medium was supplemented with 1% (v/v) of penicillin and streptomycin (PenStrep). Cells were maintained in a controlled humidified atmosphere at 37ºC and 5% (v/v) CO_2 in an autoflow CO_2 water jackted incubator (Nuaire) and monitored daily (Olympus inverted microscope).

Cell splitting was performed twice a week with a splitting ratio of 1:4 for Caco-2 cells and 1:3/1:6 for HT29 cells. Briefly, after discard the medium, cells were washed with pre-warm 0,25% Trypsin-EDTA (1x) (Gibco, Life Technologies), followed by incubation with 2.5mL of Trypsin at 37ºC for 3minutes for HT29 cells or 5minutes in the case of Caco-2 cells. Trypsin activity was neutralized by the addition of 7.5mL of pre-warm culture medium. Cell sub-cultivation in the proper ratio was made considering a

final volume of 15mL in 75 cm^2 t-flasks or 30mL in 175 cm^2 t-flasks (e.g. for a splitting ratio of 1:4, 2.5mL of cell suspension were added to 12.5mL of medium culture in a 75 cm^2 t-flask), with further incubation in the previously mentioned conditions. The remaining cell suspension, whenever necessary, was used in the assays described below.

For cell-based assays, cell counting was performed by trypan blue exclusion assay, which relies in the fact that only non-viable/dead cells with disrupted membranes are selectively marked in blue, in contrast with live/viable cells that appear bright white under the microscope. After a proper dilution of cell suspension with Trypan Blue Stain (0.4%) (Gibco) previously diluted in 1:4 in distilled water – see Table 3.2. – both cameras of the hemocytometer were filled and 4quadrants per camera were counted.

Table 3.2. ***Dilution factors applied in cell counting.*** Each cell line and/or culture condition had associated a proper dilution factor to enable reliable cell counting.

Cell Line	***Dilution***	***Observations***
Caco-2 *(in 75cm^2 T-flask)*	1:5	-----
HT29 *(in 75cm^2 T-flask)*	1:20*	-----
HT29 *(in 175cm^2 T-flask)*	1:40*	For 3D cell culture preparation
Notes	**It required a previous dilution of cell suspension in PBS.*	

After cell counting, cell density was determined by Equation (1).

$$(1)\ Cell\ density\ \left(in\frac{cells}{mL}\right) = \frac{\Sigma\ cells\ per\ quadrant}{8}\ x\ Dilution\ Factor\ x\ 5000$$

3.3.3. Cell cryopreservation and defrosting

For cell line cryopreservation, after inactivation of trypsin and cell counting, as previously described, the proper volume of cell suspension accounting for $5x10^6$ cells/mL was transferred to a 15mL Falcon tube, followed by centrifugation at 200g, 10minutes. After discarding the supernatant, the pellet was resuspended in 1mL of freezing solution (containing 95% v/v FBS + 5% v/v DMSO) and transferred to a cryovial further stored at -80ºC in a Mr. Frosty container for 1day, after that it was placed in liquid nitrogen (-180ºC) for long-term storage.

Thawing of cells was performed at 37ºC and cell suspension was placed in a 15mL Falcon tube already containing 1mL of pre-warm medium culture. After centrifugation at 200g for 10minutes, the supernatant was removed and cells were resuspended in culture medium and placed in a 25cm^2 t-flask. After 2days in culture, total cell density was transferred to a 75cm^2 t-flask, and thereafter cell passage was performed as already described.

3.3.4. 3D Cell model: Development and monitoring of tumor spheroids in stirred-tank culture system

Generation of colorectal cancer spheroids in stirred-tank bioreactors was performed based on the conditions described in (Santo et al., 2016). Before culturing the spheroids, spinner bioreactors were subject to a pre-treatment, in order to prevent cell attachment to the spinner walls. Briefly, spinner-vessel was incubated overnight with a cleaning solution (potassium hydroxide solution in ethanol) followed by a quick wash with distilled water. After drying, it was pre-coated with ~3-5mL of dimethyldichlorosilane (Merck) and washed with ~3-4mL of toluene (Merck), followed by air drying. Afterwards, spinner vessel was washed with distilled water, air dried and autoclaved.

After trypsin inactivation and cell counting, as previously described, the proper volume of cell suspension accounting for $2.5x10^5$ cells/mL, towards a final volume of 100mL, was transferred to a 15mL Falcon tube and centrifuged at 200g, 10minutes. After discarding the supernatant, the pellet was resuspended in 5mL of pre-warm medium culture and transferred to a 125mL spinner flask (Corning) already containing 55mL of culture medium, totaling 60% of the final volume.

Initially, the spinner vessel was placed on a magnetic stirrer under 40rpm, in a humidified atmosphere with 5% CO_2 at 37ºC, during 6hours post-inoculation, after which cell aggregation was evaluated to check the formation of aggregates with at least 3-5 cells. At this point, the spinner volume was filled up to 100mL by adding pre-warmed medium culture. At the time-point of 8hours and 28hours post-inoculation the stirring rate was increased to 50rpm and to 60rpm, respectively. At day4 post-inoculation it was initiated a daily procedure of medium renewal, replacing half of spinner flask medium with fresh pre-warmed medium culture. Spheroids were visualized in a Leica DM1RB inverted microscope equipped with a C295 camera (10x magnification) and average spheroid diameter was quantified using ImageJ software.

3.4. Assessment of anticancer effects of phytochemicals using cell-based assays

3.4.1. Cytotoxicity assay

In vitro cytotoxicity assays were performed using Caco-2 cells as a model to mimic the human intestinal epithelium. Although derived from a human colon adenocarcinoma, under standard culture conditions and as soon as the monolayer reaches high confluency (attained at 7^{th} day of culture), these cells differentiate spontaneously towards an enterocyte-like phenotype. At this culture stage, Caco-2 cells present “brush borders” a morphological feature accomplished by cell polarization and the expression of several enzymes typically produced by enterocytes of the intestinal barrier, among other features (Grajek and Olejnik, 2004; Meunier et al., 1995; Rousset, 1986; Sambuy et al., 2005).

Cytotoxicity assays were performed for each extract and bioactive compound through the CellTiter 96® AQ_{ueous} One Solution Cell Proliferation Assay (Promega), a colorimetric method that allows the determination of the number of viable cells. Briefly, Caco-2 cells were seeded into 96-well culture plates at a density of $2x10^4$ cells/well, with a final volume of 100µL/well, and were allowed to grow for 7days, with medium renewal every 48hours. After medium removal, cells were incubated with different concentrations of extracts, bioactive compounds and 5-Fu diluted in low-serum culture medium (RPMI medium with 0.5% v/v FBS). Two control samples were also prepared, one with cells incubated only with low-serum culture medium and other with cells incubated with the maximum %v/v of the solvent in which the extract/drug/bioactive compounds were dissolved, in order to guarantee that only the samples, and not the solvents, are responsible for cell cytotoxicity. After a 24h period incubation, cells were washed twice with Phosphate Buffered Saline (PBS, pH=7.4, Sigma) at 37ºC and incubated with MTS (3-(4,5-dimethylthiazol-2-yl)-5-(3-carboxymethoxyphenyl)-2-(4-sulfophenyl)-2H-tetrazolium, inner salt) diluted in low-serum culture medium for 3hours in a final concentration of 30µg/mL. Additionally, a blank was prepared by incubating the previous dilution in wells without cells, in order to subtract the background absorvance in all the readings. This cell viability reagent contains MTS, a tetrazolium compound, that in metabolically active cells is reduced through the activity of mitochondrial dehydrogenase enzymes into formazan, a colored compound soluble in culture medium which absorbs at 490 nm. Since the amount of formazan is proportional to the number of viable cells, by measuring the absorvance at 490 nm using a Spark® 10M Multimode Microplate Reader (Tecan Trading AG), cell viability was calculated relatively to control without treatment by Equation (2).

$$(2)\ \text{Cell Viability (in \%)} = \frac{\text{Sample Absorvance}}{\text{Control Absorvance}}\ \text{x}\ 100\ \%$$

All the assays were performed in triplicate, using three independent experiments, and the inhibitory concentration required to inhibit 50% of cell viability (IC_{50} value) for each compound was calculated using GraphPad Prism 6 software (GraphPad Software, Inc., La Jolla, CA).

3.4.2. Antiproliferative assay using 2D cell model

Antiproliferative assays were performed on HT29 cells grown in monolayer, as described elsewhere (Rodrigues et al., 2016; Serra et al., 2010). Briefly, HT29 cells were seeded into 96-well culture plates at a density of $1x10^4$ cells/well in a final volume of 100µL/well and allowed to adhere and grow until the next day, in the previous described culture conditions. After 24hours post-inoculation, the medium was removed and cells were incubated with different concentrations of natural extracts, bioactive compounds and 5-Fu diluted in low-serum culture medium. In similarity with cytotoxicity assays, two control samples were also prepared: i) cells incubated with low-serum culture medium and ii) cells incubated with the maximum %v/v of the solvent in which the extract/ITCs or 5-Fu were dissolved.

After allow cell growth and proliferation for 24hours, cells were gently washed twice with warm PBS and cell viability was assessed by MTS colorimetric assay, as already described for Cytotoxicity Assays. Cell viability was calculated relatively to control of cells incubated in low-serum culture medium by Equation (2) and results were expressed in terms of percentage of cellular viability.

All the experiments were performed in triplicate and the effective concentration required to decrease 50% of cell viability (EC_{50}) for each extract/ITC or drug was calculated using GraphPad Prism 6 software (GraphPad Software, Inc., La Jolla, CA) fit, taking into account three independent experiments.

3.4.3. Antiproliferative assay using 3D cell model

Spheroids with an average diameter of 500µm collected at day6 were seeded at a density of 5 spheroids/well in 96-well plates in a final volume of 100µL/well (to note that, for spheroid seeding it was necessary to cut tips, in order to avoid spheroid damage). A blank without spheroids and only with culture medium was considered.

Cell viability of each well prior to treatment was assessed using PrestoBlue Cell Viability Reagent (Life Technologies). To accomplish this, 10µL of PrestoBlue were added per well followed by an incubation of 2hours, after which plates were centrifuged at 200g, 5minutes (Sigma 3K15, Sigma Laborzentrifugen). The supernatant of each well was carefully removed by pipetting and transferred to black 96-microwell polystyrene plates with non-treated flat bottom (Nunc, Thermo Scientific) for fluorescence intensity measurement in a Microplate Fluorimeter FLx800 (Bioteck Instruments) at an excitation and emission wavelengths of 580 nm and 595 nm, respectively. The blank of medium with PrestoBlue Reagent was used to subtract the background fluorescence to all readings.

Natural $ScCO_2$ extracts and bioactive compounds previously diluted in low-serum culture medium were added to each well and spheroids were incubated for 24hours to allow cell growth and proliferation. Afterwards, spheroids were gently washed with warm PBS and cell viability was assessed by MTS colorimetric assay. Due to higher cell density, compared to antiproliferative assays conducted in 2D cell model, a higher concentration of MTS was required. Hence, aggregates were incubated with MTS diluted in low-serum culture medium in a ratio of 1:10, followed by a 3-4hour incubation. Notwithstanding, a blank without cells and only with MTS diluted in culture medium was considered to subtract the background absorbance to all readings.

Spheroid viability for each replicate was calculated relatively to control of spheroids incubated in low-serum culture medium by Equation (3), considering cell viability of each well at time-point 0h previously assessed by fluorescence intensity measurement.

$$(3)\ \text{Spheroid Viability (in \%)} = \frac{Abs\ 24h\ (treated\ spheroids) \Big/ FI\ 0h\ (treated\ spheroids)}{Average\ Abs\ 24h\ of\ Control \Big/ Average\ FI\ 0h\ of\ Control} \ x\ 100\ \%$$

Where FI 0h is the fluorescence intensity of spheroids prior to treatment (cell viability at time-point = 0hours) and Abs 24h is the absorvance of spheroids 24h after treatment with extracts and ITCs (cell viability at time-point = 24hours). All the experiments were performed using 6replicates and EC_{50} values for each extract/ITC were calculated using GraphPad Prism 6 software fit, taking into account at least three independent experiments.

3.4.4. Cell cycle arrest analysis

Cell cycle was analyzed by Fluorescence Activated Cell Sorting (FACS) based on the DNA content at each cell cycle phase in a given cell population. By using a fluorescence dye, such as Propidium Iodide (PI), that stoichiometrically binds to DNA, it is possible to distinguish the different cell cycle phases according to the fluorescence intensity signal that dependents on the number of DNA copies. Hence, G2 phase-arrested cells presenting 2 copies of DNA will present twice the fluorescence intensity comparing with G1 phase-arrested cells that contain only 1 copy of DNA, whereas S phase-arrested cells with presence an intermediate fluorescence signal (Darzynkiewicz et al., 2010).

Spheroids collected from spinner vessel at day6 of culture were seeded at a density of 100 spheroids/well in 12-well plates, in a final volume of 800µL/well. The colonospheres were incubated for 24hours with the concentration of natural extracts and bioactive compounds that corresponds to the EC_{30} value, i.e. with the dose that grants 30% of antiproliferative effect in 3D cell model. All the dilutions were made in low-serum culture medium (RPMI medium with 0.5% v/v FBS). Spheroids incubated only in low-serum culture medium and in medium with the maximum %v/v of the solvent in which the extract/ITCs were dissolved, were considered as controls. After allow a complete cycle of cell growth and proliferation, spheroids were collected to eppendorfs and centrifuged at 200g, 10minutes. The supernatant was discarded and the pellet washed with PBS, followed by centrifugation in the abovementioned conditions. Colonospheres were disaggregated with 200µL of trypsin for 3-4minutes followed by enzyme inactivation with 800µL of complete medium (RPMI + 10%FBS). Then, the volume equivalent to $1x10^6$ cells was centrifuged at 200g, 10minutes. The supernatant was discarded and cells were washed with cold PBS, with subsequent centrifugation in the previous conditions. After supernatant removal, cells were incubated with 1mL of a staining solution containing 0.05mg/mL of PI (Sigma), 1.5%v/v of Triton X-100 (Sigma), 0.7U/mL of DNase/protease-free Ribonuclease (RNase) A (Thermo Scientific) and 0.01M of Sodium Chloride (NaCl). Following 2hours' incubation in the dark at room temperature, samples were stored at 4ºC until further reading. Analysis of the fluorescence intensity signal was performed using a CyFlow Space flow cytometer (Partec) with a blue laser as excitation source. To avoid the presence of cell clumps and doublets, all the samples were filtered (Partec) prior to reading. Data acquisition was performed by reading 30.000 events per sample at a flow rate of 350-500 events/second whenever possible. For cell cycle analysis, it was defined a gate excluding cell debris and doublets and another gate defining the singlets population. Results were analyzed by FlowMax Software (Partec), using the mathematical model "*Fit One Cycle*".

3.4.5. Soft agar assay

To analyze anchorage-independent cell growth in semi-solid matrices, a hallmark of cell transformation and unrestrained cell growth, the Soft Agar Assay was performed. This experiment is advantageous over monolayer cell models, since cell growth in a 3D system resembles best with the *in vivo* tumor microenvironment. The tumorigenic potential is evaluated by the ability of cells to proliferate and form colonies in suspension within a semisolid milieu. In this context, normal epithelial

cells are incapable to proliferate in the absence of anchorage to the ECM and undergo anoikis, a programmed cell death driven by the loss of contact with ECM. Contrary, cancer cells are able to evade this apoptotic process and grow and form colonies within a semi-solid environment, such as that provided by the soft agar. By counting colonies and/or measuring the colony dimension, this assay enables to assess the efficacy of a certain compound in the decline of the tumorigenic potential of cancer cells.

The soft agar assay was performed in 6-well plates containing two layers of low-melting agarose (Lonza). Prior to experiments, two stock solutions of agarose were made: i) a stock solution of agarose at 1.2% w/v in distilled water and ii) a stock solution of agarose at 0.6% w/v in PBS, both with subsequent autoclaving, in order to melt agarose and for sterilization. Until further use, both agarose stock solutions were kept in an incubator at 60ºC to prevent agarose solidification.

For bottom layer preparation, a mix of a 1:1 ratio was made with agarose 1.2% in water and 2x RPMI medium supplemented with 20% v/v FBS, to obtain a final solution with 0.6% w/v agarose in 1x RPMI medium with 10%FBS. After swirl the solution, 2mL of this were added carefully to each well to prevent air bubble formation and allowed to solidify at room temperature in a sterile laminar flow chamber.

In the meanwhile, for top layer preparation, a mix of a 1:1 ratio was made with PBS and agarose 0.6% in PBS to make a final solution with 0.3% w/v agarose in PBS that was kept in a water bath at 37ºC until use. Then, 1mL of spheroids was collected from the spinner vessel at 7^{th} day of culture and cells were centrifuged at 200g for 5minutes, washed with 500µL of PBS and trypsinized for 3-4minutes at 37ºC, as already described for other assays. The 200µL of trypsin were inactivated with 800µL of RPMI medium with 10%FBS. After cell counting, cells were centrifuged in the abovementioned conditions and the pellet was resuspended in pre-warmed PBS.

The top layer of each condition was prepared in 15mL sterile falcon tubes by mixing 0.3% w/v agarose in PBS, with the volume of cell suspension that yields a concentration of 1000cells/mL and the volume of extract/ITC whose concentration one wants to test (1, 3 and 5µM). Then, after homogenization, the bottom layers of each well were carefully overlaid with 2mL of this preparation, avoiding bubble formation. Each test condition was prepared and plated one at a time to prevent premature setting of agarose. Additionally, a set of controls was prepared: i) a control with cells without any treatment; ii) with the maximum %v/v of ethanol used in the tested conditions; iii) with the maximum %v/v of DMSO used in the highest SFN concentration tested; and iv) a control with cells derived from 2D cell culture without any treatment, to compare the tumorigenic potential between 2D and 3D cell model. After allowing a brief solidification of the top layer at room temperature, cells were grown for 15 days in a humidified atmosphere with 5% CO_2 at 37ºC, with addition of 150µL of RPMI medium with 10%FBS 2-3 times per week to hydrate the exposed agar and feed the cells.

At the end of the incubation period, colonies with diameters greater than 50µm were counted visually in each well, and colony density was calculated by Equation (4):

$$(4)\ CFU\ density\ (in\ \%) = \frac{counted\ colonies\ in\ treated\ sample}{colonies\ in\ control\ sample}\ x\ 100\%$$

Colonies were photographed under a light microscope (10x magnification) and analyzed by ImageJ software. All the experiments were performed in duplicates with at least two independent experiments, and results were expressed as mean ± SD.

3.4.6. Caspase-3 activity detection

The apoptotic profile of spheroids incubated with different concentrations of natural extracts and ITCs was assessed by NucView488™ and MitoView633 ™ Apoptosis Assay Kit (Biotium), a fluorescence-based method that allows the differentiation of healthy and apoptotic cells based on the fluorescence tone and intensity. MitoView633™ is a far-red fluorescent dye that specifically accumulates in the mitochondrial lipid moiety in a manner that is dependent on the membrane potential, staining healthy cells with bright red. In contrast, NucView488™, has a dual staining action: upon entering cell's cytosol, functions as a caspase-3/7 substrate and, once cleaved, it gains DNA-binding properties and migrates towards cell nuclei. Therefore, this dye stains with bright green not only the intracellular caspase-3/7 activity, but also the nucleus's morphological changes resultant from the apoptotic process (Biotium, 2012).

Colonospheres collected at 7th day of spinner vessel culture were seeded at a density of 50 spheroids/well in 12-well plates and incubated with the concentrations of natural extracts and bioactive compounds that correspond to the EC_{50} value and half of the EC_{50} value obtained in the antiproliferative assay, in a final volume of 500µL/well. Spheroids incubated only in low-serum culture medium and in medium with the maximum %v/v of the solvent used, were considered as controls. Twenty-four hours later, the medium was removed and cells were incubated with 200µL of low-serum culture medium containing 1µL of NucView488™ and 1µL of MitoView633™ for 2hours, to allow proper spheroid staining. After centrifuging the plates at 200g for 5minutes, the aggregates were washed with PBS and further resuspended in the same buffer. Then, spheroids were placed into µ-slide 8-well glass bottom plates (Ibidi) and covered with 200µL of 1.2% agarose w/v in distilled water. After agarose solidification, each well was hydrated with 15µL of PBS. Aggregates were observed and photographed in an Andor spinning-disk confocal fluorescence microscope (10x magnification). Assessment of average spheroid diameter and image treatment were performed using ImageJ software.

3.4.7. ALDH activity detection

The CSC-like phenotype of spheroids was evaluated by ALDEFLUOR™ Assay Kit (Stem Cell Technologies), a fluorescence-based method that detects the enzymatic activity of the ALDH1 isoform. This approach relies on the passive diffusion of BODIPY-aminoacetaldehyde (BAAA or ALDEFLUOR™ reagent) into viable cells, where it serves as a subtract for ALDH1. Once converted

into the negatively-charged fluorescent product BODIPY-aminoacate (BAA-) that is retained inside cells, ALDH1$^{positive(+)}$ cells became fluorescent, being the fluorescence intensity signal proportional to the ALDH1 activity and feasible to be measured by flow cytometry. To prevent the efflux of BAAA and/or BAA- mediated by ABC transporters, this assay resorts to the utilization of a cold buffer that contains efflux inhibitors in order to avoid samples' fluorescence quenching. The control of fluorescence background is achieved by preparing a negative control for each sample, using diethylaminobenzaldehyde (DEAB) as a specific inhibitor of ALDH1 activity that prevents cells to become fluorescent (STEMCELL Technologies, 2011; STEMCELL Technologies, 2016).

Spheroids collected between day 6 and day 7 of spinner vessel culture were seeded at a density of 50 spheroids/well in 6-well plates and incubated with natural extracts and bioactive compounds, in a final volume of 2mL/well. Aggregates incubated only in low-serum culture medium and in medium with the maximum %v/v of the solvent used, were considered as controls. Then, 24hours post-incubation, colonospheres were collected to eppendorfs, centrifuged at 200g for 5minutes and the supernatant was removed. The pellet was washed with PBS and cells were centrifuged in the abovementioned conditions. After supernatant removal, spheroids were dissociated with trypsin and enzyme inactivation was done by addition of complete medium, as previously described.

The volume equivalent to 5x10^5 cells/mL was centrifuged at 200g for 5minutes, the supernatant was removed and cells were washed with PBS, with subsequent centrifugation in the former conditions. Cells were resuspended in 500µL of ALDEFLUOR^{TM} Assay Buffer. A new set of eppendorfs was settled and 2.5µL of ALDEFLUOR^{TM} DEAB Reagent were added to each tube, followed by immediate tube closure due to DEAB high volatility. Immediately, 2.5µL of ALDEFLUOR^{TM} Reagent was added to each tube containing cells in ALDEFLUOR^{TM} Assay Buffer, followed by quick homogenization and transfer of half of the volume to the respective tube containing ALDEFLUOR^{TM} DEAB Reagent followed by quick homogenization (each sample was treated individually). All the positive and negatives controls of each sample were incubated at 37ºC for 30-40minutes, after which samples were centrifuged at 200g for 5minutes, with subsequent supernatant removal and pellet resuspension in 250µL of ALDEFLUOR^{TM} Assay Buffer. Samples were kept in ice until further reading.

Data acquisition was performed by reading 10.000 events per sample at flow rate of 200-350 events/second, considering a R1 gating region that includes nucleated cells and excludes cell debris and a R2 region that encompasses the ALDH1$^+$ population (sorting gates were drawn relative to background fluorescence of DEAB-treated samples, according to manufacturer's instructions).

3.4.8. Gene expression assessment

3.4.8.1. Sample collection and RNA extraction

For RNA extraction from colorectal cancer spheroids it was used the RNeasy® Mini Kit (QIAGEN) according to the manufacturer's instructions, with some modifications. This method relies on cell lysis in the presence of a highly denaturing buffer containing guanidine-thiocyanate that inactivates RNases

and on subsequent ethanol addition to afford appropriate binding conditions of RNA to a silica-based membrane of spin columns, being the contaminants washed away (QIAGEN, 2012).

Colonospheres at the 7th day of spinner vessel culture were collected and seeded in 6-well plates at a density of 50 spheroids/well and incubated with natural extracts and ITCs, in a final volume of 2mL/well. Spheroids incubated in low-serum culture medium with the %v/v of the solvent used, were considered as controls. Twenty-four hours' post-incubation, aggregates were transferred to eppendorfs and centrifuged at 200g for 5minutes, followed by supernatant removal. Cells were resuspended in 600µL of RTL buffer (QIAGEN) with 1% v/v of β-mercaptoethanol with previous mechanic dissociation of spheroids, first by up-and-down pipetting with clipped tips and then by syringe needle-based dissociation. Biological samples were stored at -80ºC until further use in the Portuguese Oncology Institute (IPO) facilities.

After thawing samples on ice, 600µL of 70% v/v Ethanol in DEPC-treated water were added to each sample followed by homogenization. Then, 700µL of the sample were transferred to a RNeasy Mini spin column placed in a 2mL collection tube and centrifuged at 14.000 rpm for 30seconds (Centrifuge Eppendorf 5810R). The supernatant was discarded and the previous step was repeated with the remaining 500µL of each sample, reusing the same a RNeasy Mini spin column and collection tube. At this point, an additional step of on-column DNase digestion was made by adding per column 80µL of a solution containing 70µL of RDD buffer (QIAGEN) and 10µL of DNase I (with approximately 2727,3 Kunitz units/mL in RNase-free water), followed by incubation for 15minutes at room temperature. The spin column was washed with 700µL of RW1 buffer followed by centrifugation at 14.000 rpm for 30seconds, for DNase I removal. After discarding the flow-through of the collection tube, 500µL of RPE buffer were added to the spin column with subsequent centrifugation in the abovementioned conditions. The supernatant was removed from the collecting tube and the latter washing step with RPE buffer was repeated followed by centrifugation at 14.000 rpm for 2minutes. The old collection tube with the flow-through was discarded, and spin column was placed in a new collection tube followed by centrifugation at 14.000 rpm for 1minute to eliminate residual RPE buffer or supernatant traces outside the column. Then, to perform RNA elution the spin columns were placed in new 1.5mL RNase-free eppendorfs and 40µL of RNase-free water were added to each column membrane with subsequent centrifugation at 14.000 rpm for 1minute. To maximize the RNA extraction yield, the previous eluate was transferred back to the spin column membrane, followed by centrifugation in the previous conditions, with recover of the eluate RNA in the same collection eppendorf. Samples were kept on ice.

Total RNA concentration was quantified by ultraviolet spectrophotometry at 260nm using a Nanodrop 2000 Spectrophotometer (Thermo Scientific), considering that an absorbance reading of 1 at 260nm corresponds to approximately 40µg/mL of RNA. Total RNA samples were store at -80ºC until further use.

3.4.8.2. cDNA synthesis by reverse transcription

RNA samples obtained previously were used as templates for the generation of complementary DNA (cDNA) by a reverse transcriptase enzyme, using random primers that hybridize with messenger RNA templates and nucleotides for DNA synthesis (dNTPs). Approximately 600ng of total RNA were reverse transcribed into cDNA in a final reaction volume of 20µL with a final concentration of 30ng/µL, under the conditions listed in Table 3.3.

Table 3.3. ***Conditions applied for cDNA synthesis by reverse transcription.*** Discrimination of the temperatures and times for the denaturation, annealing, amplification and enzyme inactivation phases of cDNA synthesis.

Step	*Temperature (ºC)*	*Time (minutes)*
Denaturation and Annealing	70	10
Amplification	42	60
Enzyme inactivation	70	15

Briefly, in 0.2mL reaction tubes it was added the volume of total RNA corresponding to 600ng, 0.5µL of random primers at 3µg/µL and the volume of DEPC-treated nuclease-free water (Ambion) needed to make up a final volume of 7.75µL. This solution was incubated at 70ºC for 10minutes in a T3 Thermocycler (Biometra). Afterwards, samples were chilled on ice and 12.25µL of a master mix containing 4µL of 5x First Strand Buffer (Invitrogen), 4µL of dNTPs, 2µL of 0.1M DTT (Invitrogen), 0.75µL of RNase Out Recombinant Ribonuclease inhibitor 5.000U (40U/µL; Invitrogen), 1µL of Supercript II Reverse Transcriptase 10.000U (200 U/µL; Invitrogen) and 0.5µL of DEPC-treated nuclease-free water, were added to each reaction tube. The reverse transcription reaction was carried out at 42ºC for 1hour and stopped by heating for 10minutes at 70ºC. In the end, cDNA samples were store at -20ºC until further use.

3.4.8.3. Real-time quantitative polymerase chain reaction (qPCR)

The quantification of the expression of a targeted gene was accomplished by qPCR. In qPCR process each reaction cycle encompasses a melting phase with separation of the cDNA double-strand at a high temperature, followed by an annealing phase with primer binding to DNA templates and a polymerization phase carried out by a DNA polymerase enzyme, at a lower temperature. This method consists in the detection of the DNA quantity during the exponential phase of nucleic acid amplification, in the end of each cycle, based on the detection and quantification of the fluorescence intensity signal emitted by a fluorophore that intercalates with the resultant double-stranded amplification products. The fluorescence measurement is made above a given threshold (that excludes the background signal) and the number of cycles required for each sample to reach the threshold fluorescence is designated as the Ct (threshold cycle) value. Notwithstanding, samples in

which a certain target gene has increased expression will reach the threshold value faster than samples in which the target gene is less expressed and, hence, will present lower Ct values comparatively to the latter.

cDNA samples obtained previously were used as templates for the amplification of target gene sequences by qPCR and subsequently gene expression quantification. Initially, all cDNA samples were diluted in 1:4.8 in sterile water, in order to obtain reasonable Ct values within the range covered by the calibration curves and to dilute remaining reagents of the cDNA synthesis which may interfere with qPCR process. All qPCR reactions were carried out in PCR 96-Microwell plates (Axygen Scientific) in a final volume of 15µL and were set up in triplicates. For each sample a master mix was prepared to a final volume of 13µL, considering the respective components and volumes listed in Table 3.4.

Table 3.4. – ***Required components for the preparation of qPCR Master Mixes.*** Discrimination of the volumes of reverse and forward primers, qPCR mix and water, as well as primers stock concentrations.

Gene	**Primer stock**	**Reaction Master Mix**		
(marker)	**concentration (µmol)**	***Primer volume***	***Mix***	***Water***
GAPDH	10	0.75µL of reverse primer + 0.75µL of forward primer	7.5µL of SYBR® Green PCR Master Mix (Applied Biosystems)	4µL
BIRC5 (Survivin)	5			
CTNNB1 (β-Catenin)	10			
AXIN2	3.5			
TCF7L2	7.5			
PROM1 (CD133)	3		7.5µL of Kapasyber® Fast qPCR Master Mix (2x) (Kapa Biosystems) + 0.3µL of Kapasyber® Fast Rox High (50x) (Kapa Biosystems)	3.7µL
LGR5	7.5			
P21	5			
CCNA2 (Cyclin A2)	5			

In the end, 2µL of cDNA were added to the respective well and the plate was sealed with PlateMax ultra-clear sealing film (Corning Axygen), followed by centrifugation at 1200rpm for 1minute. The thermal cycling comprised an initial denaturation step at 95ºC for 10minutes, followed by 40cycles of denaturation at 95ºC for 15seconds and annealing and extension at 60ºC for 1minute. qPCR reactions were carried out in ABI PRISM 7000 Sequence Detection System (Applied Biosystems) and monitored in SDS Software (Applied Biosystems).

All the analyzes were performed in triplicate for the obtainment of the average threshold cycle (Ct) value. The comparative Ct ($2^{-\Delta\Delta CT}$) method was applied to compare the expression of the target genes. The relative gene expression was quantified as $2^{-\Delta\Delta CT}$, as outlined in Equations (5) and (6):

$$(5)\ 2^{-\Delta\Delta CT} = 2^{-[(\Delta CT \text{ of treated sample}) - (\Delta CT \text{ of untreated control})]}$$

Wherein:

$$(6)\ \Delta CT = CT_{\text{target gene}} - CT_{\text{housekeeping gene}}$$

The expression of each target gene in each treatment with phytochemicals was normalized to the corresponding housekeeping gene levels, i.e. Glyceraldehyde-3-phosphate dehydrogenase (GAPDH) levels, to determine the overall variation in gene expression.

3.5. Statistical analysis

Statistical analysis of the results was performed using GraphPad Prism 6 software (GraphPad Software, Inc., La Jolla, CA). Comparisons between samples were made by One-way ANOVA analysis, whereas comparisons with more than two variables were performed by a Two-way ANOVA analysis, both following Tukey's multiple comparison test. Values of $p<0.05$ were considered as statistically significant.

4. Results and Discussion

4.1. Phytochemical characterization of *Brassicaceae* extracts

The first task required for the prosecution of this dissertation was the development of natural extracts from two cruciferous vegetables - watercress and broccoli - using "environmentally friendly" high-pressure extraction methods. Supercritical CO_2 extraction was applied to both raw materials, whereas a CO_2 -expanded ethanol high pressure extraction was only performed for watercress. This part of the work was not included in the dissertation and was performed by the host lab pilot unit. The selection of the operating conditions was based on a previous optimization study performed by our group, aiming the isolation of PEITC from watercress (Rodrigues et al., 2016).

The obtained supercritical fluid extracts of watercress and broccoli presented an intense yellow and a light green color, respectively. Inversely, watercress extract obtained by CO_2-expanded ethanol extraction presented a dark green color (data not shown).

ITC quantification in all extracts was performed by the group, and extracts concentration was expressed as ITC equivalents (i.e. in µM of the respective main ITC). Concentrations of *Brassicaceae* extracts are displayed in Table 4.1. and, as we can see, lower PEITC content was obtained for watercress CO_2-expanded ethanol extraction. Inversely, the watercress extract obtained by supercritical CO_2 extraction presented an enhanced increment in PEITC concentration. In this way, this extraction method is more selective for PEITC isolation than the one that recurs to a co-solvent (ethanol), as already suggested (Rodrigues et al., 2016). Moreover, even after a concentration step, broccoli extract does not have shown high contents of SFN.

Table 4.1. ***ITC content of Brassicaceae extracts***

Sample	Solvent mixture	ITC concentration (in µM)
Watercress **CO_2-expanded EtOH extract**	60% CO_2 40%EtOH	1229 µM of PEITC
Watercress **ScCO_2 extract**	CO_2	7314 µM of PEITC
Broccoli **ScCO_2 extract** (with additional concentration step)	CO_2	3410 µM of SFN

Further phytochemical characterization by Folin-Ciocalteau method allowed to assess the total phenolic content of all extracts. Results showed a significant difference in the phenolic profiles of both watercress extracts, suggesting that the phenolic content of the extract is influenced by the extraction

method (Figure 4.1.). In fact, the CO_2-expanded ethanol extraction enables almost a 33-fold increase in total phenolic content (TPC) in watercress extract (Table 4.2.).

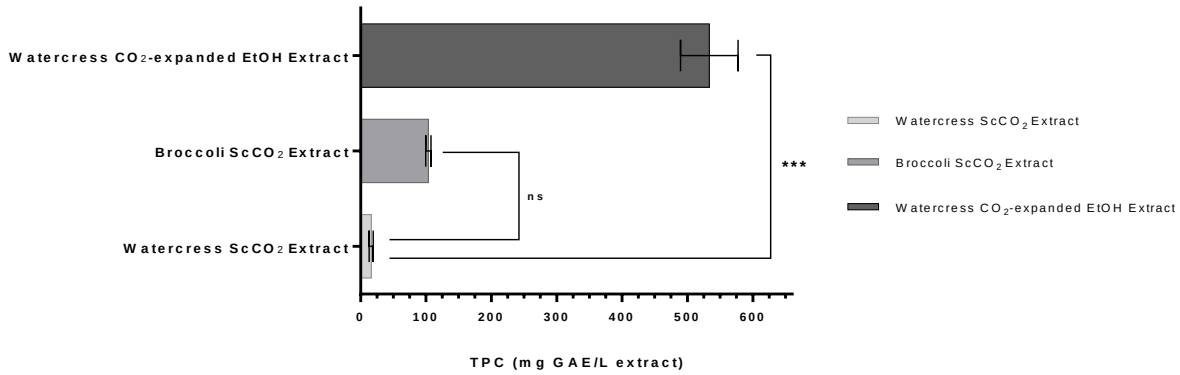

Figure 4.1. ***Phenolic profile of watercress and broccoli extracts by Folin-Ciocalteau method.*** Results are expressed as mean of two independent experiments performed at least in duplicate ± SD. ***p-value<0.001 is relative to watercress $ScCO_2$ extract.

Regardless of, between $ScCO_2$ extracts, broccoli extract appears to be more enriched in phenolic compounds than the watercress extract by the same method (Figure 4.1. and Table 4.2.). However, one could not discard the possibility of this be due to the concentration step of this extract after production.

Table 4.2. ***Phenolic content of $ScCO_2$ and CO_2-expanded EtOH Brassicaceae extracts***

***Brassicaceae* Extract**	**Total Phenolic Content (TPC in mg GAE/L extract)**
Broccoli $ScCO_2$ extract	103.8 ± 4.0
Watercress $ScCO_2$ extract	16.2 ± 3.1
Watercress CO_2-expanded EtOH extract	533.1 ± 44.0

HPLC and GC-MS analyses were further carried out by the host lab, in order to characterize the bioactive compounds in these extracts. These technical procedures were not part of the thesis experimental work, and were performed by the host lab pilot unit.

The obtained chromatographic HPLC-DAD profiles of watercress extracts (Figure 4.2.) corroborate the results obtained for watercress extracts phenolic contents. Indeed, several phenolic compounds – such as caffeic acid, caffeoylmalate, coumaric acid and rutin (co-eluted), coumaroylmalate, feruloylmalate and sinapoylmalate – were identified in CO_2-expanded EtOH watercress extract. Inversely, the prevalence of these phenolic compounds in the $ScCO_2$ watercress extract was not so significant (Figure 4.1. and Table 4.2.), which can be explained by the low solubility of phenols in the

supercritical fluid. That's way extraction of phenolic compounds usually recurs to the use of a co-solvent, like ethanol (Gil-Chávez, 2013; Pereira and Meireles, 2009).

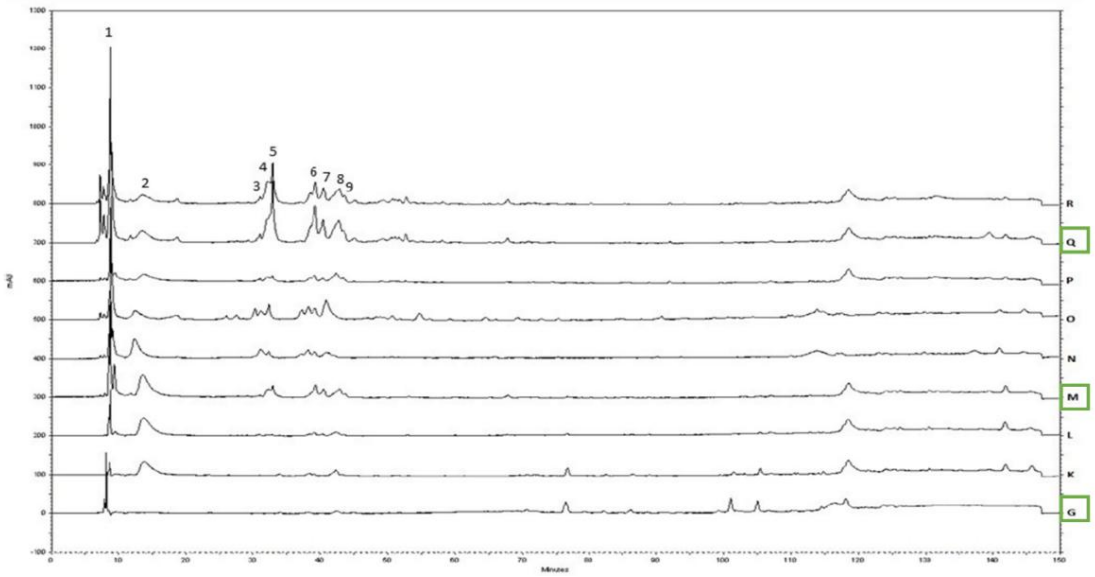

Figure 4.2. ***Chromatographic HPLC-DAD profiles of watercress extracts at 280nm*** (published work of the host lab, in (Rodrigues et al., 2016). Extract G correspond to supercritical CO_2 extraction of freeze-dried watercress; Extracts M and Q correspond to CO_2-expanded EtOH extraction with a CO_2:H_2O ratio of 60:40 using freeze-dried and fresh watercress, respectively. Legend: 1- Unidentified non-phenolic organic acid; 2 – Adenine; 3 – Caffeic acid; 4 – Tryptophan; 5 – Caffeoylmalate; 6 – Coumaric acid and rutin (co-eluted); 7 – Coumaroylmalate; 8 – Feruloylmalate; 9 – Sinapoylmalate.

Furthermore, the GC-MS chromatographic profile of watercress $ScCO_2$ extract (Figure 4.3.) exhibited a single pick at retention time = 27minutes, that was further identified as PEITC. Therefore, one can assume that $ScCO_2$ extraction was highly selective in ITC extraction from watercress matrices (Rodrigues et al., 2016).

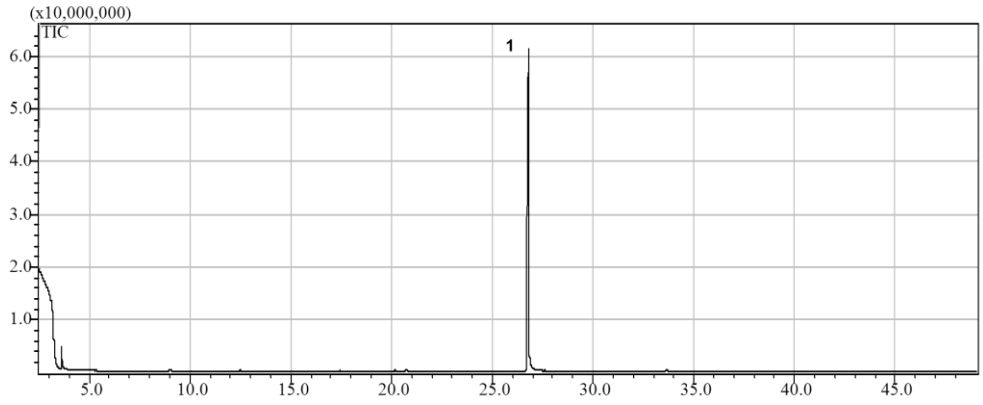

Figure 4.3. ***Chromatographic GC-MS profile of watercress extract obtained by $ScCO_2$ extraction.*** Legend: 1 – PEITC.

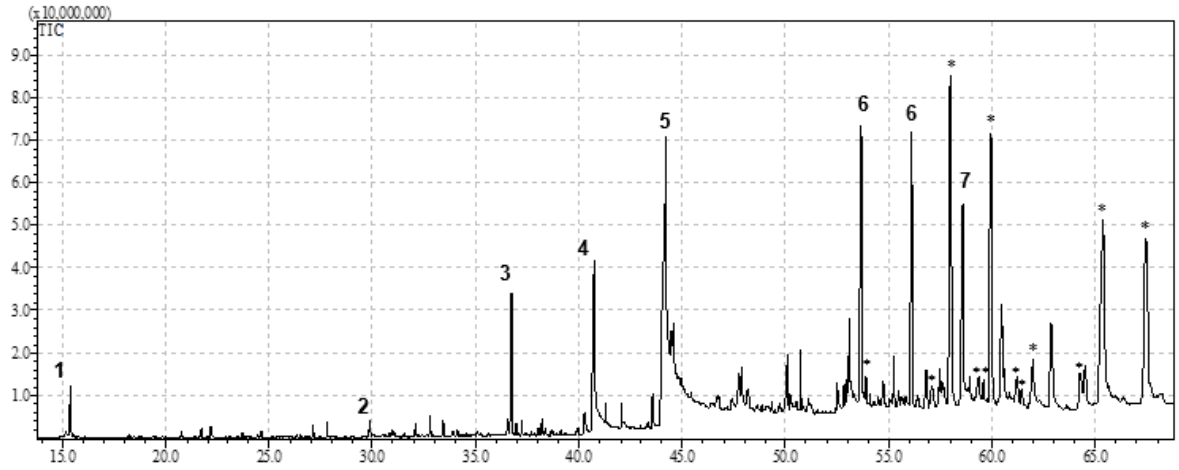

Figure 4.4. ***Chromatographic GC-MS profile of broccoli extract obtained by $ScCO_2$ extraction.*** Legend: **1 -** 3-Butenyl isothiocyanate; **2-** β-Phenylethyl isothiocyanate (β-PEITC); **3 –** Sulforaphane (SFN); **4 -** I-(+)-Asborbic acid 2,6-dihexadecanoate; **5 -** Ethyl Linoleolate; **6 –** Tetracontane; **7 -** 1-Eicosanol; (*)-compound without correspondence in the GC-MS library.

Contrary to watercress extract, the broccoli extract holds a more complex phytochemical composition, as depicted in Figure 4.4., encompassing not only SFN but also other ITCs and fatty acids (e.g. Tetracontane) and their derivatives. Fatty acids presence in broccoli extract was already reported using supercritical fluid extraction to extract compounds using broccoli leaves as raw material (Arnáiz et al., 2011).

4.2. Characterization of 2D and 3D cell models of colorectal cancer

Before performing the screening of the chemotherapeutic potential of natural extracts and bioactive compounds in colorectal cancer cells, it is important to perform the structural and functional characterization of 2D and 3D cell models (in terms of morphology, cell viability and phenotype).

HT29 colorectal cancer cells cultured in T-flasks grow in two dimensions, forming a monolayer of cells, as depicted in Figure 4.5-A. In this 2D cell model, these epithelial cells grow adherently to the surface, a phenomena known as anchorage-dependent growth. In a stage of sub-confluent growth these cells tend to form islands (data not shown), and as they grow they become polarized (Figure 4.5-A).

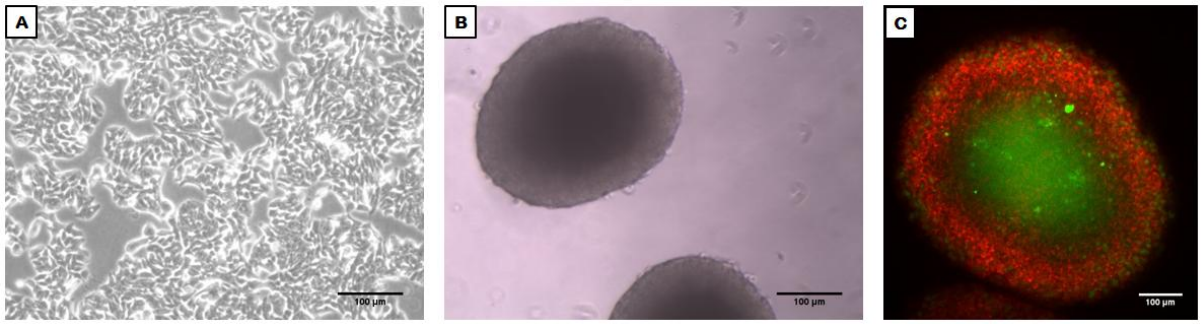

Figure 4.5. ***Morphological and structural characterization of 2D and 3D cell models of colorectal cancer.*** Morphological characterization was carried out by light microscopy for observation of HT29 cell monolayer **(A)** and colorectal cancer cell spheroids recovered at 7th day of spinner vessel culture **(B)**. Cell viability within the spheroid was assessed by fluorescence confocal microscopy through detection of caspase-3 activity **(C)**, showing a necrotic core within the spheroid (in green) and an outer layer composed of viable cells (in red). *Scale bar of 100µm.*

In the other hand, when HT29 cells are cultured in a spinner flask stirred bioreactor they have the ability to grow in the form of cell spheroids. Spheroid generation from HT29 cells is a gradual procedure that involves initial cell aggregation, followed by spheroid compaction and finally spheroid growth, during which a gradual increase in size occurs (Santo et al., 2016). Upon achieving complete aggregation, i.e. the establishment of compact spheroids, and after a daily medium renewal of the bioreactor system, it was possible to obtain at the 7th day of culture colorectal cancer spheroids that presented an average diameter of 500µm (Figure 4.5.-B).

To confirm the establishment of a structural hierarchy within these spheroids, the activity of caspase-3 was assessed. As already explained in “Materials and Methods”, the NucView488^{TM} and MitoView633^{TM} Apoptosis Assay is a fluorescence-based method that allows to differentiate between healthy and apoptotic cells, by detecting bright red or bright green fluorescence, respectively. In this assay, apoptotic cells were identified based on the activity of caspase-3, one of the most well-known markers of apoptosis.

The results showed a high activity of caspase-3 within the spheroids, which points to a high content of apoptotic cells in the core of the spheroid. In contrast, a high content of viable cells was detected in the outer/peripheral section of the spheroid (Figure 4.5.-C). Therefore, we can assume that at 7th day of culture these spheroids comprised the presence of a necrotic center and a more peripheral proliferating zone. In the conditions, it is plausible that cells in these spheroids are subject to pathophysiological gradients (as explained in “Introduction”) with the most inner cells being subject to a lower bioavailability of nutrients and oxygen, whereas cells that comprise the spheroid periphery have easier access to nutrients and oxygen. Hence, these spheroids appear to be a reliable tool to be used in cancer research since they mimic the *in vivo* bioavailability of these factors (Hirschhaeuser et al., 2010; LaBarbera et al., 2012).

Additionally, the ability of this 3D cell culture method generate cells with a phenotype that best resembles the cancer cells *in vivo* was explored by through the ALDEFLUOR ^{TM} and soft agar assays.

ALDH1 is a cytosolic detoxifying enzyme that oxidizes cellular aldehydes into carboxylic acids and confers resistance to alkylating chemotherapeutic agents, being considered as a putative CSC marker associated with tumor progression (Huang et al., 2009).

The results demonstrated that spheroids have a more CSC-like phenotype in comparison with the 2D cell model (Figure 4.6-A). Cells derived from spheroids upon enzymatic dissociation (see "Materials and Methods" section) presented a higher ALDH1 activity, and therefore we can assume that spheroids have a higher subpopulation of ALDH $^{positive/+}$ cells comparing with the 2D cell model. In this context, spheroids will recapitulate best the *in vivo tumor* chemotherapeutic response since a higher ALDH1 activity can enhance tumor chemo-resistance (Abdullah and Chow, 2013).

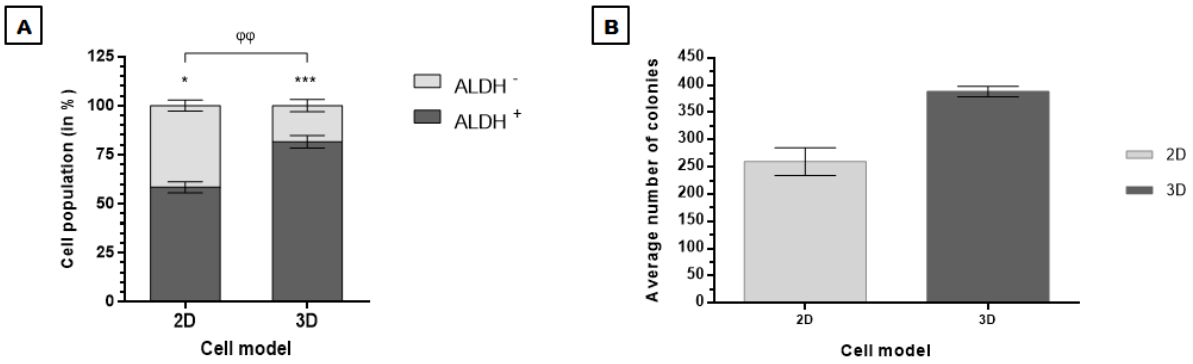

Figure 4.6. ***Phenotypical characterization of 2D and 3D cell models of colorectal cancer.*** Phenotypical characterization was carried out by detection of ALDH1 activity **(A)** and cells ability to growth in an anchorage-independent manner (soft agar assay) **(B)**. Results are expressed as mean of at least two independent experiments performed in duplicate ± SD. In (A) *p-value<0.05 and ***p-value<0.001 are relative to the overall population; ϕϕp-value<0.01 relative to 2D cell model.

The CSC-like phenotype of both models was also assessed by evaluating the ability of cells to form colonies in soft agar, a capacity that is related with anchorage-independent cell growth and with self-renewal typical of CSCs (Ricci-Vitiani et al., 2007; Vermeulen et al., 2008). In this context, spheroid-derived cells proved to be more efficient in forming colonies than monolayer-derived cells (Figure 4.6.-B). This is extremely important when considering cancer metastasis, since in this event single cells must have the ability to grow in an anchorage-independent manner and have self-renewal potential to colonize the potential secondary tumor site (Mori et al., 2009; Xu et al., 2015).

Overall, these results confirm that our 3D cell model of colorectal cancer recapitulates best the tumor microenvironment and its functional characteristics when comparing with the 2D cell model. Therefore, spheroids become a more reliable tool to perform assays with the aim to explore the anticancer effects of compounds of interest. Notwithstanding, the 2D cell model can be used to perform initial screening of the biological effect of these effects, since it is less time consuming.

4.3. Antiproliferative effects of natural extracts and bioactive compounds using 2D cell model of colorectal cancer

The efficacy of natural extracts and respective ITCs in preventing cell proliferation was first assessed using 2D cell model of colorectal cancer. The results, shown in Figure 4.7. A-B, demonstrated that all samples have the potential to inhibit colorectal cancer cell proliferation. However, the most used chemotherapeutic agent, 5-Fu, was not so effective as natural extracts and ITCs when considering the same concentrations of the bioactive principle – Figure 4.7-C.

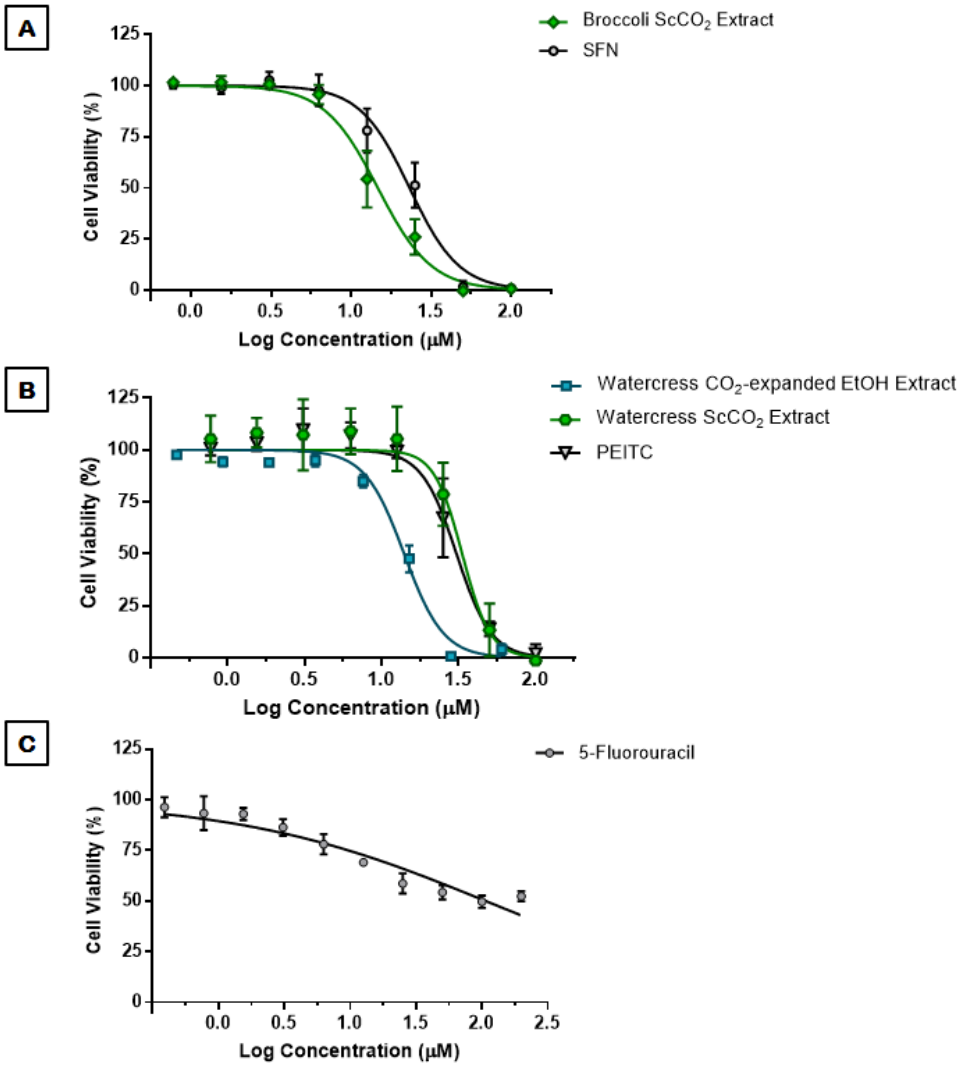

Figure 4.7. ***Antiproliferative effect of natural extracts, ITCs and 5-Fu in 2D cell model of colorectal cancer***. Dose-response profiles of the antiproliferative effect induced by *Brassicaceae* extracts, ITCs and 5-Fu after a 24h period of incubation. **(A)** Dose-response curve obtained for the antiproliferative effect of broccoli $ScCO_2$ extract and its main ITC, SFN. **(B)** Dose-response profile of the antiproliferative effect of watercress $ScCO_2$ extract, watercress CO_2-expanded EtOH extract and PEITC. **(C)** Dose-response curve obtained for the antiproliferative effect of 5-Fu in HT29 cells. *Results are means of 3 independent experiments performed in triplicate ± SD. Green stands for $ScCO_2$ extracts of Brassicaceae, blue for watercress CO_2-expanded EtOH extract, black for ITCs and grey for 5-Fu.*

The dose-response prolife of HT29 cells treated with broccoli extract showed that this extract is more effective in preventing cell proliferation than SFN (Figure 4.7-A). This was further confirmed by comparing the respective EC_{50} values of both compounds, depicted in Figure 4.8. EC_{50} values showed that broccoli extract (EC_{50} ≈ 15μM) is more effective than SFN (EC_{50} ≈ 23μM) in inhibiting 50% of cell proliferation, although this was not statistically significant. Overall, this suggests that SFN is not the only compound in the broccoli extract responsible for its biological effect. This is in line with the complex phytochemical composition of this extract (Figure 4.4.). Hence, we can assume that other compounds in broccoli extract can synergize with SFN, rendering this extract with enhanced antiproliferative efficacy.

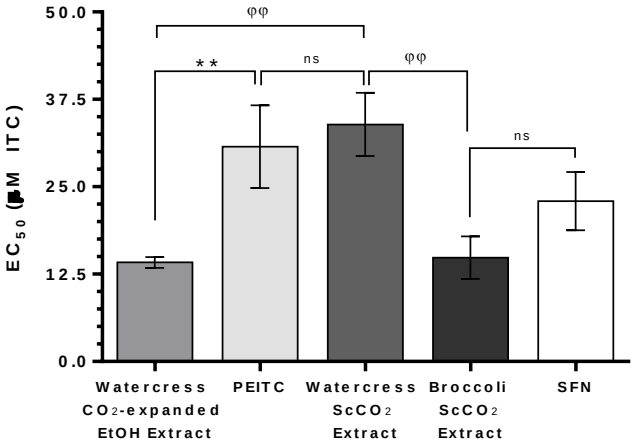

Figure 4.8. ***EC_{50} values obtained in the antiproliferative assay using 2D cell model of colorectal cancer.*** EC_{50} value (presented in μM of ITC) represents the concentration that renders a decrease of 50% in cell proliferation upon treatment with natural extracts and respective ITCs for 24h. *Results are means of 3 independent experiments performed in triplicate ± SD.* **p-value<0.01 is relative to PEITC; ϕϕp-value<0.01 is relative to watercress $ScCO_2$ extract.

On the other hand, the dose-response profiles for watercress $ScCO_2$ extract and PEITC were very similar (Figure 4.7.-B), which is further validated by their EC_{50} values. Between both samples, watercress $ScCO_2$ extract showed a slightly higher EC_{50} value (≈33 μM) than PEITC (≈31 μM), although this was not statistically significant (Figure 4.8.). The similar antiproliferative effect of this extract in comparison with PEITC could be explained based on its phytochemical composition, in which PEITC was the only compound identified by GC-MS analysis along with the poor phenolic content (detected by the Folin-Ciocalteau method). Until now, few reports have confirmed the anti-proliferative effect of PEITC in colorectal cancer cells. Nonetheless, it was demonstrated that in HT29 cells this compound promotes G1 cell cycle arrest (Cheung et al., 2008). More recently, Liu and colleagues have reported that PEITC inhibits the proliferation of SW480 colon cancer cells in a dose- and time-dependent manner (Liu et al., 2013a). Hence, we can assume that the antiproliferative activity of watercress $ScCO_2$ extract is almost entirely resultant from PEITC content. This is in line with

the highly selectivity of our CO_2 supercritical extraction method for ITC recover from watercress (Rodrigues et al., 2016).

Inversely, the CO_2-expanded EtOH watercress extract showed a higher antiproliferative response in comparison with PEITC (Figure 4.7.- B). Accordingly, this extract presented a significantly lower EC_{50} value (≈14 μM), comparing with PEITC. Similarly, this extract also showed a significantly lower EC_{50} value in comparison with its counterpart obtained by supercritical CO_2 extraction. This can be explained based on the high content in phenolic compounds (533.2 mg GAE/L extract) obtained for this extract (Figure 4.1), some of which were previously identified as being: Caffeic acid; Caffeoylmalate; Coumaric acid, rutin; Coumaroylmalate; Feruloylmalate and Sinapoylmalate (Figure 4.2.). For instance, it was recently reported the anti-proliferative effect of caffeic acid derivatives in HCT116 and SW480 colorectal cancer cells in consequence of enhanced AMP-activated protein kinase (AMPK) activation that led to G0/G1 cell cycle arrest (Chiang et al., 2014). Therefore, the phenolic compounds present in the CO_2-expanded EtOH watercress extract may synergize with PEITC, rendering an enhanced antiproliferative effect in colorectal cancer that is statistically more effective when comparing with watercress $ScCO_2$ extract.

Assumptions can also be made when comparing different *Brassicaceae* extracts obtained by the same high-pressure extraction method, i.e. supercritical CO_2 extraction. By comparing both dose-response profiles for these extracts (Figure 4.7 – A and B) it appears that broccoli extract is more effective than watercress $ScCO_2$ extract, a trend that is further corroborated when looking at EC_{50} values (Figure 4.8). In fact, broccoli extract is statistically more effective in preventing colorectal cancer cells proliferation than watercress extract, an effect that could be resultant from the phytochemical composition of broccoli. Whereas in cells treated with watercress $ScCO_2$ extract the antiproliferative effect is almost exclusively due to PEITC, in broccoli $ScCO_2$ extract treated cells the antiproliferative effect can derive from the synergy between SFN and other compounds, namely phenolic compounds (103.8 mg GAE/L extract). To note that in watercress $ScCO_2$ extract only a vestigial fraction of phenolic compounds was detected, as shown in Figure 4.1, an occurrence that can be explained by the low solubility of these compounds in the supercritical fluid (CO_2), as already explained in "*Introduction*" section.

Treatment with 5-Fu was not so effective in preventing cell proliferation, comparing with extracts and ITCs. As shown in Figure 4.7.-C, treatment with this chemotherapeutic agent rendered a more discrete dose-response profile in colorectal cancer cells, and a *plateau* in cell proliferation was reached after attaining an antiproliferative effect of 50% (EC_{50}≈100μM, data not shown). With these results one can assume that natural bioactive compounds appear to be a more effective and promising strategy for colorectal cancer therapy rather than 5-Fu.

Since the major goal of this dissertation was to explore the role of ITC-rich extracts in colorectal cancer therapy within the NutraBrass Project, the CO_2-expanded EtOH watercress extract was past behind in detriment of the watercress $ScCO_2$ extract. However, it will be interesting in a near future to test the potentially of the synergy between phenolic compounds and PEITC in colorectal cancer cells.

4.4. Antiproliferative effects of natural extracts and bioactive compounds using 3D cell model of colorectal cancer

After confirming the potential antiproliferative effect of natural extracts and bioactive compounds using a 2D cell model, we performed the same experiments using the 3D cell model (previously characterized), in order to confirm if these compounds also exert anticancer effects in a more complex biological scenario. To note that due to cell density increase, inherent to the cellular structure of the spheroid *per se*, we tested higher concentrations than in 2D cell model.

In resemblance with results obtained in 2D cell model, natural extracts and respective ITCs also induced an inhibitory effect in cell proliferation of colorectal cancer spheroids. The same trend in dose-response profile was obtained for cells treated with broccoli $ScCO_2$ extract and SFN – Figure 4.9-A. In this case, it was reinforced, once again, the higher antiproliferative effect of broccoli $ScCO_2$ extract in comparison with SFN, as described for 2D cell model. In fact, broccoli $ScCO_2$ presented a lower EC_{50} value (50.9 µM) in comparison with SFN (128.7 µM) – Figure 4.10.

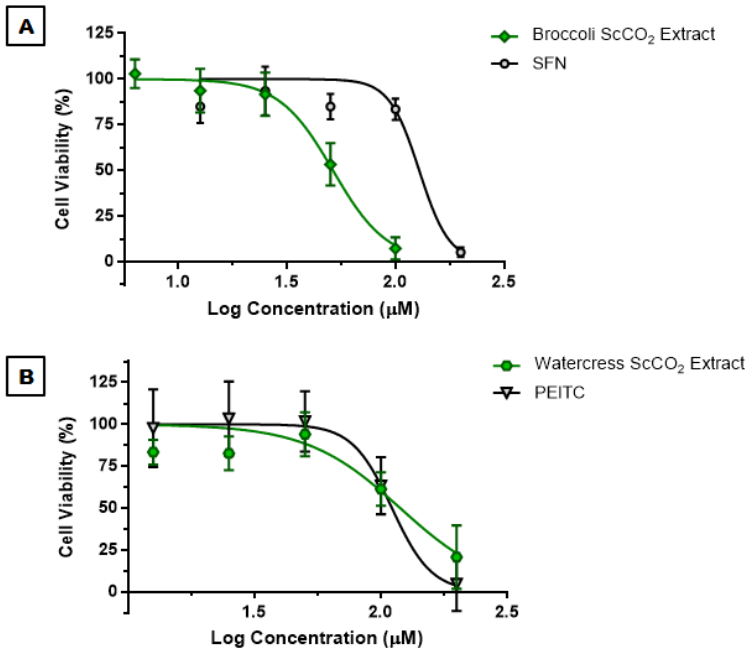

Figure 4.9. ***Antiproliferative effect of natural extracts and ITCs in 3D cell model of colorectal cancer***. Dose-response profiles of the antiproliferative effect induced by *Brassicaceae* extracts and ITCs after a 24h period of incubation. **(A)** Dose-response curve obtained for the antiproliferative effect of broccoli $ScCO_2$ extract and its main ITC, SFN. **(B)** Dose-response profile of the antiproliferative effect of watercress $ScCO_2$ extract and PEITC. *Results are means of at least 3 independent experiments performed in triplicate ± SD. Green stands for $ScCO_2$ extracts of Brassicaceae and black for ITCs.*

In contrast, watercress $ScCO_2$ extract and PEITC dose-response profiles displayed a similar behavior, as noted for 2D cell model. In a similar way to 2D cell model, also in cell spheroids was observed a

slightly decrease in EC_{50} of watercress $ScCO_2$ when comparing with PEITC (121.2 µM and 110.6 µM, respectively).

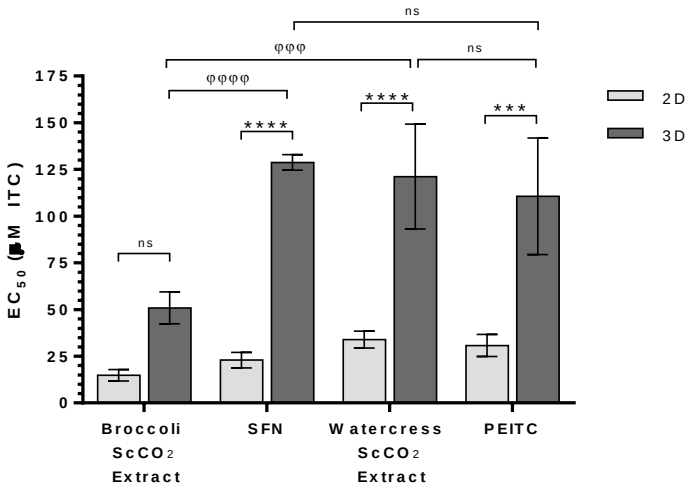

Figure 4.10. ***EC_{50} values obtained in the antiproliferative assay using 3D cell model of colorectal cancer.*** EC_{50} value (presented in µM of ITC) represents the concentration that renders a decrease of 50% in cell proliferation upon treatment with natural extracts and respective ITCs for 24h. *Results are means of at least 3 independent experiments performed in triplicate ± SD.* ***p-values<0.001 and ****p-values<0.0001 are relative to the same extract/ITC between both cell models; ϕϕϕp-values<0.001 and ϕϕϕϕp-values<0.0001 relative broccoli $ScCO_2$ extract.

Overall, the EC_{50} values obtained for all samples were much higher than those obtained in 2D cell model (Figure 4.10). For watercress $ScCO_2$ extract and PEITC an increase up to almost four times was attained in relation with 2D cell model. This fold increase was much more discrepant when comparing broccoli $ScCO_2$ extract and SFN, with an increase up to almost three and six times, respectively. This discrepancy between the fold increase of EC_{50} values for extracts and ITCs relatively to 2D cell model may be explained by the establishment of gradients within the spheroid. As already mentioned above head, when spheroids reach a mean diameter of 500µm they become "stratified" in terms of cell viability and bio-availability of nutrients, oxygen, and other possible compounds (Hirschhaeuser et al., 2010; LaBarbera et al., 2012), which in turn could explain the chemo-resistant phenotype of these cells (Karlsson et al., 2012).

Nonetheless, we then assessed the possible effects of these compounds in inducing cell cycle arrest, an analysis carried out by flow cytometry using a fluorescence marker that stoichiometrically binds to DNA. Therefore, it was possible to evaluated the different cell cycle phases considering the fluorescence intensity signal that was intrinsically dependent on the number of DNA copies. In this way, since G1 phase-arrested cells contain only 1 copy of DNA, G2 phase-arrested cells 2 copies of

DNA and S phase-arrested cells an intermediate DNA content, a gradient of fluorescence intensity can be reached according with the DNA content (Darzynkiewicz et al., 2010).

To study the effect of these compounds in cell cycle arrest, we considered a dose treatment with the concentration of extracts that rendered 30% of antiproliferative effect in 3D cell model (ITCs were tested at the same concentration of the respective extract). After a 24hour incubation with natural extracts and ITCs, the results showed that all samples inhibit cell proliferation by inducing cell cycle arrest at phase G2/M, which translates the enrichment of cells in phase G2/M relatively to control (Figure 4.11.). This effect is in accordance with previous reports in colorectal cancer cells treated with PEITC and SFN (Chen et al., 2012; Cheung et al., 2008).

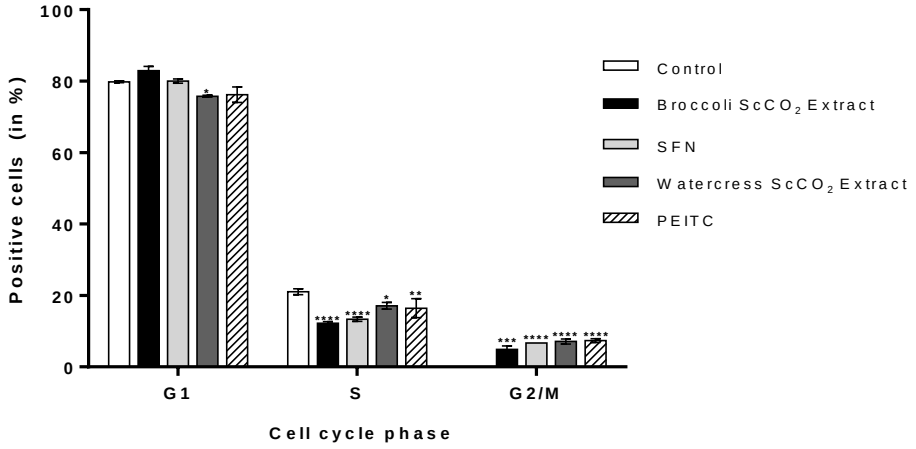

Figure 4.11. ***Cell cycle arrest induced by natural extracts and ITCs*****.** Cell cycle distribution in HT29 cell spheroids after treatment with natural extracts and respective ITCs for 24h. Tested concentrations were based on the dose of extract that corresponds to a decrease of 30% in cell proliferation (the respective ITCs were tested at the same concentration of the extract). *Results are means of two independent experiments performed in duplicate ± SD.* *p-values<0.05, **p-values<0.01, ***p-values<0.001 and ****p-values<0.0001 are relative to control.

To further confirm these results, analysis of the expression of cell cycle-related genes was performed by qPCR. Our results (Figure 4.12) demonstrated a significantly higher p21 expression after a 24h treatment with 50µM of broccoli extract and SFN, pointing out cell cycle arrest at phase G1 (Harada and Ogden, 2000). Dissimilar gene expression behaviors were observed for watercress extract and PEITC when considering the same dose, although this was not significant. This result is not in line with the flow cytometry result, which suggests that different doses can induce cell cycle arrest at different stages (since in the flow cytometry assay the tested dose was the EC_{30}, whereas in qPCR analysis the p21 increase occurred at the EC_{50} value for broccoli extract and same concentration of SFN, as well as at the EC_{50} value for SFN).

On the other hand, treatment with all samples led to an increase in Cyclin A2 expression, which do not suggest G2/M cell cycle arrest. This result is not in line with the result obtained by flow cytometry (Figure 4.11) confirming cell cycle arrest at G2/M in colorectal cancer spheroids upon treatment with ITCs and natural extracts. Cell cycle arrest at G2/M stage upon treatment with SFN was already reported in colorectal cancer cells of the same cell line with subsequent increase in Cyclin A2 expression (Gamet-Payrastre et al., 2000). Therefore, one could not exclude that increased levels in this marker might be derived from DNA damage induced by ITCs, since these compounds can elicit ROS generation in cancer cells (Trachootham et al., 2006).

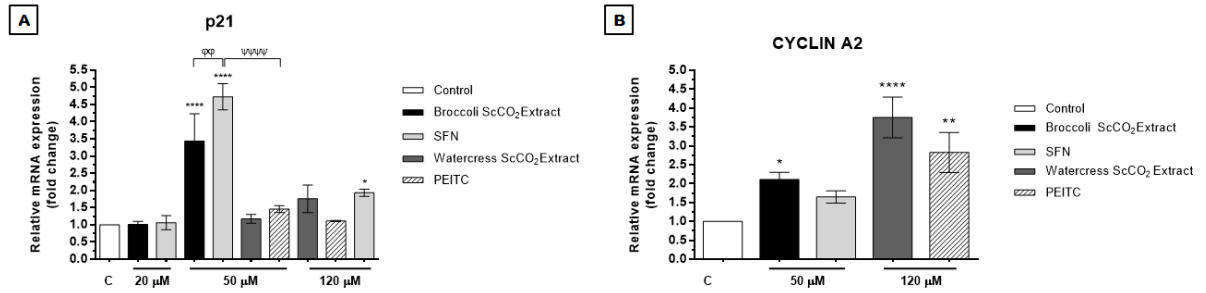

Figure 4.12. ***Analysis of p21 and cyclin A2 expression in colorectal cancer spheroids.*** Antiproliferative effect of natural extracts and ITCs measured by p21 and cyclin A2 expression, upon a 24hour's treatment. Results are expressed as mean of one experiment performed in triplicate ± SD. *p-value<0.05, **p-value<0.01, ***p-value<0.001 and ****p-value<0.0001 are relative to control; ϕϕp-value<0.01 is relative to broccoli $ScCO_2$ extract; ΨΨΨΨp-value <0.0001 relative to control PEITC.

Further studies involving different incubation times and different time-points to assess cell cycle arrest should be carried out, in order to unveil the precise mechanisms of cell cycle arrest and if it is, or not, time- and dose- dependent.

4.5. Apoptotic effects of natural extracts and bioactive compounds using 3D cell model of colorectal cancer

The potential of *Brassicaceae* natural extracts and ITCs to induce cell death in colorectal cancer cell spheroids was explored by the detection of caspase-3 activity, one of the main effectors of apoptosis (Elmore, 2007).

For both extracts and ITCs the maximum tested concentration was an approximate value to their respective EC_{50} obtained in the antiproliferative assay performed in 3D cell model (120 µM for watercress $ScCO_2$ extract, PEITC and SFN, and 50 µM for broccoli $ScCO_2$ extract). Overall, results depicted in Figure 4.13. and 4.14. showed that the EC_{50} value obtained in 3D antiproliferative assay induces apoptosis in cell spheroids. In fact, apoptosis induction increased in a dose-dependent

manner, with this effect being more prominent in the spheroid periphery, as one can see in Figures 4.13-E, F and Figure 4.14.-D, E, by the increase in apoptotic cells in the outer most layer of the spheroid. This apoptotic effect is in line with previous studies reporting apoptosis induction after treatment with PEITC and SFN in colorectal cancer cells (Andelova et al., 2007; Roy et al., 2013; Rudolf and Cervinka, 2011).

The low content of apoptotic cells in the periphery of cell spheroids at low dose treatments (Figure 4.13-B, C, D. and 4.14-B, C) could be due to low diffusion of natural extracts and ITCs towards spheroid inner milieu. Since spheroids at 7th day of spinner culture have an average diameter of 500µm and a necrotic core, as already described previously, this chemo-resistant phenotype could be derived from the spheroid cellular structure *per se*, that at this stage offers nutrient/oxygen input limitations, and therefore, phytochemical compounds input limitations (Hirschhaeuser et al., 2010; LaBarbera et al., 2012).

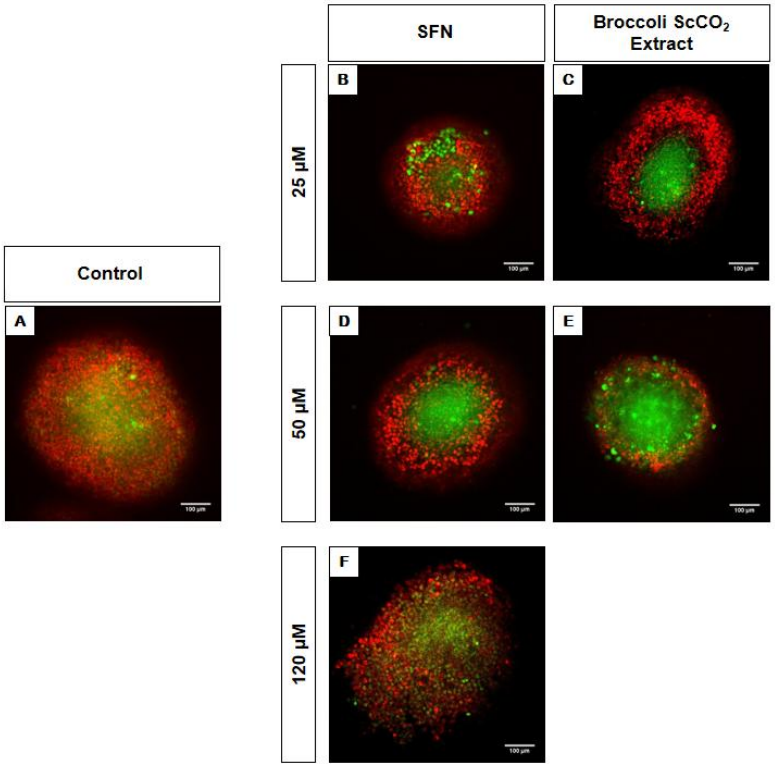

Figure 4.13. ***Detection of caspase-3 activity in colorectal cancer spheroids treated with broccoli extract and SFN.*** Apoptosis assessment in HT29 cell spheroids incubated with SFN – **(B)** 25µM, **(D)** 50 µM and **(F)** 120µM) and broccoli $ScCO_2$ extract – **(C)** 25µM and **(E)** 50 µM -, for 24hours, was carried out by fluorescence confocal microscopy. **(A)** Control without treatment. Green stands for apoptotic cells (high caspase-3 activity) and red for viable cells (high mitochondrial activity). *Scale bar of 100µm.*

To note that, at same concentrations, both extracts have a higher apoptotic effect in colorectal cancer spheroids than their respective ITCs. This increase in peripheral apoptotic cell content in spheroids

corroborates the existence of other potential compounds in $ScCO_2$ extracts with possible apoptotic activity that may synergize with ITCs.

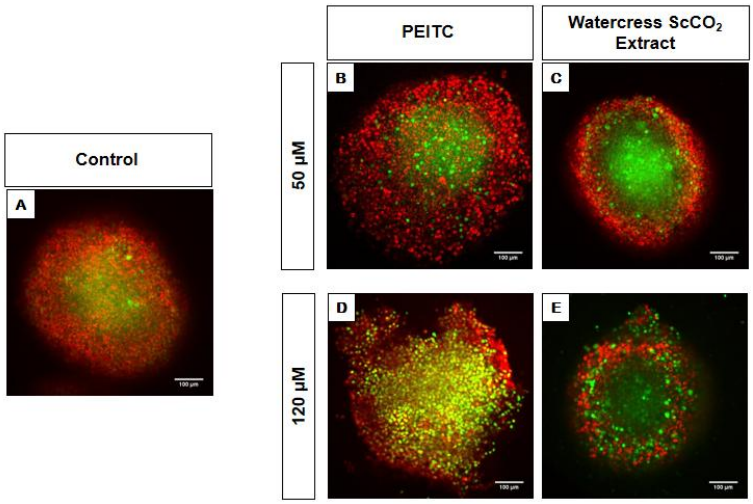

Figure 4.14. ***Detection of caspase-3 activity in colorectal cancer spheroids treated with watercress extract and PEITC.*** Apoptosis assessment in HT29 cell spheroids incubated with PEITC – **(B)** 50µM and **(D)** 120 µM and watercress $ScCO_2$ extract – **(C)** 50µM and **(E)** 120 µM -, for 24hours, was carried out by fluorescence confocal microscopy. **(A)** Control without treatment. Green stands for apoptotic cells (high caspase-3 activity) and red for viable cells (high mitochondrial activity). *Scale bar of 100µm.*

Moreover, treatment with extracts and ITCs showed no significant influence the expression of survivin (Figure 4.15), an anti-apoptosis marker (Altieri, 2003). However inconsistent results were obtained for 50µM of SFN and for the highest concentration tested in watercress $ScCO_2$ extract and PEITC. Overall, these results suggest that broccoli extract at the EC_{50} value induce less the expression of survivin and that, to avoid the expression of this marker, intermediate concentrations of watercress extract and PEITC should be used.

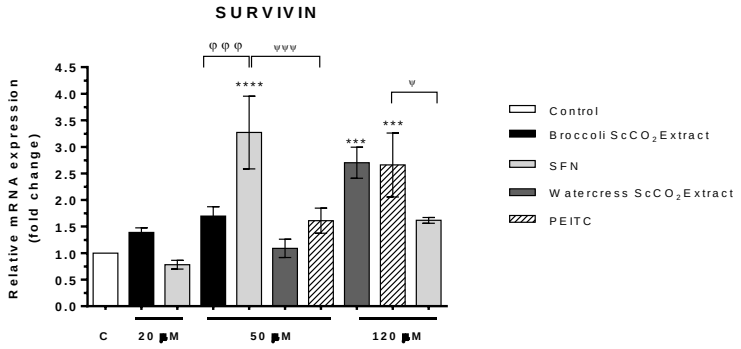

Figure 4.15. ***Analysis of survivin expression in colorectal cancer spheroids.*** Apoptotic effect of natural extracts and ITCs measured by survivin expression, upon a 24hour's treatment. Results are expressed as mean of one experiment performed in triplicate ± SD. ***p-value<0.001 and ****p-value<0.0001 are relative to control; ϕϕϕp-value<0.001 is relative to broccoli $ScCO_2$ extract; Ψ<0.05 and ΨΨΨ<0.001 relative to PEITC at same concentration.

4.6. Targeting CSC-like features of colorectal cancer cell spheroids using natural extracts and bioactive compounds

One of the most crucial aspects in colorectal cancer therapy is the prevalence of CSCs even after radio- and chemo-therapy (Saigusa et al., 2009; Saigusa et al., 2010). Therefore, is imperative to seek new therapeutic strategies to circumvent this issue. In this context, and according to epidemiological evidences pointing the chemo-preventive role of cruciferous vegetables, *Brassicaceae*-derived bio-active compounds appear to be a promising strategy. In this part of the work, the biological effect of *Brassicaceae* extracts and their respective ITCs in CSC-like related cellular events/markers was further explored, in order to unveil their potential application in colorectal cancer therapy.

4.6.1. Evaluation of anchorage-independent cell growth

The effect of *Brassicaceae* extracts and respective ITCs in preventing anchorage-independent cell growth was explored by the soft agar assay, which allowed to explore the ability of cells to form colonies from a single cell within a semisolid milieu, like the one proportionated by agarose.

Normal epithelial cells are unable to proliferate in the absence of anchorage to the ECM. In these cells the loss of contact with ECM components promote a form of programmed cell death named anoikis. In contrast, even in the absence of ECM components, cancer cells are able to evade this apoptotic process and have the potential to grow and proliferate, forming colonies (Guadamillas et al., 2011; Paoli et al., 2013). Anchorage-independent cell growth alongside with the self-renewal ability constitute one of the principal features related to CSCs (Ricci-Vitiani et al., 2007; Vermeulen et al., 2008).

Therefore, we intended to explore if the *Brassicaceae* extracts and respective ITCs have the ability to decrease the tumorigenic potential of colorectal cancer cells. To test the hypothesis, we performed the soft agar assay with single cells derived from the enzymatic dissociation of HT29 cell spheroids, since these cells have a more CSC-like phenotype compared with cells from a 2D system culture, as already discussed in section 4.2. (Figure 4.5. and Figure 4.6.). By counting colonies and measuring their average size, we tested the efficacy of extracts and ITCs in inhibiting the tumorigenic potential of these cells.

Results showed that both extracts and ITCs inhibit colony formation in a dose-dependent manner (Figure 4.16.). Between all samples, broccoli $ScCO_2$ extract and SFN were the most effective samples in inhibiting the formation of cell colonies with dose increase. In fact, the highest concentration of broccoli extract almost abolished completely the tumorigenic potential of these cells. Results demonstrated that with dose increase the anti-tumorigenic potential of broccoli extract became more accentuated.

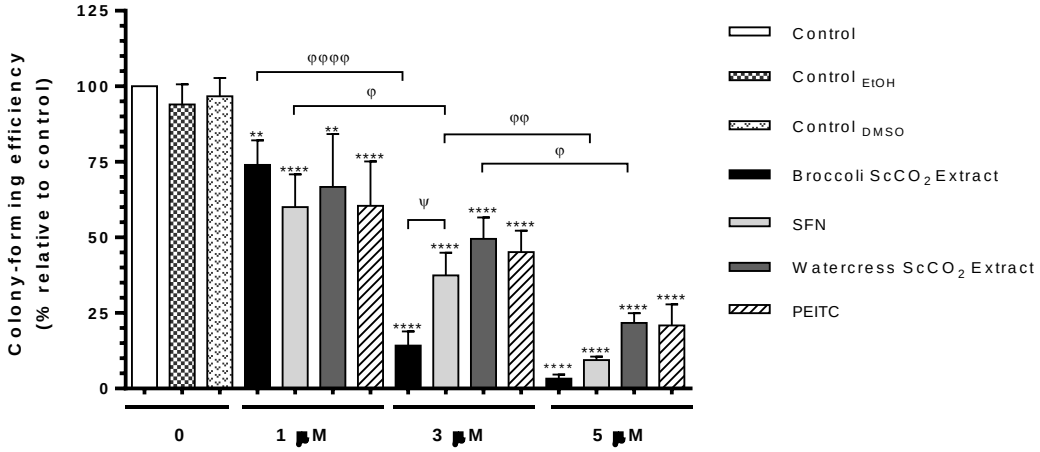

Figure 4.16. ***Inhibitory effects of natural extracts and ITCs in anchorage-independent cell growth using cells derived from HT29 spheroids.*** Inhibition of anchorage-independent cell growth upon a 15day treatment with natural extracts and ITCs. Results are means of at least two independent experiments performed in duplicate ± *SD*. **p-value<0.01 and ****p-value<0.0001 are relative to control; ϕp-value<0.05, ϕϕp-value<0.01, ϕϕϕϕp-value<0.0001 are relative to the same compound; Ψ<0.05 relative to broccoli $ScCO_2$ extract.

Besides affecting colony number, treatment with these natural compounds and respective ITCs also affected the average diameter of the colonies, as demonstrated for cells treated with SFN and broccoli extract in Figure 4.17 (data not shown for PEITC and watercress extract).

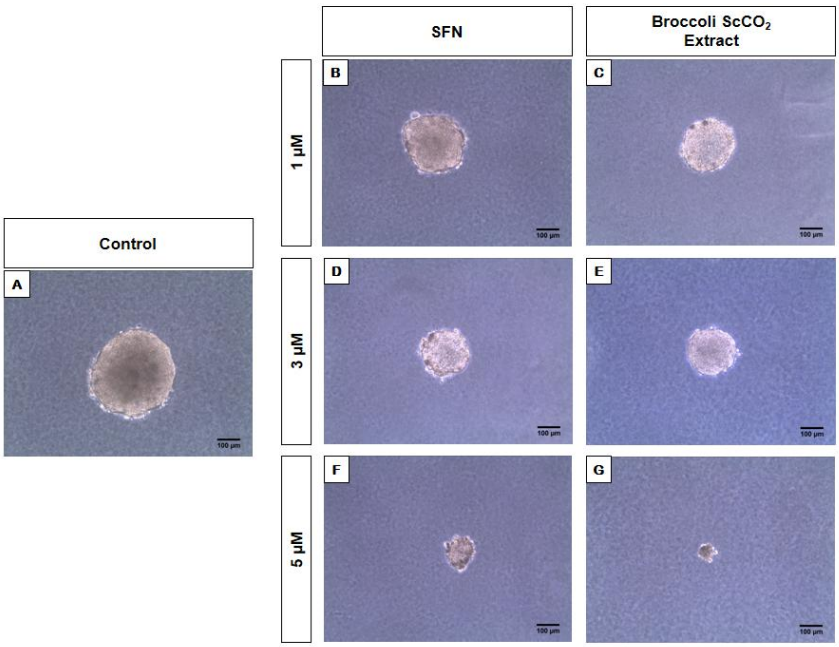

Figure 4.17. ***Inhibitory effects of broccoli extract and SFN in mean size of colonies formed by anchorage-independent cell growth and proliferation of spheroid-derived cells.*** Inhibition of anchorage-independent cell growth upon a 15day treatment with 1, 3 and 5µM of SFN **(B, D, F)** and broccoli extract **(C, E, G)**. **(A)** Control without treatment. *Scale bar = 100µm.*

Also, the treatment with watercress $ScCO_2$ extract and PEITC led to a significant decrease in the tumorigenic potential of colorectal cancer cells, in a dose-dependent manner, with a more pronounced effect at 5µM (Figure 4.16.). Moreover, both compounds exerted a similar response in these cells regardless of the dose increase (no statistically differences were observed between treatments with 1, 3 or 5 µM of bioactive compound). The same trend was previously observed in the antiproliferative effect of these compounds in cell spheroids, that rendered a similar dose-response profile, as already mentioned.

Overall, the results demonstrated that all *Brassicaceae* extracts and ITCs have the ability to induce anoikis in spheroid-derived cells and decreased their potential to grow in an anchorage-dependent manner. Therefore, one can assume that these samples decrease the metastatic and self-renewal potential of colorectal cancer cells with a CSC-like phenotype (Mori et al., 2009; Xu et al., 2015).

4.6.2. Assessment of ALDH1 activity

As already referred above, one of the dictating factors in the success of colorectal cancer therapy is the potential to successfully target and eradicate CSCs or even cells that undergo EMT.

In order to determine whether *Brassicaceae* extracts and/or respective ITCs have the potential to circumvent the detoxifying action of ALDH1 and/or decrease its activity, the detection of ALDH1 activity was carried out by flow cytometry using the ALDEFLUOR^{TM} Assay Kit.

In this experiment, spheroids between the 6-7th days of culture were incubated for 24hours with natural extracts and respective ITCs ate the same concentration. A rational for the tested concentrations was established based on the EC_{50} values obtained in the antiproliferative assay using 2D cell model, with the lower tested concentration being an approximation of the EC_{50} obtained in 2D cell model for each extract, and the higher concentration being the double of the EC_{50} value. With this, we intended to evaluate if natural extracts and ITCs were able to decrease ALDH1 activity even at “sub-therapeutic” doses comparing with other experiments in which higher doses were applied. For comparison between ITCs, SFN concentrations were extended up to 60µM.

The results depicted in Figure 4.18. demonstrated that despite the dose of broccoli extract and SFN (15 and 30µM) these samples do not have the potential to target the $ALDH^+$ subpopulation. However, to evaluate if this was a dose-dependent effect, or not, we increased the SFN concentration up to 60µM, which rendered a significantly higher effect when comparing with lower SFN doses. So, its plausible to assume that increase in broccoli extract dose could also display more promising effects in decreasing ALDH1 activity, but already outside the “sub-therapeutic” dosage.

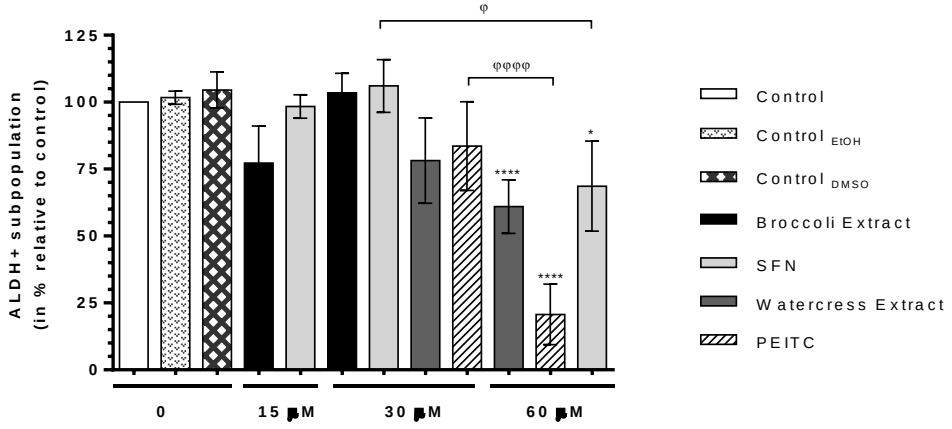

Figure 4.18. ***Inhibitory effect in ALDH1 activity by natural extracts and ITCs evaluated by ALDEFLUOR^{TM} assay using cells derived from HT29 spheroids.*** *Results are means of at least two independent experiments performed in duplicate ± SD.* *p-value<0.05 and ****p-value<0.0001 are relative to control; ϕp-value<0.05 and ϕϕϕϕp-value<0.0001 are relative to the same compound.

On the other hand, watercress extract and PEITC, at the highest concentration tested, led to a decrease in ALDH1 activity. Although both samples at 60 µM had the ability to decrease the ALDH$^+$ subpopulation, the effect of PEITC was more pronounced than that obtained in the case of watercress extract. So, it's possible to assume that other compounds (not detected by GC-MS and HPLC) may exist in the watercress extract that could explain the difference in this behavior, contrary to the similar biological effects between watercress extract and PEITC observed in other assays.

Notwithstanding, by observing the content of ALDH$^+$ cells after treatment with 60µM of PEITC and SFN we can affirm that, between ITCs, PEITC was the most effective in targeting ALDH1 activity inherent to cells with CSC-like phenotype.

In short, we can postulate that, among all samples, watercress extract and PEITC provide the highest effect in ALDH1 activity rendering a more effective decrease in the content of ALDH$^+$ cells. Therefore, since ALDH1 is responsible for tumor chemo-resistance (Abdullah and Chow, 2013) it can be assumed that these two samples are the more effective in CSCs eradication.

4.6.3. Analysis of the expression of CSC and EMT associated markers

Finally, the potential of these extracts and bioactive compounds to modulate several crucial events in tumorigenesis was further explored by the evaluation of gene expression of key target genes, namely putative CSC markers and genes related with several signaling pathways crucial to self-renewal and metastasis (Figure 4.19).

CD133 and LGR5 have been considered as colorectal CSC markers and correlated positively with metastasis and chemo-resistance (Liu et al., 2013b; Ren et al., 2013; Schneider et al., 2012; Wang et al., 2012; Wu et al., 2012). In general, *Brassicaceae* extracts showed the potential to promote the downregulation of CD133 and LGR5 markers (Figure 4.19), which suggests that these extracts have the capacity to target the CSC subpopulation. Considering the results for CD133, for watercress extract and PEITC this effect appears to be dose-dependent. A similar effect was seen for SFN, with exception of the highest concentration (120µM).

The expression of β-catenin, Axin2 and TCF7L2 was also assessed to explore if the extracts and ITCs have influence on one of the major pathways in colorectal cancer carcinogenesis, more precisely in the β-catenin /TCF7L2 axis of the Wnt signaling.

Normally, APC loss in colorectal cancer drives the deregulation of the Wnt pathway, with consequent translocation of β-catenin towards the nucleus where it accumulates and interacts with TCF7L2, resulting in unrestrained transcription of target genes, like CD44 involved in tumor progression (Fredericks, 2015; Huels and Sansom, 2015).

Our results showed that, in overall, treatment with samples, especially watercress extract and PEITC, led to a decreased β-catenin expression (with exception of SFN, although this event was not statistically significant), which is relevant when considering the most upstream activating events of the adenoma-to-carcinoma sequence of the tumorigenic process.

Attending that Axin2 functions as an oncogene in colorectal cancers with mutated APC (which is the case of HT29 cells) (Yochum, 2012) we can suggest that broccoli extract is the most promising compound for colorectal cancer therapy. In the other hand, when looking at TCFL2 expression that could be considered as a tumor suppressor gene (Angus-Hill et al., 2011), PEITC appears to be more effective in targeting tumorigenesis (at 50/120µM). However, the status of TCF7L2 as an oncogenic or tumor suppressor gene has been debatable (Angus-Hill et al., 2011).

More studies need to be performed to explore other putative CSC markers, as well as other targets of signaling pathways inherent to CSCs.

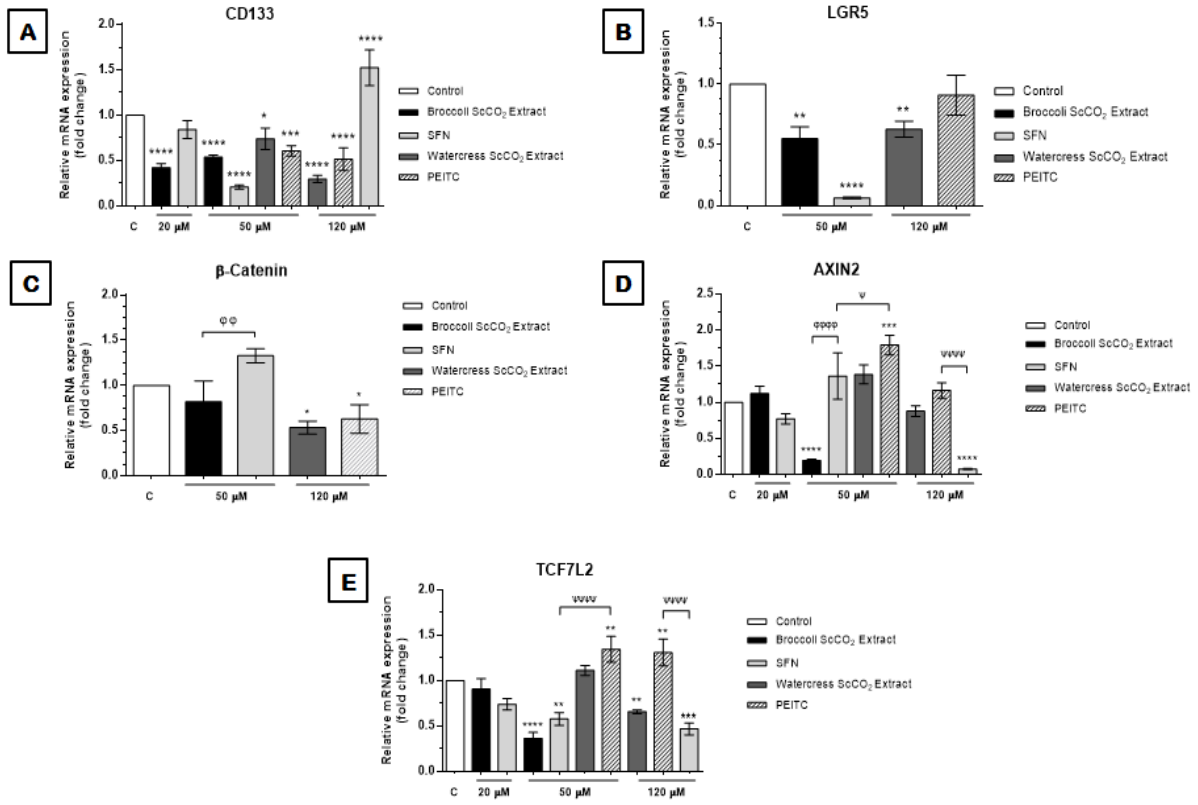

Figure 4.19. ***Effects of natural extracts and ITCs in genes related with EMT, self-renewal and stemness.*** Results are expressed as mean of one experiment performed in triplicate ± SD. *p-value<0.05, **p-value<0.01, ***p-value<0.001 and ****p-value<0.0001 are relative to control; ϕϕp-value<0.01 and ϕϕϕϕp-value<0.0001 relative to broccoli $ScCO_2$ extract; Ψp-value<0.05 and ΨΨΨΨp-value<0.0001 relative to PEITC.

4.7. Cytotoxicity of natural extracts and ITCs

The cytotoxic effect of natural extracts, ITCs and 5-Fu was tested using a Caco-2 cell model of the intestinal barrier. Results depicted in Figure 4.20 demonstrated that, excluding 5-Fu, all the samples exert cytotoxic effects in a dose-dependent manner. In Table 4.3. are summarized the IC_{50} values for each sample.

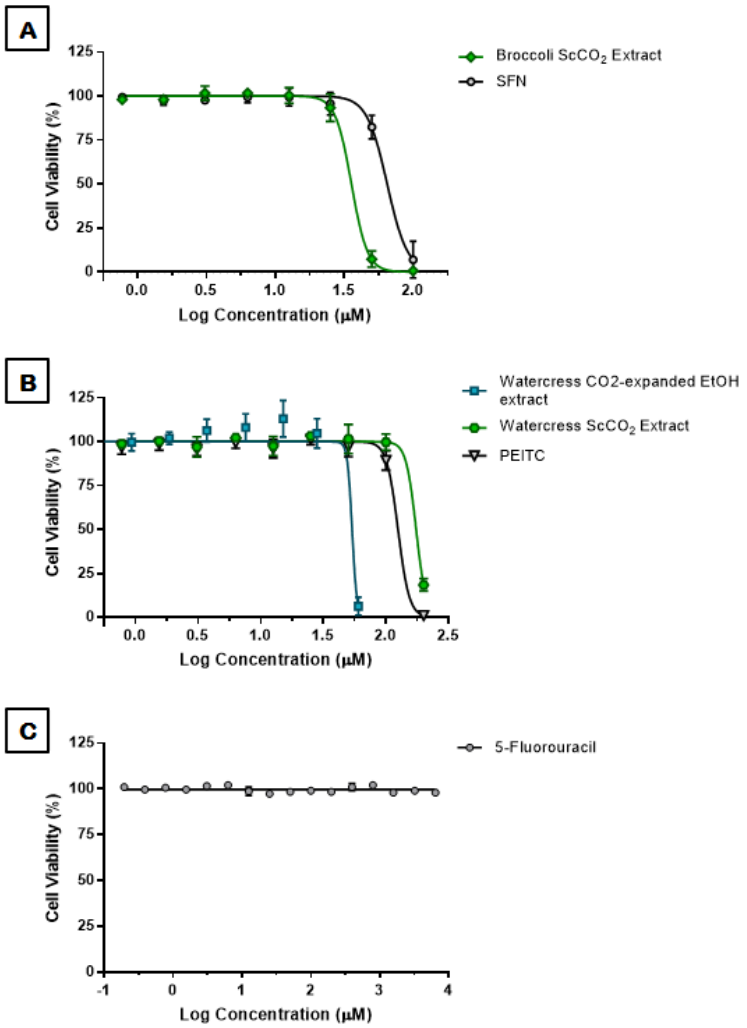

Figure 4.20. ***Cytotoxic effect of natural extracts, ITCs and 5-Fu in 2D cell model of intestinal barrier***. Dose-response profiles of the cytotoxic effect induced by *Brassicaceae* extracts, ITCs and 5-Fu in Caco-2 cells after a 24h period of incubation. **(A)** Dose-response curve obtained for the cytotoxic effect of broccoli $ScCO_2$ extract and its main ITC, SFN. **(B)** Dose-response profile of the cytotoxic effect of watercress $ScCO_2$ extract, CO_2-expanded EtOH watercress extract and PEITC. **(C)** Dose-response curve obtained for the cytotoxic effect of 5-Fu in Caco-2 cells. *Results are means of 3 independent experiments performed in triplicate ± SD. Green stands for $ScCO_2$ extracts of Brassicaceae, blue for CO_2-expanded EtOH watercress extract, black for ITCs and grey for 5-Fu.*

Table 4.3. ***IC_{50} values obtained in the cytotoxicity assay.***

Sample	IC_{50} (µM)
Broccoli $ScCO_2$ extract	35.73 ± 1.19
SFN	64.89 ± 2.48
Watercress $ScCO_2$ extract	174.00 ± 35.87
Watercress CO2-expanded EtOH extract	> 53.60
PEITC	124.70 ± 14.69
5-Fu	> 6400

Although most of all the concentrations used in the 3D-cell model assays are near the range of cytotoxicity, one cannot exclude the efficacy of these extracts and bioactive compounds in colorectal cancer therapy. Cytotoxicity issues can be circumvented by using delivery vectors that selectively target the colorectal cancer cells, more precisely the CSC niche. For instance, its plausible to design nanoparticles for extract/ITC delivery, with a coupled targeting moiety directed, for instance, to $LGR5^{+}$ or $CD133^{+}$ subpopulation.

More studies need to be addressed aiming at developing nano-carriers for these bioactive compounds, in order to couple their anticancer potential within a viable, non-toxic, therapeutic strategy.

5. Conclusions

In the present work, natural extracts from cruciferous vegetables obtained by supercritical CO_2 extraction were applied to cancer research to unveil their chemotherapeutic potential in colorectal cancer, especially in the CSC subpopulation.

The supercritical CO_2 extraction developed by the host lab was highly selective in recovering PEITC from watercress matrices, but in the case of broccoli an enormous plethora of phytochemical compounds were recovered when applying the same method. Therefore, in an over-all way, the anticancer mechanisms of PEITC and watercress $ScCO_2$ extract were similar, whereas broccoli extract and SFN displayed some discrepancies.

Nonetheless, both extracts and ITCs stand out by their antiproliferative and pro-apoptotic effects, as well as in inhibiting chemo-resistance, anchorage-independent cell growth and self-renewal. These effects alongside with their capacity to target the $LGR5^+$ and $CD133^+$ subpopulation, and hence the CSC-like phenotype, turn these extracts in potential chemotherapeutic compounds towards colorectal cancer therapy.

In our knowledge, this was the first work exploring the anticancer effects of cruciferous vegetables, as well as their respective ITCs, in colorectal cancer spheroids, which unveils an exciting start-point in this field, since the used 3D-cell model recapitulates best the tumor microenvironment *in vivo*.

Further studies are required namely in exploring other *stemness* markers, as well as other cellular phenotypes in terms of migration, as well as exosomes release, for instance, important aspects of metastasis. Additionally, a better characterization of these extracts will be required to understand if more compounds are involved in the anticancer effects of these natural extracts.

6. References

Abdullah, L.N., and E.K.H. Chow. 2013. Mechanisms of chemoresistance in cancer stem cells. *Clin Transl Med*. 2:3.

Ait Ouakrim, D., C. Pizot, M. Boniol, M. Malvezzi, E. Negri, M. Bota, M.A. Jenkins, H. Bleiberg, and P. Autier. 2015. Trends in colorectal cancer mortality in Europe: retrospective analysis of the WHO mortality database. *BMJ*. 351:h4970.

Altieri, D.C. 2003. Survivin, versatile modulation of cell division and apoptosis in cancer. *Oncogene*. 22:8581-8589.

Amann, A., G. Gamerith, J.M. Huber, M. Zwierzina, W. Hilbe, and H. Zwierzina. 2015. Predicting drug sensitivity by 3D cell culture models. *memo - Magazine of European Medical Oncology*. 8:77-80.

American Cancer Society. 2014. Colorectal Cancer Facts & Figures 2014-2016. In Atlanta: American Cancer Society.

Andelova, H., E. Rudolf, and M. Cervinka. 2007. In vitro antiproliferative effects of sulforaphane on human colon cancer cell line SW620. *Acta Medica (Hradec Kralove)*. 50:171-176.

Angus-Hill, M.L., K.M. Elbert, J. Hidalgo, and M.R. Capecchi. 2011. T-cell factor 4 functions as a tumor suppressor whose disruption modulates colon cell proliferation and tumorigenesis. *Proc Natl Acad Sci U S A*. 108:4914-4919.

Araujo, J.R., P. Goncalves, and F. Martel. 2011. Chemopreventive effect of dietary polyphenols in colorectal cancer cell lines. *Nutr Res*. 31:77-87.

Arnáiz, E., J. Bernal, M.T. Martín, C. García-Viguera, J.L. Bernal, and L. Toribio. 2011. Supercritical fluid extraction of lipids from broccoli leaves. *European Journal of Lipid Science and Technology*. 113:479-486.

Arnold, M., M.S. Sierra, M. Laversanne, I. Soerjomataram, A. Jemal, and F. Bray. 2016. Global patterns and trends in colorectal cancer incidence and mortality. *Gut*.

Aykan, N.F. 2015. Red Meat and Colorectal Cancer. *Oncol Rev*. 9:288.

Baenas, N., J.M. Silván, S. Medina, S. de Pascual-Teresa, C. García-Viguera, and D.A. Moreno. 2015. Metabolism and antiproliferative effects of sulforaphane and broccoli sprouts in human intestinal (Caco-2) and hepatic (HepG2) cells. *Phytochemistry Reviews*. 14:1035-1044.

Beachy, P.A., S.S. Karhadkar, and D.M. Berman. 2004. Tissue repair and stem cell renewal in carcinogenesis. *Nature*. 432:324-331.

Biotium. 2012. Apoptosis Assay Kit NucView™ 488 and MitoView™ 633. *In* Biotium.

Bishehsari, F., M. Mahdavinia, M. Vacca, R. Malekzadeh, and R. Mariani-Costantini. 2014. Epidemiological transition of colorectal cancer in developing countries: environmental factors, molecular pathways, and opportunities for prevention. *World J Gastroenterol*. 20:6055-6072.

Boman, B.M., and E. Huang. 2008. Human colon cancer stem cells: a new paradigm in gastrointestinal oncology. *J Clin Oncol*. 26:2828-2838.

Brabletz, T., F. Hlubek, S. Spaderna, O. Schmalhofer, E. Hiendlmeyer, A. Jung, and T. Kirchner. 2005. Invasion and metastasis in colorectal cancer: epithelial-mesenchymal transition, mesenchymal-epithelial transition, stem cells and beta-catenin. *Cells Tissues Organs*. 179:56-65.

Breslin, S., and L. O'Driscoll. 2013. Three-dimensional cell culture: the missing link in drug discovery. *Drug Discov Today*. 18:240-249.

Cappell, M.S. 2008. Pathophysiology, clinical presentation, and management of colon cancer. *Gastroenterol Clin North Am*. 37:1-24, v.

Cartea, M.E., M. Francisco, P. Soengas, and P. Velasco. 2011. Phenolic compounds in Brassica vegetables. *Molecules*. 16:251-280.

Chang, L.C., and Y.L. Yu. 2016. Dietary components as epigenetic-regulating agents against cancer. *Biomedicine (Taipei)*. 6:2.

Chemat, F., M.A. Vian, and G. Cravotto. 2012. Green extraction of natural products: concept and principles. *Int J Mol Sci*. 13:8615-8627.

Chen, J., and X. Xu. 2010. Diet, epigenetic, and cancer prevention. *Adv Genet*. 71:237-255.

Chen, M.J., W.Y. Tang, C.W. Hsu, Y.T. Tsai, J.F. Wu, C.W. Lin, Y.M. Cheng, and Y.C. Hsu. 2012. Apoptosis Induction in Primary Human Colorectal Cancer Cell Lines and Retarded Tumor Growth in SCID Mice by Sulforaphane. *Evid Based Complement Alternat Med*. 2012:415231.

Cheung, K.L., T.O. Khor, S. Yu, and A.N. Kong. 2008. PEITC induces G1 cell cycle arrest on HT-29 cells through the activation of p38 MAPK signaling pathway. *AAPS J*. 10:277-281.

Cheung, K.L., and A.N. Kong. 2010. Molecular targets of dietary phenethyl isothiocyanate and sulforaphane for cancer chemoprevention. *AAPS J*. 12:87-97.

Chiang, E.P., S.Y. Tsai, Y.H. Kuo, M.H. Pai, H.L. Chiu, R.L. Rodriguez, and F.Y. Tang. 2014. Caffeic acid derivatives inhibit the growth of colon cancer: involvement of the PI3-K/Akt and AMPK signaling pathways. *PLoS One*. 9:e99631.

Cho, H.J., and J.H. Park. 2013. Kaempferol Induces Cell Cycle Arrest in HT-29 Human Colon Cancer Cells. *J Cancer Prev*. 18:257-263.

Chung, Y.K., R. Chi-Hung Or, C.H. Lu, W.T. Ouyang, S.Y. Yang, and C.C. Chang. 2015. Sulforaphane down-regulates SKP2 to stabilize p27(KIP1) for inducing antiproliferation in human colon adenocarcinoma cells. *J Biosci Bioeng*. 119:35-42.

Colak, S., C.D. Zimberlin, E. Fessler, L. Hogdal, P.R. Prasetyanti, C.M. Grandela, A. Letai, and J.P. Medema. 2014. Decreased mitochondrial priming determines chemoresistance of colon cancer stem cells. *Cell Death Differ*. 21:1170-1177.

da Silva, R.P.F.F., T.A.P. Rocha-Santos, and A.C. Duarte. 2016. Supercritical fluid extraction of bioactive compounds. *TrAC Trends in Analytical Chemistry*. 76:40-51.

Darzynkiewicz, Z., H.D. Halicka, and H. Zhao. 2010. Analysis of cellular DNA content by flow and laser scanning cytometry. *Adv Exp Med Biol*. 676:137-147.

Degirolamo, C., S. Modica, G. Palasciano, and A. Moschetta. 2011. Bile acids and colon cancer: Solving the puzzle with nuclear receptors. *Trends Mol Med*. 17:564-572.

Dent, O.F., L. Bokey, P.H. Chapuis, C. Chan, and R.C. Newland. 2016. Trends in short-term outcomes after resection of colorectal cancer: 1971-2013. *ANZ J Surg*.

Dolznig, H., C. Rupp, C. Puri, C. Haslinger, N. Schweifer, E. Wieser, D. Kerjaschki, and P. Garin-Chesa. 2011. Modeling colon adenocarcinomas in vitro a 3D co-culture system induces cancer-relevant pathways upon tumor cell and stromal fibroblast interaction. *Am J Pathol*. 179:487-501.

Drewnowski, A., and C. Gomez-Carneros. 2000. Bitter taste, phytonutrients, and the consumer: a review. *Am J Clin Nutr*. 72:1424-1435.

Du, G.J., Z. Zhang, X.D. Wen, C. Yu, T. Calway, C.S. Yuan, and C.Z. Wang. 2012. Epigallocatechin Gallate (EGCG) is the most effective cancer chemopreventive polyphenol in green tea. *Nutrients*. 4:1679-1691.

Durko, L., and E. Malecka-Panas. 2014. Lifestyle Modifications and Colorectal Cancer. *Curr Colorectal Cancer Rep*. 10:45-54.

Dylla, S.J., L. Beviglia, I.K. Park, C. Chartier, J. Raval, L. Ngan, K. Pickell, J. Aguilar, S. Lazetic, S. Smith-Berdan, M.F. Clarke, T. Hoey, J. Lewicki, and A.L. Gurney. 2008. Colorectal Cancer Stem Cells Are Enriched in Xenogeneic Tumors Following Chemotherapy. *PLoS ONE*. 3.

Edmondson, R., J.J. Broglie, A.F. Adcock, and L. Yang. 2014. Three-dimensional cell culture systems and their applications in drug discovery and cell-based biosensors. *Assay Drug Dev Technol*. 12:207-218.

Elmore, S. 2007. Apoptosis: A Review of Programmed Cell Death. *Toxicol Pathol*. 35:495-516.

Espinoza, I., R. Pochampally, F. Xing, K. Watabe, and L. Miele. 2013. Notch signaling: targeting cancer stem cells and epithelial-to-mesenchymal transition. *Onco Targets Ther*. 6:1249-1259.

Fahey, J.W., S.L. Wehage, W.D. Holtzclaw, T.W. Kensler, P.A. Egner, T.A. Shapiro, and P. Talalay. 2012. Protection of humans by plant glucosinolates: efficiency of conversion of glucosinolates to isothiocyanates by the gastrointestinal microflora. *Cancer Prev Res (Phila)*. 5:603-611.

Favoriti, P., G. Carbone, M. Greco, F. Pirozzi, R.E. Pirozzi, and F. Corcione. 2016. Worldwide burden of colorectal cancer: a review. *Updates Surg*. 68:7-11.

Fredericks, E., Dealtry G. and Roux S. 2015. Molecular aspects of Colorectal Carcinogenesis - A Review. *J Cancer Biol Res 3(1): 1057.*

Gamet-Payrastre, L., P. Li, S. Lumeau, G. Cassar, M.A. Dupont, S. Chevolleau, N. Gasc, J. Tulliez, and F. Terce. 2000. Sulforaphane, a naturally occurring isothiocyanate, induces cell cycle arrest and apoptosis in HT29 human colon cancer cells. *Cancer Res*. 60:1426-1433.

Gil-Chávez, G.J., Villa, J. A., Ayala-Zavala, J. F., Heredia, J. B., Sepulveda, D., Yahia, E. M., González-Aguilar, G. A. 2013. Technologies for Extraction and Production of Bioactive Compounds to be Used as Nutraceuticals and Food Ingredients: An Overview. *Comprehensive Reviews in Food Science and Food Safety*. 12:5-23.

GLOBOCAN. 2012. IARC.

Golovko, D., D. Kedrin, O.H. Yilmaz, and J. Roper. 2015. Colorectal cancer models for novel drug discovery. *Expert Opin Drug Discov*. 10:1217-1229.

Gonzalez-Vallinas, M., M. Gonzalez-Castejon, A. Rodriguez-Casado, and A. Ramirez de Molina. 2013. Dietary phytochemicals in cancer prevention and therapy: a complementary approach with promising perspectives. *Nutr Rev*. 71:585-599.

Grajek, W., and A. Olejnik. 2004. Epithelial cell cultures in vitro as a model to study functional properties of food. *Polish Journal of Food and Nutrition Sciences*. 13/54.

Guadamillas, M.C., A. Cerezo, and M.A. Del Pozo. 2011. Overcoming anoikis--pathways to anchorage-independent growth in cancer. *J Cell Sci*. 124:3189-3197.

Gupta, N., J.R. Liu, B. Patel, D.E. Solomon, B. Vaidya, and V. Gupta. 2016. Microfluidics-based 3D cell culture models: Utility in novel drug discovery and delivery research. *Bioengineering & Translational Medicine*. 1:63-81.

Haggar, F.A., and R.P. Boushey. 2009. Colorectal cancer epidemiology: incidence, mortality, survival, and risk factors. *Clin Colon Rectal Surg*. 22:191-197.

Hammond, W.A., A. Swaika, and K. Mody. 2016. Pharmacologic resistance in colorectal cancer: a review. *Ther Adv Med Oncol*. 8:57-84.

Han, M., Y. Song, and X. Zhang. 2016. Quercetin Suppresses the Migration and Invasion in Human Colon Cancer Caco-2 Cells Through Regulating Toll-like Receptor 4/Nuclear Factor-kappa B Pathway. *Pharmacogn Mag*. 12:S237-244.

Hanahan, D., and R.A. Weinberg. 2011. Hallmarks of cancer: the next generation. *Cell*. 144:646-674.

Hanna, A., and L.A. Shevde. 2016. Hedgehog signaling: modulation of cancer properies and tumor mircroenvironment. *Mol Cancer*. 15:24.

Harada, K., and G.R. Ogden. 2000. An overview of the cell cycle arrest protein, p21(WAF1). *Oral Oncol*. 36:3-7.

Hellinger, M.D., and C.A. Santiago. 2006. Reoperation for recurrent colorectal cancer. *Clin Colon Rectal Surg*. 19:228-236.

Hepatology., J.H.H.D.o.G. 2016. Hereditary Colorectal Cancer: Therapy. 2016.

Herrero, M., M. Castro-Puyana, J.A. Mendiola, and E. Ibañez. 2013. Compressed fluids for the extraction of bioactive compounds. *TrAC Trends in Analytical Chemistry*. 43:67-83.

Hickman, J.A., R. Graeser, R. de Hoogt, S. Vidic, C. Brito, M. Gutekunst, and H. van der Kuip. 2014. Three-dimensional models of cancer for pharmacology and cancer cell biology: capturing tumor complexity in vitro/ex vivo. *Biotechnol J*. 9:1115-1128.

Higdon, J.V., B. Delage, D.E. Williams, and R.H. Dashwood. 2007. Cruciferous vegetables and human cancer risk: epidemiologic evidence and mechanistic basis. *Pharmacol Res*. 55:224-236.

Hirsch, D., N. Barker, N. McNeil, Y. Hu, J. Camps, K. McKinnon, H. Clevers, T. Ried, and T. Gaiser. 2014. LGR5 positivity defines stem-like cells in colorectal cancer. *Carcinogenesis*. 35:849-858.

Hirschhaeuser, F., H. Menne, C. Dittfeld, J. West, W. Mueller-Klieser, and L.A. Kunz-Schughart. 2010. Multicellular tumor spheroids: an underestimated tool is catching up again. *J Biotechnol*. 148:3-15.

Hlavata, I., B. Mohelnikova-Duchonova, R. Vaclavikova, V. Liska, P. Pitule, P. Novak, J. Bruha, O. Vycital, L. Holubec, V. Treska, P. Vodicka, and P. Soucek. 2012. The role of ABC transporters in progression and clinical outcome of colorectal cancer. *Mutagenesis*. 27:187-196.

Huang, E.H., M.J. Hynes, T. Zhang, C. Ginestier, G. Dontu, H. Appelman, J.Z. Fields, M.S. Wicha, and B.M. Boman. 2009. Aldehyde dehydrogenase 1 is a marker for normal and malignant human colonic stem cells (SC) and tracks SC overpopulation during colon tumorigenesis. *Cancer Res*. 69:3382-3389.

Huels, D.J., and O.J. Sansom. 2015. Stem vs non-stem cell origin of colorectal cancer. *Br J Cancer*. 113:1-5.

Humphries, A., and N.A. Wright. 2008. Colonic crypt organization and tumorigenesis. *Nat Rev Cancer*. 8:415-424.

Jass, J.R., V.L.J. Whitehall, J. Young, and B.A. Leggett. 2002. Emerging concepts in colorectal neoplasia. *Gastroenterology*. 123:862-876.

Jeong, S.Y., J.H. Lee, Y. Shin, S. Chung, and H.J. Kuh. 2016. Co-Culture of Tumor Spheroids and Fibroblasts in a Collagen Matrix-Incorporated Microfluidic Chip Mimics Reciprocal Activation in Solid Tumor Microenvironment. *PLoS One*. 11:e0159013.

Kapusta-Duch, J., A. Kopec, E. Piatkowska, B. Borczak, and T. Leszczynska. 2012. The beneficial effects of Brassica vegetables on human health. *Rocz Panstw Zakl Hig*. 63:389-395.

Karlsson, H., M. Fryknas, R. Larsson, and P. Nygren. 2012. Loss of cancer drug activity in colon cancer HCT-116 cells during spheroid formation in a new 3-D spheroid cell culture system. *Exp Cell Res*. 318:1577-1585.

Katt, M.E., A.L. Placone, A.D. Wong, Z.S. Xu, and P.C. Searson. 2016. In Vitro Tumor Models: Advantages, Disadvantages, Variables, and Selecting the Right Platform. *Front Bioeng Biotechnol*. 4:12.

Kim, D.H., B. Sung, Y.J. Kang, S.Y. Hwang, M.J. Kim, J.H. Yoon, E. Im, and N.D. Kim. 2015a. Sulforaphane inhibits hypoxia-induced HIF-1alpha and VEGF expression and migration of human colon cancer cells. *Int J Oncol*. 47:2226-2232.

Kim, S.-A., E.K. Lee, and H.-J. Kuh. 2015b. Co-culture of 3D tumor spheroids with fibroblasts as a model for epithelial–mesenchymal transition in vitro. *Experimental Cell Research*. 335:187-196.

Krausova, M., and V. Korinek. 2014. Wnt signaling in adult intestinal stem cells and cancer. *Cell Signal*. 26:570-579.

Kuppusamy, P., M.M. Yusoff, G.P. Maniam, S.J. Ichwan, I. Soundharrajan, and N. Govindan. 2014. Nutraceuticals as potential therapeutic agents for colon cancer: a review. *Acta Pharm Sin B*. 4:173-181.

LaBarbera, D.V., B.G. Reid, and B.H. Yoo. 2012. The multicellular tumor spheroid model for high-throughput cancer drug discovery. *Expert Opin Drug Discov*. 7:819-830.

Lai, K.-C., S.-C. Hsu, C.-L. Kuo, S.-W. Ip, J.-S. Yang, Y.-M. Hsu, H.-Y. Huang, S.-H. Wu, and J.-G. Chung. 2010. Phenethyl Isothiocyanate Inhibited Tumor Migration and Invasion via Suppressing Multiple Signal Transduction Pathways in Human Colon Cancer HT29 Cells. *Journal of Agricultural and Food Chemistry*. 58:11148-11155.

Lai, K.C., C.C. Lu, Y.J. Tang, J.H. Chiang, D.H. Kuo, F.A. Chen, I.L. Chen, and J.S. Yang. 2014. Allyl isothiocyanate inhibits cell metastasis through suppression of the MAPK pathways in epidermal growth factorstimulated HT29 human colorectal adenocarcinoma cells. *Oncol Rep*. 31:189-196.

Lampe, J.W., and S. Peterson. 2002. Brassica, biotransformation and cancer risk: genetic polymorphisms alter the preventive effects of cruciferous vegetables. *J Nutr*. 132:2991-2994.

Lamprecht, S., and A. Fich. 2015. The cancer cells-of-origin in the gastrointestinal tract: progenitors revisited. *Carcinogenesis*. 36:811-816.

Lanou, A.J., and B. Svenson. 2010. Reduced cancer risk in vegetarians: an analysis of recent reports. *Cancer Manag Res*. 3:1-8.

Li, L., W. Lee, W.J. Lee, J.H. Auh, S.S. Kim, and J. Yoon. 2010a. Extraction of allyl isothiocyanate from wasabi (Wasabia japonica Matsum) using supercritical carbon dioxide. *Food Science and Biotechnology*. 19:405-410.

Li, L., Y. Luo, M. Lu, X. Xu, H. Lin, and Z. Zheng. 2015. Cruciferous vegetable consumption and the risk of pancreatic cancer: a meta-analysis. *World J Surg Oncol*. 13.

Li, S.H., J. Fu, D.N. Watkins, R.K. Srivastava, and S. Shankar. 2013. Sulforaphane regulates self-renewal of pancreatic cancer stem cells through the modulation of Sonic hedgehog-GLI pathway. *Mol Cell Biochem*. 373:217-227.

Li, Y., T. Zhang, H. Korkaya, S. Liu, H.F. Lee, B. Newman, Y. Yu, S.G. Clouthier, S.J. Schwartz, M.S. Wicha, and D. Sun. 2010b. Sulforaphane, a dietary component of broccoli/broccoli sprouts, inhibits breast cancer stem cells. *Clin Cancer Res*. 16:2580-2590.

Lin, Y.U., T. Wu, Q. Yao, S. Zi, L. Cui, M. Yang, and J. Li. 2015. LGR5 promotes the proliferation of colorectal cancer cells via the Wnt/beta-catenin signaling pathway. *Oncol Lett*. 9:2859-2863.

Liu, R.H. 2004. Potential synergy of phytochemicals in cancer prevention: mechanism of action. *J Nutr*. 134:3479S-3485S.

Liu, X., and K. Lv. 2013. Cruciferous vegetables intake is inversely associated with risk of breast cancer: a meta-analysis. *Breast*. 22:309-313.

Liu, Y., S. Chakravarty, and M. Dey. 2013a. Phenethylisothiocyanate alters site- and promoter-specific histone tail modifications in cancer cells. *PLoS One*. 8:e64535.

Liu, Y.S., H.C. Hsu, K.C. Tseng, H.C. Chen, and S.J. Chen. 2013b. Lgr5 promotes cancer stemness and confers chemoresistance through ABCB1 in colorectal cancer. *Biomed Pharmacother*. 67:791-799.

Lynn, A., A. Collins, Z. Fuller, K. Hillman, and B. Ratcliffe. 2006. Cruciferous vegetables and colo-rectal cancer. *Proc Nutr Soc*. 65:135-144.

Mann, S.K., and N. Khanna. 2013. Health Promoting Effects of Phytochemicals from Brassicaceae: A Review. *Indian J. Pharm. Biol. Res*. 1.

Marshall, J.R. 2008. Prevention of colorectal cancer: diet, chemoprevention, and lifestyle. *Gastroenterol Clin North Am*. 37:73-82, vi.

Mathonnet, M., A. Perraud, N. Christou, H. Akil, C. Melin, S. Battu, M.O. Jauberteau, and Y. Denizot. 2014. Hallmarks in colorectal cancer: angiogenesis and cancer stem-like cells. *World J Gastroenterol*. 20:4189-4196.

McDonald, S.A., S.L. Preston, M.J. Lovell, N.A. Wright, and J.A. Jankowski. 2006. Mechanisms of disease: from stem cells to colorectal cancer. *Nat Clin Pract Gastroenterol Hepatol*. 3:267-274.

Mehta, G., A.Y. Hsiao, M. Ingram, G.D. Luker, and S. Takayama. 2012. Opportunities and challenges for use of tumor spheroids as models to test drug delivery and efficacy. *J Control Release*. 164:192-204.

Mertins, S.D. 2014. Cancer stem cells: a systems biology view of their role in prognosis and therapy. *Anticancer Drugs*. 25:353-367.

Meunier, V., M. Bourrie, Y. Berger, and G. Fabre. 1995. The human intestinal epithelial cell line Caco-2; pharmacological and pharmacokinetic applications. *Cell Biol Toxicol*. 11:187-194.

Mori, S., J.T. Chang, E.R. Andrechek, N. Matsumura, T. Baba, G. Yao, J.W. Kim, M. Gatza, S. Murphy, and J.R. Nevins. 2009. Anchorage-independent cell growth signature identifies tumors with metastatic potential. *Oncogene*. 28:2796-2805.

Myzak, M.C., P.A. Karplus, F.L. Chung, and R.H. Dashwood. 2004. A novel mechanism of chemoprotection by sulforaphane: inhibition of histone deacetylase. *Cancer Res*. 64:5767-5774.

National Institutes of Health, N.C.I. 2016. National Center for Biotechnology Information, U.S. National Library of Medicine. (2016). Colon (Bowel). National Center for Biotechnology Information, U.S. National Library of Medicine

Navarro, S.L., F. Li, and J.W. Lampe. 2011. Mechanisms of action of isothiocyanates in cancer chemoprevention: an update. *Food Funct*. 2:579-587.

Nelson, W.J., and R. Nusse. 2004. Convergence of Wnt, beta-catenin, and cadherin pathways. *Science*. 303:1483-1487.

Orlich, M.J., P.N. Singh, J. Sabate, J. Fan, L. Sveen, H. Bennett, S.F. Knutsen, W.L. Beeson, K. Jaceldo-Siegl, T.L. Butler, R.P. Herring, and G.E. Fraser. 2015. Vegetarian dietary patterns and the risk of colorectal cancers. *JAMA Intern Med*. 175:767-776.

Pan, M.H., C.S. Lai, J.C. Wu, and C.T. Ho. 2011. Molecular mechanisms for chemoprevention of colorectal cancer by natural dietary compounds. *Mol Nutr Food Res*. 55:32-45.

Paoli, P., E. Giannoni, and P. Chiarugi. 2013. Anoikis molecular pathways and its role in cancer progression. *Biochimica et Biophysica Acta (BBA) - Molecular Cell Research*. 1833:3481-3498.

Park, J.I., J. Lee, J.L. Kwon, H.B. Park, S.Y. Lee, J.Y. Kim, J. Sung, J.M. Kim, K.S. Song, and K.H. Kim. 2016. Scaffold-Free Coculture Spheroids of Human Colonic Adenocarcinoma Cells and Normal Colonic Fibroblasts Promote Tumorigenicity in Nude Mice. *Transl Oncol*. 9:79-88.

Pereira, C.G., and M.A.A. Meireles. 2009. Supercritical Fluid Extraction of Bioactive Compounds: Fundamentals, Applications and Economic Perspectives. *Food and Bioprocess Technology*. 3:340-372.

Pericleous, M., D. Mandair, and M.E. Caplin. 2013. Diet and supplements and their impact on colorectal cancer. *J Gastrointest Oncol*. 4:409-423.

Pistollato, F., F. Giampieri, and M. Battino. 2015. The use of plant-derived bioactive compounds to target cancer stem cells and modulate tumor microenvironment. *Food Chem Toxicol*. 75:58-70.

Priyadarsini, R.V., and S. Nagini. 2012. Cancer chemoprevention by dietary phytochemicals: promises and pitfalls. *Curr Pharm Biotechnol*. 13:125-136.

QIAGEN. 2012. RNeasy® Mini Handbook, QIAGEN.

Qiao, L., and B.C. Wong. 2009. Role of Notch signaling in colorectal cancer. *Carcinogenesis*. 30:1979-1986.

Qu, Q., J. Qu, Y. Guo, B.T. Zhou, and H.H. Zhou. 2014. Luteolin potentiates the sensitivity of colorectal cancer cell lines to oxaliplatin through the PPARgamma/OCTN2 pathway. *Anticancer Drugs*. 25:1016-1027.

Rajagopalan, H., M.A. Nowak, B. Vogelstein, and C. Lengauer. 2003. The significance of unstable chromosomes in colorectal cancer. *Nat Rev Cancer*. 3:695-701.

Ren, F., W.Q. Sheng, and X. Du. 2013. CD133: a cancer stem cells marker, is used in colorectal cancers. *World J Gastroenterol*. 19:2603-2611.

Ricci-Vitiani, L., D.G. Lombardi, E. Pilozzi, M. Biffoni, M. Todaro, C. Peschle, and R. De Maria. 2007. Identification and expansion of human colon-cancer-initiating cells. *Nature*. 445:111-115.

Rimann, M., and U. Graf-Hausner. 2012. Synthetic 3D multicellular systems for drug development. *Curr Opin Biotechnol*. 23:803-809.

Rodrigues, L., I. Silva, J. Poejo, A.T. Serra, A.A. Matias, A.L. Simplício, M.R. Bronze, and C.M.M. Duarte. 2016. Recovery of antioxidant and antiproliferative compounds from watercress using pressurized fluid extraction. *RSC Adv.* 6:30905-30918.

Rousset, M. 1986. The human colon carcinoma cell lines HT-29 and Caco-2: two in vitro models for the study of intestinal differentiation. *Biochimie*. 68:1035-1040.

Roy, N., I. Elangovan, D. Kopanja, S. Bagchi, and P. Raychaudhuri. 2013. Tumor regression by phenethyl isothiocyanate involves DDB2. *Cancer Biol Ther*. 14:108-116.

Rudolf, E., and M. Cervinka. 2011. Sulforaphane induces cytotoxicity and lysosome- and mitochondria-dependent cell death in colon cancer cells with deleted p53. *Toxicol In Vitro*. 25:1302-1309.

Saigusa, S., K. Tanaka, Y. Toiyama, T. Yokoe, Y. Okugawa, Y. Ioue, C. Miki, and M. Kusunoki. 2009. Correlation of CD133, OCT4, and SOX2 in rectal cancer and their association with distant recurrence after chemoradiotherapy. *Ann Surg Oncol*. 16:3488-3498.

Saigusa, S., K. Tanaka, Y. Toiyama, T. Yokoe, Y. Okugawa, A. Kawamoto, H. Yasuda, Y. Morimoto, H. Fujikawa, Y. Inoue, C. Miki, and M. Kusunoki. 2010. Immunohistochemical features of CD133

expression: association with resistance to chemoradiotherapy in rectal cancer. *Oncol Rep*. 24:345-350.

Salama, P., and C. Platell. 2009. Colorectal cancer stem cells. *ANZ J Surg*. 79:697-702.

Sambuy, Y., I. De Angelis, G. Ranaldi, M.L. Scarino, A. Stammati, and F. Zucco. 2005. The Caco-2 cell line as a model of the intestinal barrier: influence of cell and culture-related factors on Caco-2 cell functional characteristics. *Cell Biol Toxicol*. 21:1-26.

Santo, V.E., M.F. Estrada, S.P. Rebelo, S. Abreu, I. Silva, C. Pinto, S.C. Veloso, A.T. Serra, E. Boghaert, P.M. Alves, and C. Brito. 2016. Adaptable stirred-tank culture strategies for large scale production of multicellular spheroid-based tumor cell models. *J Biotechnol*. 221:118-129.

Scalbert, A., and G. Williamson. 2000. Dietary intake and bioavailability of polyphenols. *J Nutr*. 130:2073S-2085S.

Schneider, M., J. Huber, B. Hadaschik, G.M. Siegers, H.H. Fiebig, and J. Schuler. 2012. Characterization of colon cancer cells: a functional approach characterizing CD133 as a potential stem cell marker. *BMC Cancer*. 12:96.

Serra, A.T., I.J. Seabra, M.E.M. Braga, M.R. Bronze, H.C. de Sousa, and C.M.M. Duarte. 2010. Processing cherries (Prunus avium) using supercritical fluid technology. Part 1: Recovery of extract fractions rich in bioactive compounds. *The Journal of Supercritical Fluids*. 55:184-191.

Singleton, V.L., and J.A. Rossi. 1965. Colorimetry of Total Phenolics with Phosphomolybdic-Phosphotungstic Acid Reagents. *American Journal of Enology and Viticulture*. 16:144-158.

Solana, M., S. Mirofci, and A. Bertucco. 2016. Production of phenolic and glucosinolate extracts from rocket salad by supercritical fluid extraction: Process design and cost benefits analysis. *Journal of Food Engineering*. 168:35-41.

Song, M., W.S. Garrett, and A.T. Chan. 2015. Nutrients, foods, and colorectal cancer prevention. *Gastroenterology*. 148:1244-1260 e1216.

STEMCELL Technologies, I. 2011. TECHNICAL BULLETIN ALDEFLUOR™ Assay Optimization, STEMCELL Technologies.

STEMCELL Technologies, I. 2016. ALDEFLUOR™ Kit: For the Identification, Evaluation and Isolation of Stem and Progenitor Cells Expressing High Levels of ALDH, STEMCELL TECHNOLOGIES

Subramaniam, D., S. Ramalingam, C. Houchen, and S. Anant. 2010. Cancer Stem Cells: A Novel Paradigm for Cancer Prevention and Treatment. *Mini Rev Med Chem*. 10:359-371.

Suh, Y., F. Afaq, J.J. Johnson, and H. Mukhtar. 2009. A plant flavonoid fisetin induces apoptosis in colon cancer cells by inhibition of COX2 and Wnt/EGFR/NF-kappaB-signaling pathways. *Carcinogenesis*. 30:300-307.

Tang, F.Y., C.J. Shih, L.H. Cheng, H.J. Ho, and H.J. Chen. 2008a. Lycopene inhibits growth of human colon cancer cells via suppression of the Akt signaling pathway. *Mol Nutr Food Res*. 52:646-654.

Tang, L., G.R. Zirpoli, K. Guru, K.B. Moysich, Y. Zhang, C.B. Ambrosone, and S.E. McCann. 2008b. Consumption of raw cruciferous vegetables is inversely associated with bladder cancer risk. *Cancer Epidemiol Biomarkers Prev*. 17:938-944.

Tang, L., G.R. Zirpoli, V. Jayaprakash, M.E. Reid, S.E. McCann, C.E. Nwogu, Y. Zhang, C.B. Ambrosone, and K.B. Moysich. 2010. Cruciferous vegetable intake is inversely associated with lung cancer risk among smokers: a case-control study. *BMC Cancer*. 10:162.

Trachootham, D., Y. Zhou, H. Zhang, Y. Demizu, Z. Chen, H. Pelicano, P.J. Chiao, G. Achanta, R.B. Arlinghaus, J. Liu, and P. Huang. 2006. Selective killing of oncogenically transformed cells through a ROS-mediated mechanism by beta-phenylethyl isothiocyanate. *Cancer Cell*. 10:241-252.

University., M. 2015. Biomarker discovery offers clearer prognosis for bowel and rectal cancer patients. Last Updated: 29 September, 2015. Vol. 2016. Macquarie University, Sydney Australia, http://www.mq.edu.au/newsroom/2015/02/19/biomarker-discovery-offers-clearer-prognosis-for-bowel-and-rectal-cancer-patients/.

Vaiopoulos, A.G., I.D. Kostakis, M. Koutsilieris, and A.G. Papavassiliou. 2012. Colorectal cancer stem cells. *Stem Cells*. 30:363-371.

Vanamala, J., L. Reddivari, S. Radhakrishnan, and C. Tarver. 2010. Resveratrol suppresses IGF-1 induced human colon cancer cell proliferation and elevates apoptosis via suppression of IGF-1R/Wnt and activation of p53 signaling pathways. *BMC Cancer*. 10:238.

Varnat, F., A. Duquet, M. Malerba, M. Zbinden, C. Mas, P. Gervaz, and A. Ruiz i Altaba. 2009. Human colon cancer epithelial cells harbour active HEDGEHOG-GLI signalling that is essential for tumour growth, recurrence, metastasis and stem cell survival and expansion. *EMBO Mol Med*. 1:338-351.

Verhoeven, D.T., R.A. Goldbohm, G. van Poppel, H. Verhagen, and P.A. van den Brandt. 1996. Epidemiological studies on brassica vegetables and cancer risk. *Cancer Epidemiol Biomarkers Prev*. 5:733-748.

Vermeulen, L., M. Todaro, F. de Sousa Mello, M.R. Sprick, K. Kemper, M. Perez Alea, D.J. Richel, G. Stassi, and J.P. Medema. 2008. Single-cell cloning of colon cancer stem cells reveals a multi-lineage differentiation capacity. *Proceedings of the National Academy of Sciences*. 105:13427-13432.

Wahle, K.W., I. Brown, D. Rotondo, and S.D. Heys. 2010. Plant phenolics in the prevention and treatment of cancer. *Adv Exp Med Biol*. 698:36-51.

Wang, K., J. Xu, J. Zhang, and J. Huang. 2012. Prognostic role of CD133 expression in colorectal cancer: a meta-analysis. *BMC Cancer*. 12:1-6.

Wu, H., G.A. Zhang, S. Zeng, and K.C. Lin. 2009. Extraction of allyl isothiocyanate from horseradish (Armoracia rusticana) and its fumigant insecticidal activity on four stored-product pests of paddy. *Pest Manag Sci*. 65:1003-1008.

Wu, Q.J., Y. Yang, E. Vogtmann, J. Wang, L.H. Han, H.L. Li, and Y.B. Xiang. 2013a. Cruciferous vegetables intake and the risk of colorectal cancer: a meta-analysis of observational studies. *Ann Oncol*. 24:1079-1087.

Wu, Q.J., Y. Yang, J. Wang, L.H. Han, and Y.B. Xiang. 2013b. Cruciferous vegetable consumption and gastric cancer risk: a meta-analysis of epidemiological studies. *Cancer Sci*. 104:1067-1073.

Wu, X.S., H.Q. Xi, and L. Chen. 2012. Lgr5 is a potential marker of colorectal carcinoma stem cells that correlates with patient survival. *World J Surg Oncol*. 10:244.

Xu, S., Z. Wen, Q. Jiang, L. Zhu, S. Feng, Y. Zhao, J. Wu, Q. Dong, J. Mao, and Y. Zhu. 2015. CD58, a novel surface marker, promotes self-renewal of tumor-initiating cells in colorectal cancer. *Oncogene*. 34:1520-1531.

Yochum, G.S. 2012. AXIN2: Tumor Suppressor, Oncogene or Both in Colorectal Cancer? *J Cancer Sci Ther*. 4:xii-xiii.

Zeuner, A., M. Todaro, G. Stassi, and R. De Maria. 2014. Colorectal cancer stem cells: from the crypt to the clinic. *Cell Stem Cell*. 15:692-705.

Zhang, X.A., S. Zhang, Q. Yin, and J. Zhang. 2015. Quercetin induces human colon cancer cells apoptosis by inhibiting the nuclear factor-kappa B Pathway. *Pharmacogn Mag*. 11:404-409.
Zhang, Y. 2012. The molecular basis that unifies the metabolism, cellular uptake and chemopreventive activities of dietary isothiocyanates. *Carcinogenesis*. 33:2-9.
zur Hausen, H. 2012. Red meat consumption and cancer: reasons to suspect involvement of bovine infectious factors in colorectal cancer. *Int J Cancer*. 130:2475-2483.